NASA/TM—2004-213114

Strategic Research to Enable NASA's Exploration Missions Conference

Abstracts

June 2004

The NASA STI Program Office . . . in Profile

Since its founding, NASA has been dedicated to the advancement of aeronautics and space science. The NASA Scientific and Technical Information (STI) Program Office plays a key part in helping NASA maintain this important role.

The NASA STI Program Office is operated by Langley Research Center, the Lead Center for NASA's scientific and technical information. The NASA STI Program Office provides access to the NASA STI Database, the largest collection of aeronautical and space science STI in the world. The Program Office is also NASA's institutional mechanism for disseminating the results of its research and development activities. These results are published by NASA in the NASA STI Report Series, which includes the following report types:

- TECHNICAL PUBLICATION. Reports of completed research or a major significant phase of research that present the results of NASA programs and include extensive data or theoretical analysis. Includes compilations of significant scientific and technical data and information deemed to be of continuing reference value. NASA's counterpart of peer-reviewed formal professional papers but has less stringent limitations on manuscript length and extent of graphic presentations.

- TECHNICAL MEMORANDUM. Scientific and technical findings that are preliminary or of specialized interest, e.g., quick release reports, working papers, and bibliographies that contain minimal annotation. Does not contain extensive analysis.

- CONTRACTOR REPORT. Scientific and technical findings by NASA-sponsored contractors and grantees.

- CONFERENCE PUBLICATION. Collected papers from scientific and technical conferences, symposia, seminars, or other meetings sponsored or cosponsored by NASA.

- SPECIAL PUBLICATION. Scientific, technical, or historical information from NASA programs, projects, and missions, often concerned with subjects having substantial public interest.

- TECHNICAL TRANSLATION. English-language translations of foreign scientific and technical material pertinent to NASA's mission.

Specialized services that complement the STI Program Office's diverse offerings include creating custom thesauri, building customized databases, organizing and publishing research results . . . even providing videos.

For more information about the NASA STI Program Office, see the following:

- Access the NASA STI Program Home Page at ***http://www.sti.nasa.gov***

- E-mail your question via the Internet to help@sti.nasa.gov

- Fax your question to the NASA Access Help Desk at 301–621–0134

- Telephone the NASA Access Help Desk at 301–621–0390

- Write to:
  NASA Access Help Desk
  NASA Center for AeroSpace Information
  7121 Standard Drive
  Hanover, MD 21076

NASA/TM—2004-213114

Strategic Research to Enable NASA's Exploration Missions Conference

Abstracts

Abstracts from a conference sponsored by
the NASA Office of Biological and Physical Research
and hosted by NASA Glenn Research Center and
the National Center for Microgravity Research on Fluids and Combustion
Cleveland, Ohio, June 22–23, 2004

National Aeronautics and
Space Administration

Glenn Research Center

June 2004

Trade names or manufacturers' names are used in this report for identification only. This usage does not constitute an official endorsement, either expressed or implied, by the National Aeronautics and Space Administration.

This work was sponsored by the Low Emissions Alternative Power Project of the Vehicle Systems Program at the NASA Glenn Research Center.

Available from

NASA Center for Aerospace Information
7121 Standard Drive
Hanover, MD 21076

National Technical Information Service
5285 Port Royal Road
Springfield, VA 22100

Available electronically at http://gltrs.grc.nasa.gov

TABLE OF CONTENTS
PRESENTATIONS

Baker, James R., Jr.
NANOMOLECULAR BIOSENSORS AND THERAPEUTICS
Session 3C 3

Behringer, Bob
GRAVITY AND GRANULAR MATERIALS
Session 3A 5

Burns, Mark A.; Johnson, Brian N.; Pal, Rohit; Yang, Ming; Lin, Rongsheng; Srivastava, Nimisha; Razzacki, S. Zafar; Chomistek, Kenneth J.; Heldsinger, Dylan; Yim, Moon-Bin; Ugaz, Victor; Krishnan, Madhavi; Namasivayam, Vijay; Fuller, Oveta; Larson, Ronald G.; and Burke, David T.
MEDICAL LAB ON A CHIP
Session 3C 7

D'Andrea, Susan E.; Kahelin, Michael W.; Horowitz, Jay G.; and O'Connor, Philip A.
A DUAL TRACK TREADMILL IN A VIRTUAL REALITY ENVIRONMENT AS A COUNTERMEASURE FOR NEUROVESTIBULAR ADAPTATIONS IN MICROGRAVITY
Session 2C 9

Gaver III, Donald P.; Bilek, A.M.; Kay, S.; and Dee, K.C.
INVESTIGATIONS OF PULMONARY EPITHELIAL CELL DAMAGE DUE TO AIR-LIQUID INTERFACIAL STRESSES IN A MICROGRAVITY ENVIRONMENT
Session 1C 11

Gazda, Daniel B.; Fritz, James S.; Lipert, Robert J.; Porter, Marc D.; Mudgett, Paul; Rutz, Jeff; and Schultz, John
COLORIMETRIC SOLID PHASE EXTRACTION: A METHOD FOR THE RAPID, LOW LEVEL DETERMINATIONS OF BIOCIDE LEVELS IN SPACECRAFT WATER
Session 2A 13

Hirschl, Ronald B.; Bull, Joseph L.; and Grotberg, James B.
AN EARTH-BASED MODEL OF MICROGRAVITY PULMONARY PHYSIOLOGY
Session 1C 15

Israelachvili, Jacob; and Leal, Gary
INTERACTIONS, DEFORMATIONS AND BIOLUBRICATION OF LIQUID-LIQUID AND BIOFLUID INTERFACES
Session 3A 17

Jenkins, James T.; and Louge, Michel Y.
PARTICLE SEGREGATION IN COLLISIONAL SHEARING FLOWS
Session 3A 19

Kim, Jungho
BOILING HEAT TRANSFER MECHANISMS IN EARTH AND LOW GRAVITY: BOUNDARY CONDITION AND HEATER ASPECT RATIO EFFECTS
Session 3A 21

Knothe, Ulf R.; Berglund, Ryan; O'Leary, Jared; Ziegler, Jennifer; and Knothe Tate, Melissa L.
EXTRACORPOREAL SHOCK WAVE THERAPY AS A COUNTERMEASURE FOR BONE LOSS ON EARTH AND IN SPACE
Session 2C 23

Koch, Donald L.; and Sangani, Ashok
MOBI: MICROGRAVITY OBSERVATIONS OF BUBBLE INTERACTIONS
Session 3A 25

Larson, Ronald G.; Fang, Lin; Li, Lei; Namasivayam, Vijay; and Burns, Mark A.
MICROFLUIDIC AND DIELECTRIC PROCESSING OF DNA
Session 1C 27

Louge, Michel Y.; and Jenkins, James T.
SOLIDS INTERACTING WITH A GAS IN A MICROGRAVITY APPARATUS
Session 3A 29

Lueptow, Richard M.; Yoon, Yeomin; and Pederson, Cynthia
ROTATING REVERSE OSMOSIS FOR WASTEWATER REUSE
Session 2A 31

Mitchell, Kenny
PAST, PRESENT AND FUTURE ADVANCED ECLS SYSTEMS FOR HUMAN EXPLORATION OF SPACE
Session 2A 33

Motil, Brian J.; Balakotaiah, Vemuri; Kamotani, Yasuhiro; and McCready, Mark J.
FIXED PACKED BED REACTORS IN REDUCED GRAVITY
Session 3A 35

Plawsky, Joel L.; and Wayner, Peter C., Jr.
CONSTRAINED VAPOR BUBBLE
Session 3A 37

Shaqfeh, Eric S.G.; Beck, Victor; Teclemeriam, Nerayo; and Muller, Susan J.
DNA CONFIGURATIONS IN THE FLOW THROUGH ARRAYS WITH APPLICATION TO BIOSENSORS
Session 1C 39

Tohda, Koji; and Gratzl, Miklos
MICROMINIATURE MONITOR FOR VITAL ELECTROLYTE AND METABOLITE LEVELS OF ASTRONAUTS
Session 3C 41

Zimmerli, Gregory; Fischer, David; Asipauskas, Marius; Chauhan, Chirag; Compitello, Nicole; Burke, Jamie; and Knothe Tate, Melissa
BIOPHOTONICS AND BONE BIOLOGY
Session 2C 43

POSTER SESSION

Avedisian, C.T.; Chandra, S.; and Mostaghimi, J.
THE FLUID MECHANICS OF LIQUID JET IMPINGEMENT: THE HYDRAULIC JUMP IN MICROGRAVITY 47

Banerjee, H.; Blackshear, M.; Mahaffey, K.; Knight, C.; Khan, A.A.; and Delucas, L.
EFFECT OF MICROGRAVITY ON MAMMALIAN LYMPHOCYTES 51

Bar-Ilan, A.; Putzeys, O.; Rein, G.; and Fernandez-Pello, A.C.
TRANSITION FROM FORWARD SMOLDERING TO FLAMING IN SMALL POLYURETHANE FOAM SAMPLES 53

Bergroth, M.; Solomon, T.; Gebremichael, Y.; Keys, A.S.; Vogel, M.; Solomon, M.J.; and Glotzer, S.C.
SPATIALLY HETEROGENEOUS DYNAMICS AND THE EARLY STAGES OF CRYSTAL NUCLEATION AND GROWTH IN METASTABLE LIQUIDS AND COLLOIDS 55

Bhattacharjee, Subrata; Paolini, Chris; Wakai, Kazunori; and Takahashi, Shuhei
FLAMMABILITY MAP FOR MICROGRAVITY FLAME SPREAD 57

Bhunia, Avijit; Chandrasekaran, Sriram; and Chen, Chung-Lung
LIQUID MICRO-JET IMPINGEMENT COOLING OF A POWER CONVERSION MODULE 59

Buckley, Steven G.; Rangwala, Ali S.; and Torero, Jose L.
MODELING AND ANALYSIS OF CO-CURRENT FLAME SPREAD APPLIED TO THE UPWARD BURNING OF PMMA 61

Cavanagh, Jane M.; Torvi, David A.; Gabriel, Kamiel S.; and Ruff, Gary A.
TESTS OF FLAMMABILITY OF COTTON FABRICS AND EXPECTED SKIN BURNS IN MICROGRAVITY 63

Colver, Gerald M.; Greene, Nate; and Xu, Hua
EPS (ELECTRIC PARTICULATE SUSPENSION) MICROGRAVITY TECHNOLOGY PROVIDES NASA WITH NEW TOOLS 65

Colwell, Joshua E.; Horányi, Mihály; Robertson, Scott; Sture, Stein; Batiste, Susan; and Sternovsky, Zoltan
LUNAR SURFACE ENVIRONMENT LABORATORY 67

Dreyer, Michael E.; Rosendahl, Uwe; and Ohlhoff, Antje
CRITICAL VELOCITIES IN OPEN CAPILLARY CHANNEL FLOWS (CCF) 69

Ettema, R.; Marshall, J.S.; and McAlister, G.
WIND-DRIVEN RIVULET BREAK-OFF IN CONDITIONS RANGING FROM 0G TO 1G 71

Faghri, M.; and Charmchi, M.
MELTING AND SOLIDIFICATION IN A RECTANGULAR CAVITY UNDER ELECTROMAGNETICALLY SIMULATED LOW GRAVITY 73

Fernandez-Pello, A.C.; Bar-Ilan, A.; Putzeys, O.M.; Rein, G.; and Urban, D.L.
TRANSITION FROM FORWARD SMOLDERING TO FLAMING IN SMALL POLYURETHANE FOAM SAMPLES..... 75

Gillis, Keith A.; Shinder, Iosif I.; and Moldover, Michael R.
PROGRESS ON ACOUSTIC MEASUREMENTS OF THE BULK VISCOSITY OF NEAR-CRITICAL XENON (BVX) 77

Glushko, Vladimir
STUDYING BIOLOGICAL RHYTHMS OF PERSON'S SKIN-GALVANIC REACTION AND DYNAMICS OF LIGHT TRANSMISSION BY ISOMERIC SUBSTANCE IN SPACE FLIGHT CONDITIONS 79

Goree, John
ELECTROSTATIC RELEASE OF FINE PARTICLES ADHERED TO SURFACES ON THE MOON OR MARS 81

Hermanson, J.C.; Johari, H.; Ghaem-Maghami, E.; Stocker, D.P.; and Hegde, U.G.
BUOYANCY EFFECTS IN STRONGLY-PULSED, TURBULENT DIFFUSION FLAMES..... 83

Ishii, Mamoru; Sun, Xiaodong; and Vasavada, Shilp
TWO-FLUID MODEL AND INTERFACIAL AREA TRANSPORT IN MICROGRAVITY CONDITION..... 85

Jenkins, James T.; Pasini, José Miguel; and Valance, Alexandre
AEOLIAN SAND TRANSPORT WITH COLLISIONAL SUSPENSION 87

Jun, Yonggun; Zhang, Jie; and Wu, Xiao-Lun
TWO DIMENSIONAL TURBULENCE IN PRESENCE OF POLYMER..... 89

Kashiwagi, Takashi; Nakamura, Yuji; Olson, Sandra L.; and Mell, William
TRANSITION FROM IGNITION TO FLAME GROWTH UNDER EXTERNAL RADIATION IN THREE DIMENSIONS (TIGER-3D)..... 91

Kazakov, A.; Kroenlein, K.G.; Dryer, F.L.; Williams, F.A.; and Nayagam, V.
ISOLATED LIQUID DROPLET COMBUSTION: INHIBITION AND EXTINCTION STUDIES..... 93

Khusid, Boris; and Acrivos, Andreas
ELECTRIC-FIELD-DRIVEN PHENOMENA FOR MANIPULATING PARTICLES IN MICRO-DEVICES 95

Kopacka, Wesley M.; Hollingsworth, Andrew D.; Russel, William B.; and Chaikin, Paul M.
A STUDY OF COLLOIDAL CRYSTALLIZATION 97

Kuhlman, John; Gray, Donald D.; Glaspell, Shannon; Kreitzer, Paul; Battleson, Charlie; Lechliter, Michelle; Campanelli, Michael; Fredrick, Nicholas; Sunderlin, Christopher; and Williams, Brianne
POSITIONING OF SIMULATED VAPOR BUBBLES IN MICROGRAVITY BY THE KELVIN FORCE 99

Lastochkin, Dmitri; Wang, Ping; and Chang, Hsueh-Chia
AC ELECTROKINETIC JETS AND SPRAYS FOR SPACE APPLICATIONS 101

Lebedev, Nikolai; Trammell, Scott A.; and Spano, Anthony
PHOTOREGULATED ELECTRON TRANSFER AT BIO-INORGANIC INTERFACES 103

Lee, C. Ted, Jr.
MIMICKING MICROGRAVITY IN BIO- AND NANO-COLLOIDAL SYSTEMS USING SUPERCRITICAL CARBON DIOXIDE 105

Lin, Yiqiang; Lei, Zhiheng; Farouk, Bakhtier; and Oran, Elaine S.
THERMOACOUSTIC CONVECTION AND TRANSPORT IN GASES AND NEAR-CRITICAL FLUIDS UNDER NORMAL AND MICRO-GRAVITY CONDITIONS 107

Lipa, J.
FLUID PHYSICS AND TRANSPORT PHENOMENA IN A SIMULATED REDUCED GRAVITY ENVIRONMENT 109

Martineau, R.; Piccini, M.; and Towe, B.
A CONTINUOUS MICROCULTURE DEVICE FOR MONITORING THE EFFECTS OF SPACE ENVIRONMENTS ON LIVING SYSTEMS 111

Mikofski, M.A.; Blevins, L.G.; Williams, T.C.; and Shaddix, C.R.
EFFECT OF VARIED AIR FLOW ON FLAME STRUCTURE OF LAMINAR INVERSE DIFFUSION FLAMES 113

Mohraz, Ali; and Solomon, Michael J.
LIGHT SCATTERING AND DIRECT VISUALIZATION STUDIES OF ANISOMETRIC COLLOIDAL AGGREGATES AND GELS 115

Nakagawa, Masami
MECHANICAL PROPERTIES OF FINE PARTICLE ASSEMBLIES 117

Nave, Jean-Christophe; and Banerjee, Sanjoy
DIRECT NUMERICAL SIMULATION OF GAS-LIQUID SYSTEMS IN VARIABLE GRAVITY ENVIRONMENTS 119

Olson, S.L.; Beeson, H.D.; Haas, J.P.; and Baas, J.S.
A NEW TEST METHOD FOR MATERIAL FLAMMABILITY ASSESSMENT IN MICROGRAVITY AND EXTRATERRESTRIAL ENVIRONMENTS 121

Olson, S.L.
MOST PROBABLE FIRE SCENARIOS IN SPACECRAFT AND EXTRATERRESTRIAL HABITATS—WHY NASA'S CURRENT TEST 1 MIGHT NOT ALWAYS BE CONSERVATIVE 123

Ozen, Ozgur
INTERFACIAL INSTABILITIES DURING EVAPORATION 125

Panzarella, Charles
MICROFLUIDIC BIOCHIP DESIGN..... 127

Pillai, Dilip; Rosenbaum, David S.; Liszka, Kathy J.; York, David W.; Mackin, Michael A.; and Lichter, Michael J.
DETECTION AND PREVENTION OF CARDIAC ARRHYTHMIAS DURING SPACE FLIGHT 129

Popova, Natalya
THE EFFECT OF GRAVITY MODULATION ON FILTRATIONAL CONVECTION IN A HORIZONTAL LAYER..... 131

Potember, Richard S.
MINIATURE TIME OF FLIGHT MASS SPECTROMETER..... 133

Puri, Ishwar K.; Aggarwal, Suresh K.; Lock, Andrew J.; and Hegde, Uday
PARTIALLY PREMIXED FLAME (PPF) RESEARCH FOR FIRE SAFETY 135

Qiao, L.; Kim, C.H.; and Faeth, G.M.
EFFECTS OF CHEMICALLY-PASSIVE SUPPRESSANTS ON LAMINAR PREMIXED HYDROGEN/AIR FLAMES 137

Ramé, Enrique
DYNAMIC WETTING OF ROOM TEMPERATURE POLYMER MELTS: DEVIATIONS FROM NEWTONIAN BEHAVIOR..... 139

Revankar, Shripad T.; and Kong, Xiangcheng
STUDY OF CO-CURRENT AND COUNTER-CURRENT GAS-LIQUID TWO-PHASE FLOW THROUGH PACKED BED IN MICROGRAVITY 141

Rich, D.B.; Lautenberger, C.W.; Yuan, Z.; and Fernandez-Pello, A.C.
EFFECTS OF HEAT FLUX, OXYGEN CONCENTRATION AND GLASS FIBER VOLUME FRACTION ON PYROLYSATE MASS FLUX FROM COMPOSITE SOLIDS 143

Roby, Richard; Zhang, Wei; Gaines, Glenn; Olenick, Stephen; Klassen, Michael; and Torero, Jose L.
THE INTEGRATION OF A SMOKE DETECTOR MODEL WITH LARGE EDDY SIMULATION FIRE MODELING FOR PREDICTING SMOKE DETECTOR ACTIVATION IN MICROGRAVITY 145

Roushan, Pedram; and Wu, Xiao-Lun
STUDY OF THE VON-KÁRMÁN VORTEX STREET CLOSE TO ONSET OF SHEDDING..... 147

Sankaran, Subramanian; and Allen, Jeffrey S.
VISUALIZATION OF ELECTRIC FIELD EFFECTS ON NUCLEATE AND FILM BOILING 149

Shafirovich, Evgeny; and Varma, Arvind
NICKEL-COATED ALUMINUM PARTICLES: A PROMISING FUEL FOR MARS MISSIONS 151

Sharp, M. Keith
COMPUTER MODELING OF CARDIOVASCULAR RESPONSES TO GRAVITY 153

Shaw, Benjamin D.
BI-COMPONENT DROPLET COMBUSTION IN REDUCED GRAVITY 155

Shaw, Benjamin D.
REDUCED GRAVITY STUDIES OF SORET TRANSPORT EFFECTS IN LIQUID FUEL COMBUSTION 157

Son,Youngjin; Ronney, Paul D., and Gokoglu, Suleyman
COMPARISON OF CARBON DIOXIDE AND HELIUM AS FIRE EXTINGUISHING AGENTS FOR SPACECRAFT 159

Sorensen, C.M.; Kim, W.; Fry, D.; and Chakrabarti, A.
AGGREGATES AND SUPERAGGREGATES OF SOOT WITH FOUR DISTINCT FRACTAL MORPHOLOGIES 161

Steen, Paul H.; Bhandar, Anand; Vogel, Michael J.; and Hirsa, Amir H.
DYNAMICS AND STABILITY OF CAPILLARY SURFACES: LIQUID SWITCHES AT SMALL SCALES 163

Takahashi, Fumiaki; Linteris, Gregory T.; and Katta, Viswanath R.
FIRE SUPPRESSION IN LOW GRAVITY USING A CUP BURNER 165

Teclemariam, Nerayo P.; Muller, Susan J.; Beck, Victor A.; and Shaqfeh, Eric S.G.
A BIOSENSOR FOR SINGLE-MOLECULE DNA SEQUENCING 167

Thiessen, David B.; and Marston, Philip L.
SUPPORTED CAPILLARY PIPES 169

Thomas, Aaron
OSCILLATORY FLOWS AS A MEANS OF SEPARATION OF CONTAMINANTS FROM AIR 171

Tolmachoff, Erik; and Kezirian, Michael T.
REDUCING FUEL SLOSH IN SPACECRAFT PROPULSION SYSTEMS 173

Uguz, A. Kerem; and Narayanan, R.
COMPARISON OF THE STABILITY OF AN ELLIPTICAL LIQUID BRIDGE WITH A COMPANION CIRCULAR LIQUID BRIDGE 175

Unuvar, C.; Fredrick, D.; Anselmi-Tamburini, U.; Manerbino, A.; Guigne, J.Y.; Munir, Z.A.; and Shaw, B.D.
ELECTRIC CURRENT ACTIVATED COMBUSTION SYNTHESIS AND CHEMICAL OVENS UNDER TERRESTRIAL AND REDUCED GRAVITY CONDITIONS 177

Vander Wal, Randy L.; Kizito, John P.; Tryggvason, Gretar; Berger, Gordon M.; and Mozes, Steven D.
DROPLET-SURFACE IMPINGEMENT DYNAMICS FOR INTELLIGENT SPRAY DESIGN 179

Veretennikov, Igor; and Glazier, James A.
CONVECTIVE INSTABILITIES IN LIQUID FOAMS 181

Walton, Krista S.; and LeVan, M. Douglas
SEPARATION OF CARBON MONOXIDE AND CARBON DIOXIDE FOR MARS ISRU 183

Wei, Wei; Thiessen, David B.; and Marston, Philip L.
ENHANCED DAMPING FOR CAPILLARY BRIDGE OSCILLATION USING VELOCITY FEEDBACK 185

Zhang, Jie; Jun, Yonggun; and Wu, X.L.
THE STUDY OF TOPOLOGICAL STRUCTURE DISTRIBUTIONS IN STRATIFIED SOAP FILM CONVECTIONS 187

Presentations

NANOMOLECULAR BIOSENSORS AND THERAPEUTICS

James R. Baker, Jr. MD
Center for Biologic Nanotechnology
University of Michigan
Ann Arbor, MI

We are developing nanoscale biosensors and bioactuators for use in astronaut health and safety monitoring. This involves nanoscale polymer structures less than 20 nm in diameter as the basis of the sensor/actuators. The structures would be designed to target into specific cells of an astronaut and be able to monitor health issues such as the exposure to radiation or infectious agents. These molecules would also be able to administer therapeutics in response to the needs of the astronaut, and act as actuators to remotely manipulate an astronaut as necessary to ensure their safety. A multidisciplinary team, involving disciplines including nanotechnology-based materials science, bioengineering, bioinformatics and medical sciences, performs these studies. We will use these different disciplines to converge on the design and manipulation of the nanosensors, and the development of a non-invasive system to interact with the sensors through multi-spectral fluorescence analysis. Because of these broad requirements, the research involves a multidisciplinary team from the Medical, Engineering and LS&A schools at the University of Michigan, and is funded to train multidisciplinary scientists at the pre-graduate level.

GRAVITY AND GRANULAR MATERIALS

Bob Behringer
Department of Physics
Duke University
Durham, N.C.27708-0305
Phone: 919-660-2550; Fax: 919-660-2525; Email: bob@phy.duke.edu

Granular materials present a host of challenging questions that must be addressed if mankind is to successfully deal with locomotion on uncertain soils and to process soils from lunar or Martian surfaces for key life-sustaining materials. Here, we are particularly concerned with the behavior of dense granular materials, and the way in which such materials change from effective solids to fluids. It is critical that we understand this type of behavior in particular if we are to have rovers that do not get stuck and handling systems that do not jam or break. We begin by noting that granular handling systems on earth are sources of significant problems for industry. Failures of granular devices occurs on the order of 100 times more often than fluid-related devices. And granular processing facilities typically operate well below design. Unlike fluid flows, the basic equations for describing dense granular flow are still a matter of open debate. It is crucial to have careful well-designed experiments and simulations that provide the basis for theory. The Gravity and Granular Materials Flight project involves such a study. In particular, it focuses on the transition between dense and more fluid-like states. A key point here is that earth's gravity consistently compacts granular materials, so that it is impossible to provide a true characterization of the rheological properties of granular materials. Nevertheless, a ground based study has shown that this transition has a particularly novel character. The experimental part of this project is carried out in an annular channel that allows shearing from above and vibration from below. The latter feature gives us the ability both to partially compensate for gravity and to provide a kind of 'thermalization'. The fluid-solid transition see in these experiments is particularly striking because the system freezes--becomes an ordered solid, as a result of increasing the effective temperature due to vibration. A parallel aspect of these studies are Molecular Dynamics (MD) simulations in both 2D and 3D. These simulations provide insights into the expected behavior of a flight experiment--information that cannot be easily accessed with earth-based experiments. And it also provides key insight into new ways of modelling granular systems. In particular, in these studies, we have investigated the role played by order-disorder associated with the elastic energy stored in the grains. This work is in collaboration with Drs. O. Baran, K. Daniels, and L. Kondic.

MEDICAL LAB ON A CHIP

Mark A. Burns,[*†] Brian N. Johnson,[*] Rohit Pal,[*] Ming Yang,[*] Rongsheng Lin,[*]
Nimisha Srivastava,[*] S. Zafar Razzacki,[*] Kenneth J. Chomistek,[*] Dylan Heldsinger,[*]
Moon-Bin Yim,[*] Victor Ugaz,[*] Madhavi Krishnan,[*] Vijay Namasivayam,[*]
Oveta Fuller,[‡] Ronald G. Larson,[*] and David T. Burke[¥]

[*]Department of Chemical Engineering
[†]Department of Biomedical Engineering
[‡]Department of Microbiology and Immunology
[¥]Department of Human Genetics
University of Michigan
Ann Arbor, MI 48109-2136

The low per-unit cost of microfabricated devices along with the ability to integrate multiple components on a single device allows for the construction of a variety of complex chemical analysis system. These complex systems can be only a squared centimeter or less in size but can perform functions normally associated with benchtop equipment. Such devices can, in essence, function as micron-scale intelligent sensors. We are constructing such devices on silicon, glass, and polymer substrates for the analysis saliva, blood, and other medially relevant fluids. The devices consist of a combination of micron-scale fluidic channels, reaction chambers, and/or electrophoresis units. The devices can also include electronic control and sensing systems such as resistive heaters, temperature sensors, and fluorescence detectors. Liquid samples are injected into these devices and moved between components by a variety of techniques including hydrophobic/hydrophilic patterning, pressure manifolds, and/or phase-change valves. The output from these devices can then be used to determine physical and/or chemical properties of the liquid sample and ultimately the medical condition of the patient from which the sample was obtained. Results will be presented for the analysis of both physical (e.g., viscosity) and chemical (e.g., DNA) properties.

A DUAL TRACK TREADMILL IN A VIRTUAL REALITY ENVIRONMENT AS A COUNTERMEASURE FOR NEUROVESTIBULAR ADAPTATIONS IN MICROGRAVITY

Susan E. D'Andrea Ph.D.*, Michael W. Kahelin B.S.
Department of Biomedical Engineering, The Cleveland Clinic Foundation, Cleveland, OH

Jay G. Horowitz Ph.D., Philip A. O'Connor M.S.
NASA Glenn Research Center, Cleveland, OH

INTRODUCTION

While the neurovestibular system is capable of adapting to altered environments such as microgravity, the adaptive state achieved in space in inadequate for 1G [1]. This leads to gait and postural instabilities when returning to a gravity environment and may create serious problems in future missions to Mars. New methods are needed to improve the understanding of the adaptive capabilities of the human neurovestibular system and to develop more effective countermeasures [2]. The concept behind the current study is that by challenging the neurovestibular system while walking or running, a treadmill can help to readjust the relationship between the visual, vestibular and proprioceptive signals that are altered in a microgravity environment. As a countermeasure, this device could also benefit the musculoskeletal and cardiovascular systems and at the same time decrease the overall time spent exercising. The overall goal of this research is to design, develop, build and test a dual track treadmill, which utilizes virtual reality, VR, displays (Figure 1).

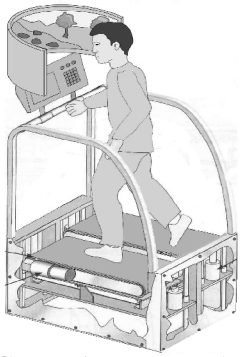

FIGURE 1: Dual Track Treadmill

PILOT STUDIES

Pilot studies were performed to evaluate the potential of the system to stimulate the neurovestibular system. Twenty subjects were tested running on a dual-track treadmill in simulated curve walking scenes. Subjects also participated in an extended trial consisting of walking 30 minutes in one randomly assigned condition. Before and immediately following testing, subjects ran a timed obstacle course. Results revealed that the combination of visual and proprioceptive stimuli provided by the VR system and the movement of the treadmill respectively, will significantly increase the stimulus to the neurovestibular system.

TREADMILL DESIGN

The proposed treadmill has been designed to function with two belts and four actuators to both elevate and incline the tracks independently (Figure 2). Along with dual speed control, this arrangement will enable the system to replicate motion found during ascending and descending hills, going over rough terrain, turning corners and climbing stairs. Working in conjunction with the VR display, the treadmill system will provide an immersive environment for testing effects on the neurovestibular system.

The system's motion is governed by six independently controlled axes: two AC motor-driven treads and four servo-driven linear actuators. The system can be simplified as a hierarchical structure composed of three levels and ten components (Figure 3). The highest level of the hierarchy is the main user interface which governs all functions of the system, including manual control, programmed control, and path generation. It is also responsible for synchronizing the system's motion with its visual display. The user interface level communicates directly with the motor controller and visualization application. The visualization application, created by NASA, uses a "morphing hallway" algorithm to create a visual environment that simulates motion in three dimensions, as well as a variety of terrains including stairs. This application outputs the visual effects to a display unit. The motor controller is responsible for the motion of the motors. This component is linked to the user interface via component object model (COM) interface. The controller is responsible for the PID control of the servomotors and the translation of the user interface's mnemonic code to machine code. The lowest level of the hierarchy represents the hardware of the system. This level is responsible for providing the physical stimulation to the subject. It is composed of the visual display and the actuation devices working through the treadmill frame.

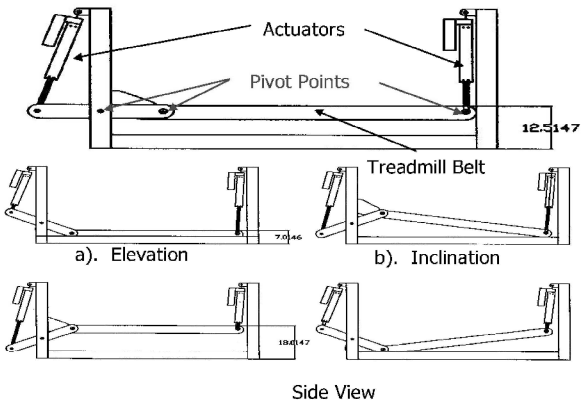

Figure 2: Treadmill Schematic

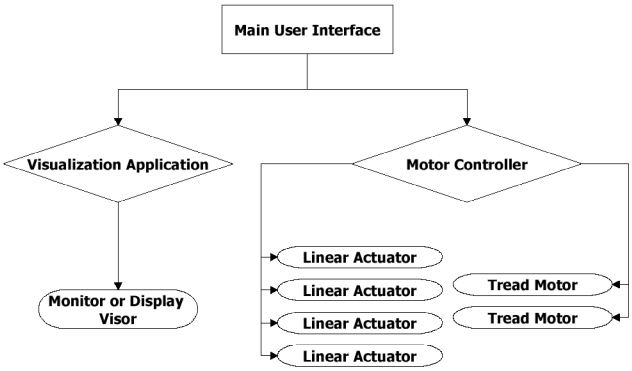

Figure 3: System Overview

Biomechanical testing will concentrate on establishing the extent to which the treadmill will stimulate the neurovestibular system. This will include motion analysis, electromyography, accelerometry and pupil tracking data. It is expected that these biomechanical parameters indicating neurovestibular response will differ significantly while walking and running on a standard treadmill from those recorded using the novel virtual reality dual track system.

REFERENCES

1. Bloomberg, *et al.*, 1997. Journal of Vestibular Research, Vol. 7, Nos 2/3, pp 161-177.
2. Oman, C.M *et al.*, 1996. Journal of Applied Physiology, Vol. 81, No. 1, pp. 69-81.

ACKNOWLEDGEMENTS

The authors would like to thank the **John Glenn Biomedical Engineering Consortium** for support and funding of this project.

*Susan E. D'Andrea, Ph.D.
Department of Biomedical Engineering/ND20
The Cleveland Clinic Foundation
9500 Euclid Avenue
Cleveland, OH 44195

Phone: 216.444..5347
Fax: 216.444.9198
Email: dandreas@bme.ri.ccf.org

Investigations of pulmonary epithelial cell damage due to air-liquid interfacial stresses in a microgravity environment

Donald P. Gaver III
Department of Biomedical Engineering, Tulane University, New Orleans, LA, USA
A.M. Bilek, S. Kay and K.C Dee
Department of Biomedical Engineering, Tulane University, New Orleans, LA, USA

Pulmonary airway closure is a potentially dangerous event that can occur in microgravity environments and may result in limited gas exchange for flight crew during long-term space flight. Repetitive airway collapse and reopening subjects the pulmonary epithelium to large, dynamic, and potentially injurious mechanical stresses. During ventilation at low lung volumes and pressures, airway instability leads to repetitive collapse and reopening. During reopening, air must progress through a collapsed airway, generating stresses on the airway walls, potentially damaging airway tissues. The normal lung can tolerate repetitive collapse and reopening. However, combined with insufficient or dysfunctional pulmonary surfactant, repetitive airway collapse and reopening produces severe lung injury. Particularly at risk is the pulmonary epithelium. As an important regulator of lung function and physiology, the degree of pulmonary epithelial damage influences the course and outcome of lung injury. In this paper we present experimental and computational studies to explore the hypothesis that the mechanical stresses associated with airway reopening inflict injury to the pulmonary epithelium.

Experimental Investigations

Experiments were performed in a parallel plate chamber lined with pulmonary epithelial cells, which was constructed as an idealized model of a collapsed segment of an airway where the walls are held in opposition by a viscous fluid. These experiments were conducted to determine whether air-liquid interfacial stresses can cause damage to epithelial cells, and to provide response behavior that can be correlated to the mechanical stimuli determined from computational investigations (below).

In a first set of experiments, a fetal rat pulmonary epithelial cell line (CCL-149, ATCC) was cultured to confluence on a small (1 cm^2), square region of the upper plate. The narrow channel was filled a model airway lining fluid. Phosphate buffered saline including 0.1 mg/mL $CaCl_2$ and $MgSO_4$ (PBS) was used to model a surfactant-deficient airway lining fluid. A surfactant-containing airway lining fluid was approximated using Infasurf (ONY, Inc.) diluted to 1 mg/mL phospholipid concentration in PBS. Airway "reopening" was generated by the steady progression of a semi-infinite bubble of air down the length of the channel using a constant rate infusion pump (7 or 70 mL/min). A digital camera mounted above the channel collected sequential overhead images of the progressing bubble, which were used to calculate bubble velocity. Once removed from the apparatus, the slide was incubated with 1.2 μM Ethidium homodimer-1 (Eth-1) and 1.2 μM calcein AM (Molecular Probes). For each slide, the number of injured cells was recorded as the average number of Eth-1 stained nuclei counted in fluorescence microscopic images.

In a second experimental study, we attempted to discriminate the stress magnitude from the stimulus duration. To do so, the stress magnitude is modified by varying the viscosity of the

occlusion fluid while fixing the reopening velocity across experiments. This approach causes the stimulus duration to be inversely related to the magnitude of the pressure gradient. We also explore the mechanism for acute damage and demonstrate that repeated reopening and closure is shown to damage the epithelial cell layer even under conditions that would not lead to extensive damage from a single reopening event.

Fluid Dynamic Simulations

The bubble and parallel-plate flow chamber was modeled as a semi-infinite bubble progressing within a Hele-Shaw cell. In this model the walls were separated by a distance $2H$, with the semi-infinite bubble progressing in the x-direction with tip velocity U. The surface tension, γ, was constant. The capillary number, $Ca = \mu U/\gamma$, representing the relative importance of viscous to surface tension effects on the bubble determines the dynamic response of the system. Stokes equations, $\nabla \mathbf{P} = \mu \nabla^2 u$ and $\nabla \bullet u = 0$, were solved using the boundary element method. The interfacial stress condition applied at the air-liquid interface was $|\sigma \bullet \hat{n}| = \gamma \kappa \hat{n}$, where $\sigma = -P\mathbf{I} + \mu(\nabla u + \nabla u^T)$ was the stress tensor, $\hat{n}$ was the unit normal, and κ was the interfacial curvature. For a given Ca, the system was simulated until a steady-state meniscus had developed and the stress-field and bubble geometry were determined.

Three potentially injurious components of the stress cycle associated with bubble progression – the shear stress, the shear stress gradient, and the pressure gradient – were analyzed. Regression relationships describing the behavior of these components as a function of Ca were determined for very small Ca ($5 \times 10^{-4} \leq Ca \leq 2 \times 10^{-3}$). Additionally, the thickness of the thin film deposited by bubble progression was estimated. Dimensionless values for the experimental flow conditions were extrapolated from the regression equations and redimensionalized.

Results and Discussion

For each condition the average number of injured cells per square centimeter was measured. For the saline-occluded channels, bubble progression at both velocities produced significantly increased numbers of injured cells when compared to the control. The slow velocity resulted in a 66-fold increase in the number of injured cells and the fast velocity produced a 20-fold increase. The addition of Infasurf to the occlusion fluid reduced the number of injured cells to a level similar to the control. These results support the hypotheses that mechanical stresses associated with airway reopening injure pulmonary epithelial cells and that pulmonary surfactant in the normal lung protects the epithelium from injury due to airway reopening.

The stress component that best agrees with the experimentally observed trauma is the maximal pressure gradient. Pressure gradients create a force imbalance on the cell membrane over the length of the cell. In addition, cell damage remains directly correlated with the pressure gradient, not the duration of stress exposure. For a low profile predominately flat cell (or region of a cell), the non-uniformly distributed load can depress the cell and stretch the membrane. For high profile cells or regions of a cell, such as the protrusion cause by the nucleus, where the normal forces of the cell surface are nearly opposite, the pressure gradient will pinch that region. The pinching can tear the membrane at the base of the protrusion or force fluid upward rupturing the top surface of the cell. The present study thus provides additional evidence that the magnitude of the pressure gradient induces cellular damage in this model of airway reopening.

COLORIMETRIC SOLID PHASE EXTRACTION: A METHOD FOR THE RAPID, LOW LEVEL DETERMINATIONS OF BIOCIDE LEVELS IN SPACECRAFT WATER

Daniel B. Gazda, James S. Fritz, Robert J. Lipert, and Marc D. Porter
Institute for Combinatorial Discovery, Ames Laboratory-U.S.D.O.E. and Department of Chemistry
Iowa State University
Ames, IA 50011

Paul Mudgett, Jeff Rutz, and John Schultz
Wyle Laboratories
Houston TX 77058

Monitoring and maintaining biocide concentrations is vital for assuring safe drinking water both in ground and spacecraft applications. Currently, there are no available methods to measure biocide concentrations (i.e., silver ion or iodine) on-orbit. Sensitive, rapid, simple colorimetric methods for the determination of silver(I) and iodine are described. The apparatus consists of a 13-mm extraction disk (Empore® membrane) impregnated with a colorimetric reagent and placed in a plastic filter holder. A Luer tip syringe containing the aqueous sample is attached to the holder and a predetermined volume of sample is forced through the disk in ~30 s. Silver(I) is retained by a disk impregnated with 5-(p-dimethylaminobenzylidene)-rhodanine (DMABR), and iodine is retained as a yellow complex on a membrane impregnated with polyvinylpyrrolidone (PVP). After passage of a water sample, the colorimetric response generated by the interaction between analyte and reagent is measured by use of a hand-held, commercial reflectance spectrophotometer. This simple solid-phase extraction (SPE) method gives a high concentration factor. The sensitivity for both measurements is excellent: 0.005 mg/L for Ag(I) and 0.1 mg/L for I2. Furthermore, the methodology minimizes sample handling and potential contamination events, produces only a small volume of waste, and requires only ~60 s for completion. Details related to membrane impregnation, calibration, and interferences are presented, as well as the results of ground-based analysis of samples of actual Space Shuttle and International Space Station (ISS) drinking water. Findings from KC-135 microgravity flight simulations and challenges for the eventual deployment on ISS will also be described.

AN EARTH-BASED MODEL OF MICROGRAVITY PULMONARY PHYSIOLOGY

Ronald B. Hirschl, M.D., Joseph L. Bull, Ph.D, and James B. Grotberg, Ph.D., M.D.

There are currently only two practical methods of achieving μG for experimentation: parabolic flight in an aircraft or space flight, both of which have limitations. As a result, there are many important aspects of pulmonary physiology that have not been investigated in μG. We propose to develop an earth-based animal model of μG by using liquid ventilation, which will allow us to fill the lungs with perfluorocarbon, and submersing the animal in water such that the density of the lungs is the same as the surrounding environment. By so doing, we will eliminate the effects of gravity on respiration. We will first validate the model by comparing measures of pulmonary physiology, including cardiac output, central venous pressures, lung volumes, and pulmonary mechanics, to previous space flight and parabolic flight measurements. After validating the model, we will investigate the impact of μG on aspects of lung physiology that have not been previously measured. These will include pulmonary blood flow distribution, ventilation distribution, pulmonary capillary wedge pressure, ventilation-perfusion matching, and pleural pressures and flows. We expect that this earth-based model of μG will enhance our knowledge and understanding of lung physiology in space which will increase in importance as space flights increase in time and distance.

INTERACTIONS, DEFORMATIONS AND BIOLUBRICATION OF LIQUID-LIQUID AND BIOFLUID INTERFACES

Jacob Israelachvili and Gary Leal
Department of Chemical Engineering, Materials Department, and Biomolecular Science & Engineering Program (BMSE), University of California at Santa Barbara (UCSB)
Santa Barbara, California 93106

Recent experiments have allowed for the molecular forces and deformations of liquid-liquid and biofluid-soft solid interfaces to be visualized and measured with unprecedented precision in real time. The talk will describe recent measurements and new theoretical treatments of the interactions and deformations of liquid-liquid interfaces [1] such as suspended droplets during collisions, coalescence and detachment, and the implications of the results to predictions of droplet coalescence and biological cell-cell interactions in general. The effects of van der Waals and other short-range molecular and thermal fluctuation forces on droplet coalescence and film instability will be described, as will the role of buoyancy forces and dissolved gases on the hydrophobic interaction between oil droplets and gas bubbles in water [2, 3], this interaction being one of the major forces between biological molecules and surfaces in aqueous solutions. Current work is also focusing on the role of surfactants and other amphiphilic molecules at the liquid-liquid interfaces. Preliminary results on the thin film rheology ('lubricity' and 'wear') of model biological and real cartilage surfaces in various model biofluids and synovial fluid will also be presented, with a discussion of the implications of the results to cartilage, bone and joint degeneration.

[1] Large deformations during the coalescence of fluid interfaces. Nianhuan Chen, Tonya Kuhl, Rafael Tadmor, Qi Lin and Jacob Israelachvili. Phys. Rev. Letters 92 (2004) 024501-04.
[2] Further studies on the effect of de-gassing on the dispersion and stability of surfactant-free emulsions. N. Maeda, K. Rosenberg, J. Israelachvili and R. Pashley. Langmuir 20 (2004) 3129-3137.
[3] Measurements of hydrophobic interactions at short-range. Tonya Kuhl, Qi Lin, Maria Tadmor, Jacob Israelachvili (submitted).

PARTICLE SEGREGATION IN COLLISIONAL SHEARING FLOWS

James T. Jenkins, PI
Department of Theoretical and Applied Mechanics
Cornell University, Ithaca, NY 14853

Michel Y. Louge, CoI
Sibley School of Mechanical and Aerospace Engineering
Cornell University, Ithaca, NY 14853

This research concerns flowing granular materials and the development of ways to predict the behavior of such flows and the means to control them. Granular flows are common in industrial processes, mining operations, and in nature. In general, they are poorly understood. The research treats flows in which the particles interact through collisions rather than enduring contacts. Such flows are expected to be important in materials processing activities carried out in space and in mining operations on the surface of the Moon and Mars.

The specific phenomenon of interest in the research is the segregation of the particles in a flow due to differences in their size and/or mass. In many industrial processes a homogeneous aggregate is desired; in these, segregation is undesirable. However, in the mining industry, segregation is exploited in sorting and crushing operations. Because segregation is not well understood, attempts to suppress it or exploit it proceed on an ad hoc basis and are expensive.

In systems that do not involve much agitation of the grains, several mechanisms that involve gravity have been identified as leading to segregation. However, in highly agitated flows there is a mechanism independent of gravity that is available to drive segregation. This is associated with spatial gradients in the energy of the velocity fluctuations of the grains. Collisional interactions between and among different types of grains require that, in general, differences in their concentrations exist to balance differences in particle fluctuation energy.

This segregation mechanism is often masked by gravitational segregation mechanisms on Earth. It is expected to be of equal importance to gravitational segregation in the reduced gravity on Mars and to be the dominant mechanism for segregation on the Moon. It is the only mechanism for segregation in space.

The segregation of colliding particles of different size and mass will be studied on the International Space Station in an axisymmetric shear cell in which the flow is created by the relative motion of bumpy boundaries of a cylindrical annulus. The profile of particle agitation across the cell is controlled by employing boundaries with different bumpiness. The particle segregation is observed using digital video, image analysis, and sophisticated particle tracking algorithms. Two basic systems are to be examined: in one, the spheres are of equal size but differ in mass; in the other, they are of equal mass but differ in size. The observations will be compared to results of simulations and the predictions of theory to establish their respective limits and suggest possible improvements.

Studies of a segregation mechanism that is especially important in reduced gravity should benefit mining and materials-handling activities associated with in-situ resource utilization applications on Mars and the Moon. It should also assist in the interpretation of geologic deposits, particularly in low gravity. It will eventually benefit the design of manufacturing operations and in-space fabrication technologies in zero gravity in support of exploration.

BOILING HEAT TRANSFER MECHANISMS IN EARTH AND LOW GRAVITY: BOUNDARY CONDITION AND HEATER ASPECT RATIO EFFECTS

Jungho Kim
University of Maryland
Dept. of Mechanical Engineering
College Park, MD 20742

Boiling is a complex phenomenon where hydrodynamics, heat transfer, mass transfer, and interfacial phenomena are tightly interwoven. An understanding of boiling and critical heat flux in microgravity environments is of importance to space based hardware and processes such as heat exchange, cryogenic fuel storage and transportation, electronic cooling, and material processing due to the large amounts of heat that can be removed with relatively little increase in temperature. Although research in this area has been performed in the past four decades, the mechanisms by which heat is removed from surfaces in microgravity are still unclear. Recently, time and space resolved heat transfer data were obtained in both earth and low gravity environments using an array of microheaters varying in size between 100 microns to 700 microns. These heaters were operated in both constant temperature as well as constant heat flux mode.

Heat transfer under nucleating bubbles in earth gravity were directly measured using a microheater array with 100 μm resolution operated in constant temperature mode with low and high subcooled bulk liquid along with images from below and from the side. The individual bubble departure diameter and energy transfer were larger with low subcooling but the departure frequency increased at high subcooling, resulting in higher overall heat transfer. The bubble growth for both subcoolings was primarily due to energy transfer from the superheated liquid layer–relatively little was due to wall heat transfer during the bubble growth process. Oscillating bubbles and sliding bubbles were also observed in highly subcooled boiling. Transient conduction and/or microconvection was the dominant heat transfer mechanism in the above cases. A transient conduction model was developed and compared with the experimental data with good agreement.

Data was also obtained with the heater array operated in a constant heat flux mode and measuring the temperature distribution across the array during boiling. The instantaneous heat transfer into the substrate was numerically determined and subtracted from the supplied heat to obtain the wall to liquid heat flux. This data was then correlated with high speed (>1000Hz) visual recordings of the bubble growth and departure from the heater surface acquired through the bottom of the heater. The data indicated that microlayer evaporation and contact line heat transfer were not major heat transfer mechanisms for bubble growth, similar to the conclusions for constant wall temperature. The dominant heat transfer mechanism appeared to be transient conduction into the liquid as the liquid rewetted the wall during the bubble departure process.

Pool boiling heat transfer measurements from heaters of varying aspect ratio were obtained in low-g (0.01 g ±0.025 g) and high-g (1.7 g ±0.5 g) using the KC-135 aircraft. The heater aspect

ratio was varied by selectively powering arrays of heaters (2x2, 2x4, 2x6, 2x8, and 2x10) in a 10x10 heater array containing individual heaters 700x700 μm^2 in size. The liquid was degassed to an air concentration below 3 ppm by repeatedly pulling a vacuum on the vapor/gas above the liquid before measurements were made. The heat fluxes were generally observed to decrease as the heater aspect ratio increased. As the wall superheat increased, Marangoni convection appeared to increase and cause the large bubbles that formed on the heater to shrink, allowing liquid to rewet the surface, increasing the heat transfer. Why Marangoni convection was observed in what is essentially a fully degassed fluid is unclear, but may be due to contaminants or isomers within the fluid.

EXTRACORPOREAL SHOCK WAVE THERAPY AS A COUNTERMEASURE FOR BONE LOSS ON EARTH AND IN SPACE

Ulf R. Knothe
Department of Orthopaedic Surgery, Orthopaedic Research Center
The Cleveland Clinic Foundation

Ryan Berglund
Glickman Urological Institute,
The Cleveland Clinic Foundation

Jared O'Leary, Jennifer Ziegler, Melissa L. Knothe Tate
Department of Biomedical Engineering, Orthopaedic Research Center,
The Cleveland Clinic Foundation

INTRODUCTION

The purpose of this study is to apply extracorporeal shock waves in an ex vivo rat model with the intent to mimic naturally occurring microdamage that stimulates bone tissue to rebuild. Whereas a continued lack of physiological activity will result in disuse osteopenia, our working hypothesis is that prophylactic application of extracorporeal shock waves will cause microdamage in bone that will stimulate the remodeling, repair and renewal cascade.

METHODS

Extracorporeal shock waves were applied to the anterior surface of the femoral middiaphysis of the prone rat, using the Lithotriptor Modulith® SLX . Waves were applied toward the periosteal surface of the bone in the planar direction. One of six different regimes was applied; wave number and peak pressures were varied, e.g. 500, 1000 and 1500 waves at 43, 76 or 100 MPa. Tissues were explanted and fixed in ethanol prior to bulk staining with calcein blue and embedding in polymethylmethacrylate. Using commercially available image analysis software (OpenLab), the number and mean length of microcracks, observed under an epifluorescent microscope, was compared between the treated side and the contralateral control.

RESULTS

In six of nine experimental groups, more cracks were visible in femoral cross sections from the treated side. These differences were highly significant in the experimental group exposed to 1500 shocks, at all peak pressures, in the lower two peak pressure regimes in the group exposed to 1000 shocks and in the highest peak pressure regime in the group exposed to 500 shocks.. Furthermore, the mean microcrack length was comparable to that occurring in response to mechanical loading in physiological and fatigue studies.

DISCUSSION/CONCLUSION

This study proves the feasibility of using exogeneously produced microdamage in bone to mimic that occurring in vivo due to physiological loading and is a first step toward development of a prophylaxis for osteopenia. Currently we are applying the same protocols in an in vivo model to determine whether the presence of exogeneously produced microdamage triggers the remodeling cascade associated with maintenance of healthy bone tissue.

Corresponding author and contact information:
Ulf R. Knothe, M.D, Dr. Med.
Department of Orthopaedic Surgery, A41,
9500 Euclid Avenue
Cleveland Clinic Foundation
Cleveland, OH 44195

knotheu@ccf.org
216-445-6513 office
216-445-6255 fax

MOBI: MICROGRAVITY OBSERVATIONS OF BUBBLE INTERACTIONS

Donald L. Koch
Cornell University

Ashok Sangani
Syracuse University

One of the greatest uncertainties affecting the design of multiphase flow technologies for space exploration is the spatial distribution of phases that will arise in microgravity or reduced gravity. On Earth, buoyancy-driven motion predominates whereas the shearing of the bubble suspension controls its behavior in microgravity. We are conducting a series of ground-based experiments and a flight experiment spanning the full range of ratios of buoyancy to shear. These include: (1) bubbles rising in a quiescent liquid in a vertical channel; (2) weak shear flow induced by slightly inclining the channel; (3) moderate shear flow in a terrestrial vertical pipe flow; and (4) shearing of a bubble suspension in a cylindrical Couette cell in microgravity. We consider nearly monodisperse suspensions of 1 to 1.8 mm diameter bubbles in aqueous electrolyte solutions. The liquid velocity disturbance produced by bubbles in this size range can often be described using an inviscid analysis. Electrolytic solutions lead to hydrophilic repulsion forces that stabilize the bubble suspension without causing Marangoni stresses. We will discuss the mechanisms that control the flow behavior and phase distribution in the ground-based experiments and speculate on the factors that may influence the suspension flow and bubble volume fraction distribution in the flight experiment.

MICROFLUIDIC AND DIELECTRIC PROCESSING OF DNA

Ronald G. Larson, Lin Fang, Lei Li, Vijay Namasivayam, and Mark A. Burns

Department of Chemical Engineering, University of Michigan, Ann Arbor, MI 48109-2136, U.S.A.

ABSTRACT

The manipulation of DNA polymers for genomics, health monitoring, and other applications can be in principle be carried out in microfluidic devices. Using single-molecule experiments and Brownian dynamics simulations we have considered isolated DNA molecules near adsorbing and non-adsorbing walls in the presence of a simple shearing flow and in an evaporating droplet. We have also used electric fields to stretch DNA molecules and adhere them to surfaces, where we might eventually study their interactions with proteins, including proteins that repair or protect DNA from radiation or other damage.

As a test problem, we have chosen the flow in a drying water droplet resting on a substrate. Because of the pinned contact line, the droplet does not shrink its radius until the very last stages of drying, but instead shrinks its height. As a result, fluid that evaporates from the edge of the droplet must be replaced by fluid flowing to the edge from the droplet center [1]; see Fig. 1.

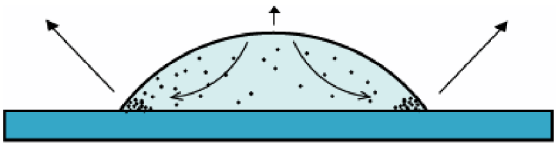

Figure 1. The flow in a drying droplet with pinned contact line.

This flow convects solute towards the droplet edge, where it deposits it in a ring [1], or "water spot," frequently seen on dishware that has been left to dry. The "coffee ring" effect can be used to advantage in genomics applications. Schwartz and coworkers have shown that the flow in a drying droplet can be used to stretch out and deposit DNA molecules onto a glass surface treated with 3-aminopropyltriethoxysilane (APTES) to make them strongly bind DNA molecules, which can then be subjected to a restriction enzyme digestion, and the length and relative positions of the fragments measured by simple fluorescence optical microscopy, using DNA stained by intercalating dyes.

We also studied a second flow, the torsional shearing flow produced by motor-driven rotation of a glass disc rotating about its axis above a parallel cover slip. In this simple shearing flow, Brownian dynamics simulations *in the absence of hydrodynamic interactions* predict that the molecules will become highly stretched as they become adsorbed irreversibly onto a surface [2]. Surprisingly, the observed stretch was much weaker than predicted, even weaker than that

observed in the droplet-drying flow. This reduced stretch was observed not only for DNA chains adsorbed to the surface, but also for chains in the fluid at distances from the surface less than around 1/3 the contour length L of the DNA molecules, which was around L = 21 microns for lambda-phage DNA and L = 67 microns for T2 DNA [3].

To investigate further the weak stretch of DNA molecules near surfaces in simple shearing flows, we chose another simple shearing flow, namely the pressure-driven channel flow. In this flow, as in torsional shearing flow, we found very weak stretch near the surface, and, moreover, found that the concentration of DNA molecules near the surface was depleted relative to that in the bulk, qualitatively in agreement with recent Brownian dynamics simulations of Jendrejack et al. [4], who included hydrodynamic interactions in their simulations. The hydrodynamic interactions therefore appear to induce migration of stretched DNA molecules from the surface. In this flow, as in torsional shearing flow, we found very weak stretch near the surface, and, moreover, found that the concentration of DNA molecules near the surface was depleted relative to that in the bulk, qualitatively in agreement with recent Brownian dynamics simulations of Jendrejack et al., who included hydrodynamic interactions in their simulations. The hydrodynamic interactions therefore appear to induce migration of stretched DNA molecules from the surface.

Given the imperfect stretch obtained in fluid flows, we have been investigating the use of AC electric fields to stretch DNA molecules. Following the work of Washizu et al., we used a microfabricated device to impose a high frequency, high gradient electric field onto stained DNA molecules, which responded by stretching and migrating to the nearest electrode. The stretching is greatly enhanced by the presence of an entangled polymer matrix for reasons that are still poorly understood (5).

REFERENCES

1. Deegan, R. D., Bakajin, O., Dupont, T. F., Huber, G., Nagel, S. R., Witten, T. A., *Nature* **389**, 827-829 (1997).
2. Chopra, M. and Larson, R.G., *J. Rheol.*, **46**, 831-862, (2002).
3. Lei, L., Hu, H., and Larson, R.G., *Rheol Acta*, submitted (2003).
4. Jendrejack, R.M., J.J. de Pablo, and M.D. Graham, J. Chem. Phys. **116**, 7752-7759 (2002).
5. Namasivayam, V. Larson, R.G., Burke, D.T., and Burns, M.A., Analytical Chem., **74**, 3378-3385 (2002).

SOLIDS INTERACTING WITH A GAS IN A MICROGRAVITY APPARATUS

Michel Y. Louge, PI
Sibley School of Mechanical and Aerospace Engineering
Cornell University, Ithaca, NY 14853

James T. Jenkins, CoI
Department of Theoretical and Applied Mechanics
Cornell University, Ithaca, NY 14853

The long-term human or robotic exploration of the Moon and Mars requires the exploitation of indigenous mineral and/or atmospheric resources. Technologies for In-Situ Resource Utilization (ISRU) must be developed for propellant production, habitat, infrastructure, extraction of water and breathable gas, etc.

Although a few of the required minerals are abundant (silicon, sulfur, iron, magnesium, aluminum), others are mainly present in trace amounts (sodium, potassium, chromium, titanium, He3, etc). Consequently, ISRU requires mining, transporting, processing, and separating massive quantities of solid materials.

On Earth, these activities have been carried out on a large scale for more than a century in the oil, chemical, pharmaceutical, mining, food, and infrastructure industries. However, because the basic principles governing the interactions of solids and gases are poorly understood, the design of reliable solids plants still involves three empirical steps: (1) process conception on the lab scale; (2) exhaustive tests in a pilot unit; and (3) operation of a demonstration plant.

Research in the lab answers basic questions of reactivity, contacting, grinding, particle-size-distribution, etc. The pilot unit then reveals practical challenges in scale-up, control, waste disposal, transport, start-up, safety, long-term reliability, wear, maintenance, filtration, product separation, etc. Finally, the demonstration plant showcases commercial viability of the process.

Technology development for ISRU must strike a different balance between empirical design and rational predictions than industrial activities on Earth. While for example new gas-solid processes can be tested on the KC-135, it is more difficult to realistically mimic conditions of reduced gravity at the pilot scale. Thus, ISRU development must also rely on simulations and theory to understand the cost of scale-up.

In computer simulations, solids are followed as discrete entities. Here, the challenge is to model accurately the interactions with the surrounding gas and the collisions amongst particles.

Theories, on the other hand, derive a set of differential equations, usually treating the gas and solid phases as inter-penetrating continua. Neither method should be used blindly for design.

A weakness of simulations is that they simplify interactions to be tractable. A limitation of theories is that basic constitutive laws, drag relations and boundary conditions are not well established, mainly because practical gas-solid suspensions are dense, agitated, inhomogeneous and unstable. For example, in large facilities, solids form clusters that degrade performance. Thus it is harder to scale-up a process involving solids than it is to do so with a single fluid.

Encouragingly, direct numerical simulations (e.g., lattice-Boltzmann) have begun to inform basic gas-solid interactions. However, they must first be tested against well-controlled experiments before using them in reliable process design.

In this context, our main objective is to produce an experimental benchmark for theories and simulations. To do so, the SiGMA flight hardware uses an axisymmetric shearing cell that is shared with other experiments. Unlike experiments such as fluidized beds where the gas velocity must be large enough to defeat particle weight, microgravity will permit us to control independently particle agitation and gas flow.

So far, we have used theories and simulations to design the experiment; we have tested a prototype on the ground and on the KC-135; and the NASA-Glenn team has made progress designing the SiGMA flight hardware. Developers of realistic simulations and theories await our results.

In the talk, we will illustrate the convenience of a long-lasting microgravity environment for studying flows of granular materials with and without gas interaction. We consider collisional granular flows of nearly elastic spheres featuring a single constituent or binary mixtures in various bounded geometries. We review the equations of the kinetic theory for the conservation of mass, momentum, fluctuation energy and species concentration. We illustrate their solutions for shear flows in rectilinear or axisymmetric rectangular channels with or without a body force. We show that proper boundary conditions yield numerical solutions in good agreement with molecular dynamical simulations and with data from physical experiments carried out in microgravity.

Rotating Reverse Osmosis for Wastewater Reuse

Richard M. Lueptow*, Yeomin Yoon, Cynthia Pederson

Department of Mechanical Engineering, Northwestern University, 2145 Sheridan Road, Evanston, IL, 60208, USA

*Email: r-lueptow@northwestern.edu, Telephone: 1-847-491-4265, Fax: 1-847-491-3915

Background: Reverse osmosis (RO) has long been in use as a physical membrane separation technology, and it may be useful for wastewater reuse for long-term space missions. However, concentration polarization decreases the flux of solvent through the membrane and the rejection of contaminants as a result of an increase in the solute concentration near the membrane surface. Urea, sodium chloride, and detergent (Geropon TC-42) are major contaminants in spacecraft wastewater. In addition, numerous organic contaminants such as 2-(2-butoxyethoxy) ethanol, caprolactam, 2-propanol, formaldehyde, and methanol have also been found at low concentrations in condensate collected from the cabin of the spacecraft. As the length of space missions increases and wastewater is reclaimed for use as potable water, it is necessary to remove all of these contaminants.

Objectives: Our previous work established the concept of a low-pressure rotating reverse osmosis membrane system. The rotation of the cylindrical RO filter produces shear and Taylor vortices in the annulus of the device that decrease the concentration polarization and fouling commonly seen with conventional RO filtration techniques. A mathematical model based on the film theory and the solution-diffusion model agrees well with the experimental results obtained using this first generation prototype. However, based on the model, the filtrate flux and contaminant rejection depend strongly on the transmembrane pressure. Therefore, the goal of our current work is to improve the flux of the device by increasing the transmembrane pressure by a factor of 3 to 4. In addition, the rejections for a wider variety of inorganic and organic compounds typically found in space mission wastewater are measured.

Rejection of Target Contaminants by Selected Membranes: Flat sheet samples of commercially available reverse osmosis, low pressure RO (LPRO), and nanofiltration (NF) membranes have been tested using a dead-end stirred-cell to remove conventional wastewater contaminants (sodium chloride, urea, and ammonium carbonate) and organic contaminants found in spacecraft condensate. By combining experimental rejection results for various compounds with a model based on the size and electrostatic exclusion properties of the membranes, the pore sizes of the membranes are estimated to be 0.33 nm for RO, 0.34 nm for LPRO, and 0.44 nm for NF membranes. The rejections for both organic and inorganic compounds for these membranes are shown in Figure 1. The rejections of 2-(2-butoxyethoxy) ethanol (BEE) and caprolactam are approximately 80% for the RO and LPRO membranes, because their molecular weights/molecular radii, 162 Da/0.32 nm for BEE and 113 Da/0.28 nm for caprolactam, are large enough to be rejected due to size exclusion. The rejection of these compounds is also relatively high (over 60 %) for the NF membrane. The rejection of ionic compounds is also high (over 80 %) for all membranes due to electrostatic exclusion effects. The rejection of 2-propanol is lower than that of NaCl even though these compounds have similar molecular weights due to electrostatic exclusion of the ionic compound. Urea, formaldehyde, and methanol rejections are quite low because the molecules are small and uncharged. As a result, they are difficult to reject

by size exclusion or by electrostatic exclusion. Furthermore, the rejection of urea is substantially lower than 2-propanol even though they have the same molecular weight of 60.1 Da. This is because the molecular radius of urea (0.18 nm) is smaller than that of 2-propanol (0.26 nm).

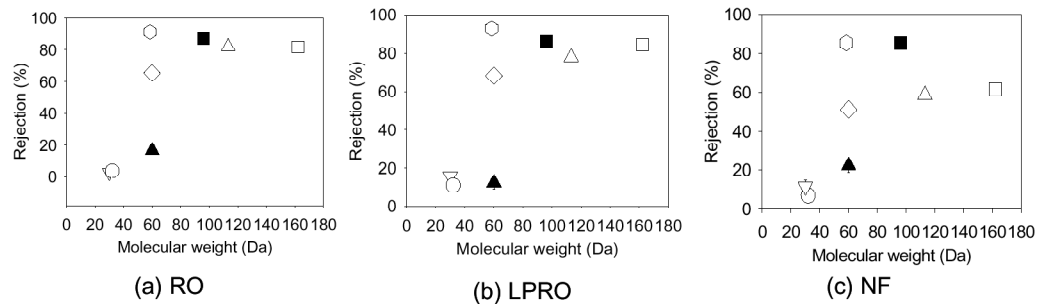

Figure 1. Rejection of different compounds for RO, LPRO, and NF. Operating conditions: • P=800 kPa; stirring speed=400 rpm; feed concentration=1 mM; recovery=60 %. (a) RO (AK), (b) LPRO (ESPA), and (c) NF (ESNA) (• ; urea; • ; ammonium carbonate; ⬡, sodium chloride; • ; methanol; • ; 2-(2-butoxyethoxy) ethanol; • ; caprolactam; • ; formaldehyde; • ; 2-propanol).

Rotating Reverse Osmosis: A second generation rotating reverse osmosis system has been designed and fabricated to function at a much higher transmembrane pressure than the original system. The new device operates at 500 psi (3450 kPa) compared to the first generation prototype that operated at 150 psi (1035 kPa). The second generation prototype and fluid circuit (Figure 2a) have also been designed so that testing can be conducted for much longer time periods: tests lasting 4 weeks or more compared to a maximum of a 6-hour test conducted with the first-generation prototype.

Preliminary three day tests exhibit high flux (Figure 2b) and high rejection (over 70 % for NaCl, 80 % for $(NH_4)_2CO_3$, 97 % for detergent) for the duration of the experiment while maintaining a high recovery ranging from 75 to 90 %. This recovery is significantly higher than the average of recovery of 25 % for typical spiral wound RO systems, a property that is particular advantageous for maximum water recovery. The second generation device exhibits a flux four times greater than that of the first generation prototype primarily due to the higher operating pressure. These experiments are the first step in the validation of rotating reverse osmosis at high transmembrane pressures over long time periods.

(a)

(b)

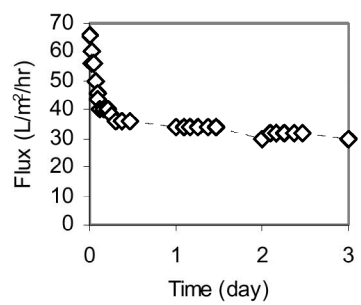

Figure 2. (a) Photograph of second generation rotating reverse osmosis filter and fluid circuit and (b) Flux as a function of time for a 3 day experiment. Operating conditions: LPRO (ESPA); • P=500 psi; rotation rate=90 rpm; recovery=75 to 90 %; wastewater composed of NaCl (1,000 mg/L), $(NH_4)_2CO_3$ (3,429 mg/L), and detergent (2,000 mg/L).

Funded by NASA.

PAST, PRESENT AND FUTURE ADVANCED ECLS SYSTEMS FOR HUMAN EXPLORATION OF SPACE

Kenny Mitchell
MSFC Manager for Advanced ECLSS/New Space Exploration Initiative

This paper will review the historical record of NASA's regenerative life support systems flight hardware with emphasis on the complexity of spiral development of technology as related to the International Space Station program. A brief summary of what constitutes ECLSS designs for human habitation will be included and will provide illustrations of the complex system/system integration issues. The new technology areas which need to be addressed in our future Code T initiatives will be highlighted. The development status of the current regenerative ECLSS for Space Station will be provided for the Oxygen Generation System and the Water Recovery System. In addition, the NASA is planning to augment the existing ISS capability with a new technology development effort by Code U/Code T for CO2 reduction (Sabatier Reactor). This latest ISS spiral development activity will be highlighted in this paper.

FIXED PACKED BED REACTORS IN REDUCED GRAVITY

Brian J. Motil
NASA Glenn Research Center
Cleveland, OH 44135

Vemuri Balakotaiah
Department of Chemical Engineering
University of Houston
Houston, TX 77204

Yasuhiro Kamotani
Department of Mechanical and Aerospace Engineering,
Case Western Reserve University
Cleveland, OH

Mark J. McCready
Department of Chemical Engineering
University of Notre Dame
Notre Dame, IN

We present experimental data on flow pattern transitions, pressure drop and flow characteristics for cocurrent gas-liquid flow through packed columns in microgravity. The flow pattern transition data indicates that the pulse flow regime exists over a wider range of gas and liquid flow rates under microgravity conditions compared to 1-g and the widely used Talmor map in 1-g is not applicable for predicting the transition boundaries. A new transition criterion between bubble and pulse flow in microgravity is proposed and tested using the data. Since there is no static head in microgravity, the pressure drop measured is the true frictional pressure drop. The pressure drop data, which has much smaller scatter than most reported 1-g data clearly shows that capillary effects can enhance the pressure drop (especially in the bubble flow regime) as much as 200% compared to that predicted by the single phase Ergun equation. The pressure drop data are correlated in terms of a two-phase friction factor and its dependence on the gas and liquid Reynolds numbers and the Suratman number. The influence of gravity on the pulse amplitude and frequency is also discussed and compared to that under normal gravity conditions.

Experimental work is planned to determine the gas-liquid and liquid-solid mass transfer coefficients. Because of enhanced interfacial effects, we expect the gas-liquid transfer coefficients k_La and k_Ga (where a is the gas-liquid interfacial area) to be higher in microgravity than in normal gravity at the same flow conditions. This will be verified by gas absorption experiments, with and without reaction in the liquid phase, using oxygen, carbon dioxide, water and dilute aqueous amine solutions. The liquid-solid mass transfer coefficient will also be determined in the bubble as well as the pulse flow regimes using solid benzoic acid particles in the packing and measuring their rate of dissolution. The mass transfer coefficients in microgravity will be compared to those in normal gravity cocurrent flow to determine the mass transfer enhancement and propose new mass transfer correlations for two-phase gas-liquid flows through packed beds in microgravity.

CONSTRAINED VAPOR BUBBLE

Joel L. Plawsky and Peter C. Wayner, Jr.
Isermann Department of Chemical and Biological Engineering
Rensselaer Polytechnic Institute
Troy, NY 12180

The use of interfacial free energy gradients to control liquid and vapor flows naturally leads to simpler and lighter change-of-phase heat transfer systems because of the absence of mechanical pumps. These "passive" engineering (PE) systems are ideal candidates for the thermal control of spacecraft. The non-isothermal constrained vapor bubble (CVB) is a generic PE system without porous material. A common example is a heat pipe without porous material. The particular CVB system being studied is in the shape of a heat pipe fin.

The dynamic thermophysical principles underlying these heat transfer systems, especially under equivalent microgravity conditions, are not well understood and its uses have not been optimized. Within this project, the CVB is being studied under both earth and microgravity flight conditions to remedy this undesirable situation. The study is multi-faceted: 1) it is a study of a passive heat exchanger; 2) it is a basic engineering study of thermal transport; and 3) it is a basic scientific study of interfacial phenomena, physics and thermodynamics. Although the basic engineering Facets (1) and (2) are emphasized for heat exchanger development, the research is also naturally a basic scientific study in interfacial phenomena, microgravity physics and thermodynamics.

The body force field for fluid flow is a function of the shape dependent pressure field, temperature field, composition field and the equivalent microgravity conditions of the system. We propose that relatively large systems (millimeter compared to micro) with regions of small pressure gradients are needed for both optimum performance (high heat fluxes) and convenient experimental study. Therefore, in this project, relatively large systems with high heat fluxes and small capillary pressure levels set in the condenser are emphasized. However, these large systems are easily distorted by the earth's gravitational field where they are inefficient. "Axisymmetric" systems with small Bond numbers are needed to optimize performance. The term axisymmetric is used herein to mean reflective symmetry with respect to the length axis of the CVB. Due to the sensitivity of systems of this size to gravity and to small temperature and pressure gradients, these thermal control systems need to be studied in the microgravitational environment of intended use.

The use of a transparent quartz cell and related optical techniques increase the understanding of the observed transport processes because the PE system is viewed directly. Based on the augmented Young-Laplace model, the pressure gradient field is obtained using interferometry to measure the liquid thickness profile. The temperature field is obtained using external thermal sensors and the measured vapor pressure in the cell. The Kelvin-Clapeyron model relates the heat flux to the temperature and pressure fields. Using earth-based studies, experimental techniques are being developed with polar and apolar fluids in a quartz cuvette with a square cross-section [inside dimensions of 3x3x40mm]. Under contract with NASA Glenn, Northrop-Grumman is using these results to build a CVB heat exchanger for studies in the Fluids Integrated Rack section of the International Space Station using the Light Microscopy Module. Results obtained under Earth and Space Station conditions will be analyzed and compared.

The *macroscopic* objectives are to determine the stability, the fluid flow characteristics, the average heat transfer coefficient in the evaporator, and the overall heat conductance of the CVB as a function of the heat flow rate and vapor volume. The *microscopic* objective is to determine the detail characteristics of

the transport processes in the curved liquid film, which has the shape of an extended meniscus with regions where both the capillary and disjoining pressure are important. The local conditions under which cavitation and instability occur with the formation of a dry region will be determined as a function of heat flux, film thickness and stress.

To date, stable and oscillating regions of evaporation or condensation using pentane, 2-propanol, n-butanol, ethanol, and fluorocarbons have been experimentally studied in the earth's gravitational field and analyzed. The film thickness profiles were obtained using the Image Analyzing Interferometric (IAI) technique developed in our laboratory with improved analytical procedures. The spreading coefficients, the Hamaker constants, and the contact angles were determined as a function of heat flow rate conditions and related using free energy principles. For example, the pentane/quartz system is a simple completely wetting apolar system during evaporation and condensation. Whereas, the polar 2-propanal/quartz system was found to be partially wetting during low heat flux dropwise condensation. A flat adsorbed film of 2-propanol, approximately 6 nm thick, was found to be unstable during film condensation and convert to dropwise condensation. However, due to flooding, this system can also be completely wetting during condensation at high heat fluxes. Publications reporting on these and other results are available.

DNA Configurations in the Flow Through Arrays with Application to Biosensors

Eric S.G. Shaqfeh, Victor Beck
Department of Chemical Engineering,
Stanford University, Stanford CA 94305-5025

Nerayo Teclemeriam, Susan J. Muller
Department of Chemical Engineering,
University of California, Berkeley, CA 94720-1462

The miniaturization of lab analysis via microfluidics now allows one to consider designing devices for the manipulation of individual molecules. Manipulation of DNA in microfluidic devices has now received an enormous attention in this context, primarily through sieving and sorting applications. However, new results in flow suggest that reactions in flow including concatenation or hybridization may be many times faster than under equilibrium conditions and thus flow can be used ton control the access to the chain for any number of sequence specific linkers. Such an scheme could form the basis for a sensor for DNA damage either for military or space applications. At the heart of this the molecule to a significant fraction of its extensibility, keep it stretched to allow hybridization to linker groups, and then sieve any unlinked species from the mixture for analysis of hybridization downstream. Engineering of such a sensor is most efficiently done if large scale simulation of DNA in flow is used as an engineering tool to narrow the possible designs. A suggested device design is shown below .

Figure 1. Schematic for single molecule sequencing microdevice.

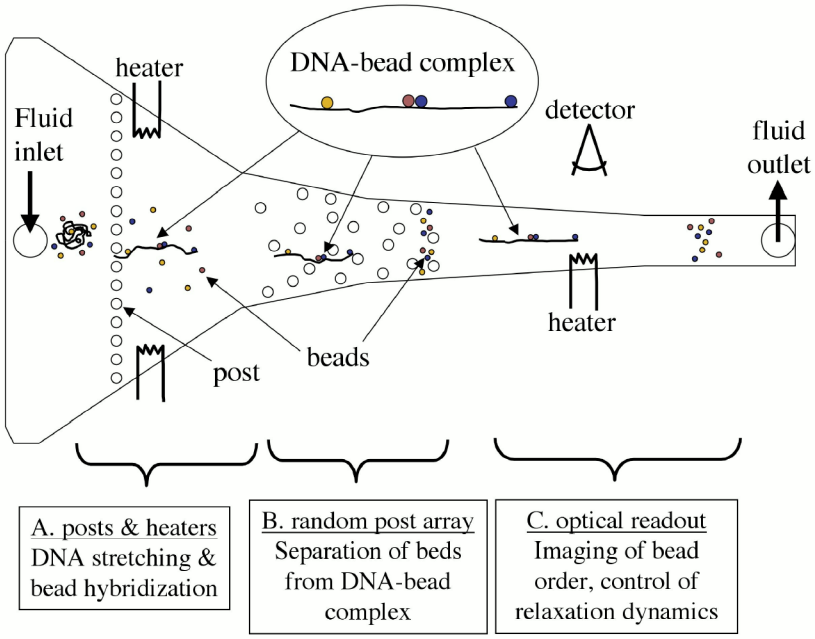

Stretching and sieving of DNA in the microdevice above involves understanding DNA configurations in the flow through post arrays of various concentrations, arrangements, and sizes. We review the large scale numerical simulation of DNA in flow through post arrays with a focus on the applications associated with the development of this biosensor including answering the following questions:

1) How does pressure driven flow differ from electrophoresis through an array?
2) Are there optimal arrangements and optimal post sizes for each in order to achieve stretch and separation?

We then demonstrate how such simulation can guide design of such a device and make preliminary comparison to experiments regarding the configuration distributions in the flow though fabricated post arrays.

MICROMINIATURE MONITOR FOR VITAL ELECTROLYTE AND METABOLITE LEVELS OF ASTRONAUTS

Koji Tohda and Miklos Gratzl

Ions, such as proton (pH) and potassium, play a crucial role in body fluids to maintain proper basic functioning of cells and tissues. Metabolites, such as glucose, control the energy available to the entire human body in normal as well as stress situations, and before, during, and after meals. These molecules diffuse easily between blood in the capillaries and the interstitial fluid residing between cells and tissues. We have developed an approach to monitoring of critical ions (called electrolytes) and glucose in the interstitial fluid under the human skin. Proton and potassium levels sensed using optode technology that translates the respective ionic concentrations into variable colors of corresponding ionophore/dye/polymeric liquid membranes. Glucose is monitored indirectly, by coupling through immobilized glucose oxidase with local pH that is then detected using a similar color scheme. The monitor consists of a tiny plastic bar, 100-200 µm wide and 1-2 mm long, placed just under the skin, with color changing spots for each analyte as well as blanks. The colors are read and translated into concentration values by a CCD camera. Direct optical coupling between the in vivo sensing bar and the ex vivo detector device requires no power, and thus eliminates the need for wires or optical fibers crossing the skin. The microminiature bar penetrates the skin easily and painlessly, so that astronauts could insert it themselves. The approach is fully compatible with telemetry in space, and thus, in vivo clinical data will be available real time in the Earth based command center once the device is fully developed. The information provided can be used for collecting hitherto unavailable vital data on clinical effects of space travel. Managing clinical emergencies in space with the sensor already in place should also become much more efficient than without a continuous monitor, as is currently the case. Civilian applications may include better glucose control of patients with moderate to sever diabetes: a growing health problem in the US and World-wide.

BIOPHOTONICS AND BONE BIOLOGY

Gregory Zimmerli and David Fischer
NASA Glenn Research Center, Cleveland, OH

Marius Asipauskas, Chirag Chauhan, Nicole Compitello, and Jamie Burke
National Center for Microgravity Research, Cleveland, OH

Melissa Knothe Tate
Cleveland Clinic Foundation, Lerner Research Institute, Cleveland, OH

One of the more-serious side effects of extended space flight is an accelerated bone loss [Bioastronautics Critical Path Roadmap, http://research.hq.nasa.gov/code_u/bcpr/index.cfm]. Rates of bone loss are highest in the weight-bearing bones of the hip and spine regions, and the average rate of bone loss as measured by bone mineral density measurements is around 1.2% per month for persons in a microgravity environment [T. Lang et al., *JBMR* 2004]. Figure 1 shows that an extrapolation of the microgravity-induced bone loss rates to longer time scales, such as a 2.5 year round-trip to Mars (6 months out at 0 g, 1.5 year stay on Mars at 0.38 g, 6 months back at 0 g), could severely compromise the skeletal system of such a person.

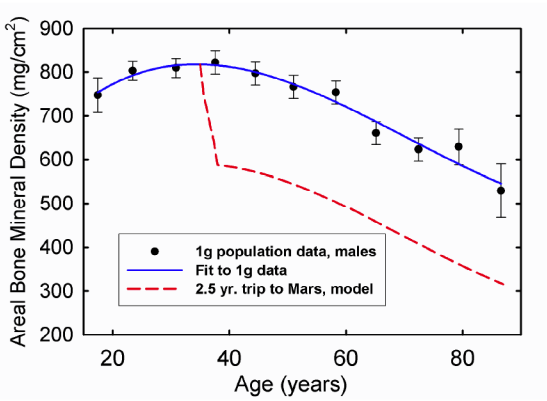

Figure 1. Age-related bone loss in a 1g population of males (data from Atlas of Clinical Endocrinology: Osteoporosis, 2003) compared to a hypothetical person exposed to microgravity and partial gravity during a 2.5 year Mars trip. The model assumes a linear response of bone loss with g-level, and does not account for the possibility of new bone growth upon returning to 1 g, as no data yet exists for such an effect.

It is well known that bone remodeling responds to mechanical forces. We are developing two-photon microscopy techniques to study bone tissue and bone cell cultures to better understand the fundamental response mechanism in bone remodeling. Osteoblast and osteoclast cell cultures are being studied, and the goal is to use molecular biology techniques in conjunction with Fluorescence Lifetime Imaging Microscopy (FLIM) to study the physiology of in-vitro cell cultures in response to various stimuli, such as fluid flow induced shear stress and mechanical stress. We have constructed a two-photon fluorescence microscope for these studies, and are currently incorporating FLIM detection. Current progress will be reviewed. This work is supported by the NASA John Glenn Biomedical Engineering Consortium.

Contact: Gregory.A.Zimmerli@nasa.gov
NASA GRC, 21000 Brookpark Road, MS 110-3, Cleveland, OH 44135

Poster Session

The Fluid Mechanics of Liquid Jet Impingement: the hydraulic jump in microgravity

C. T. Avedisian[1], S. Chandra[2] and J. Mostaghimi[2]
[1]Cornell University
[2]University of Toronto

Introduction

Liquid jet impingement is an important process for thermal management to dissipate very high heat fluxes [1] and for coating solid surfaces with a liquid (e.g., applying thin films on paper to produce a high-gloss finish). Rapid cooling is achieved by taking advantage of the high liquid velocity in the thin film flowing away from the stagnation point. If a hydraulic jump forms (figure 1a for a circular hydraulic jump) the physical extent of cooling, or uniformity of a film coating, degrades because the film thickness increases substantially downstream of the jump. The discovery of steady noncircular jump shapes in normal gravity experimentation ([2-4]; figure 1b illustrates an example at G=1 for polygonal jumps) shows unusual patterns in the flow near to the jump boundary and downstream of it (figure 1c [3] which shows fluid ejection at the corners) that are poorly understood, yet which could hold some promise for heat transfer.

This project is the first phase of an anticipated two-part effort to understand the mechanisms of heat transfer from impinging liquid jets at reduced gravity. The first part focuses on the fluid mechanics of isothermal flows and the conditions under which hydraulic jumps form. An emphasis is on the formation of noncircular jumps and the conditions and flow patterns associated with them at reduced gravity. As we have just begun the research in 2004, we describe briefly some of the objectives and methods we will pursue during the first phase.

Objectives

The overall objectives of this phase are to examine the fluid dynamics of hydraulic jumps of various shapes at normal and reduced gravity. The following aspects will be addressed: response time of the fluid to changes in the jump position due to a sudden reduction of gravity; flow conditions that polygonal jumps will form; stability of polygonal jumps in microgravity; change (if any) of jump shape after the transition to G<<1 (where $G=g/g_o$ and $g_o=9.8 m/s^2$); effect of a sudden change from G=1 to G<<1 on the curvature of the free surface across a polygonal jump; downstream flow pattern and possible jetting in the corners of polygonal jumps. The work includes a combination of experiment, direct numerical simulation (DNS) and theoretical modeling.

Noncircular jumps have thus far been observed for flows in which a toroidal vortex exists just behind the jump (schematically illustrated in figure 2a). The vortex shows the presence of a tangential velocity component in the roller which can distort the circular symmetry and lead to steady jumps of noncircular shape. Thus far, polygonal jumps have been observed at G=1 for ethylene glycol (which has a viscosity about ten times larger than water) while water tends to produce circular jumps.

Gravity's influence on the jump will be investigated experimentally by determining how a hydraulic jump (of whatever shape) responds to a sudden change to low gravity. For circular jumps the transition zone across a hydraulic jump is much more gradual in microgravity than normal gravity and the jump radius is larger. Figure 2b [5] shows how a circular hydraulic jump transitions from normal to microgravity. The increase in jump radius (r_j) as gravity is lowered (figure 2c) is a consequence of the Froude number increasing from G=1 to G<<1. There are no companion observations for noncircular jumps.

Plan of Research

The DNS portion of the research will be carried out to predict the jump shape, radial position of the jump, the flow pattern downstream of the jump, and the evolution of these quantities due to a sudden transition of the flow from G=1 to G<<1. The computations will be carried out using a 3-D Eulerian structured grid. Free surface and shape deformations will be tracked using the volume-of-fluid (VOF) algorithm [6]. The grid will be fixed so that mesh variations have to be analyzed to ensure that gradients are accurately captured and with a reasonable computational time.

We did some preliminary coding assuming G=1 for a 8m/s water jet created by a 0.45mm diameter tube (Reynolds number of 227) impinging onto a dry surface (in the experiments the target surface will be submerged to a controlled depth so that the downstream fluid height is known). Since the surface was initially dry in this simulation, a hydraulic jump does not form. The DNS was started when the jet just touched the surface and the subsequent evolution of the spreading liquid along the surface was tracked. We chose a fixed 3D grid of 768,000 points (160x160x30) structured in a rectangular fashion. This appeared like a sufficiently dense grid to give a useful result. Figure 3 is a computed snapshot of the flow 0.7ms after the jet contacted the solid surface. The simulation shows details of the liquid film break-up into droplets at the rim. A jump does not form since, as noted previously, the plate was initially dry.

The DNS will be coded for a submerged plate to match the experiments. A tangential velocity component will be assumed for the rim of the jet just as it contacts the surface. Growth/decay of the velocity should determine the jump stability, for example producing a circular jump if the tangential component decays. This general approach of perturbing the velocity has been effective for simulating instabilities in liquid droplet impingement [7,8].

For the experiments, a flow loop will be constructed for a drop tower. The general experimental methodology will be to first establish a jump at G=1 - either circular or noncircular – and to use digital photography to record the jump shape, position and flow pattern as G is suddenly reduced. This situation should be suitable for drop towers with their limited experimental run time, in that prior work [5] showed that steady (circular) jumps are created within 400ms of transitioning from normal to microgravity within drop towers. The output of the experimental phase will be photographs from which physical dimensions of the impingement process will be extracted. These include the jump shape and physical size. The data will be compared with the output of the DNS.

References

1. Liu, X. and Lienhard, J.H. 1993a J. Heat Transf. 115, 472.
2. Ellegaard, C., Hanse, A.E., Haaning, A, Hansen, K., Marcussen, A., Bohr, T., Hansen, J.L. and Watanabe, S. 1999 Nonlinearity 12, 1-7.
3. Ellegaard, C., Hansen, A.E., Haaning, A. and Bohr, T. 1996 Physicq Scripta, T67, 105.
4. Ellegaard, C., Hanse, A.E., Haaning, A, Hansen, K., Marcussen, A., Bohr, T., Hansen, J.L. and Watanabe, S. 1998 Nature, 392, 767.
5. Avedisian, C.T. and Zhao, Z. 2000 Proc. R. Soc. Lond. A, 456, 2127-2151.
6. Hirt, C.W. and B. D. Nichols 1981 Journal of Computational Physics 39, 201-225
7. Bussmann, M., J. Mostaghimi and S. Chandra 1999 Physics of Fluids 11, 1406-1417.
8. Bussmann, M, S. Chandra and J. Mostaghimi 2000 Physics of Fluids 12, 3121-3132.

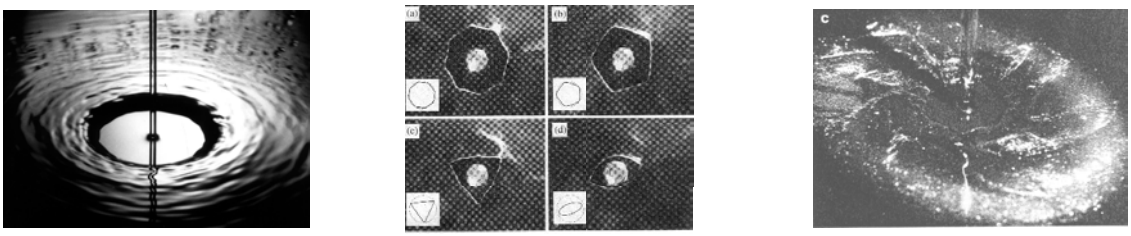

a) b) c)

Figure 1: a) circular hydraulic jump for water; b) polygonal jumps for ethylene glycol [2]; c) downstream flow pattern for a 6-sided polygon [3].

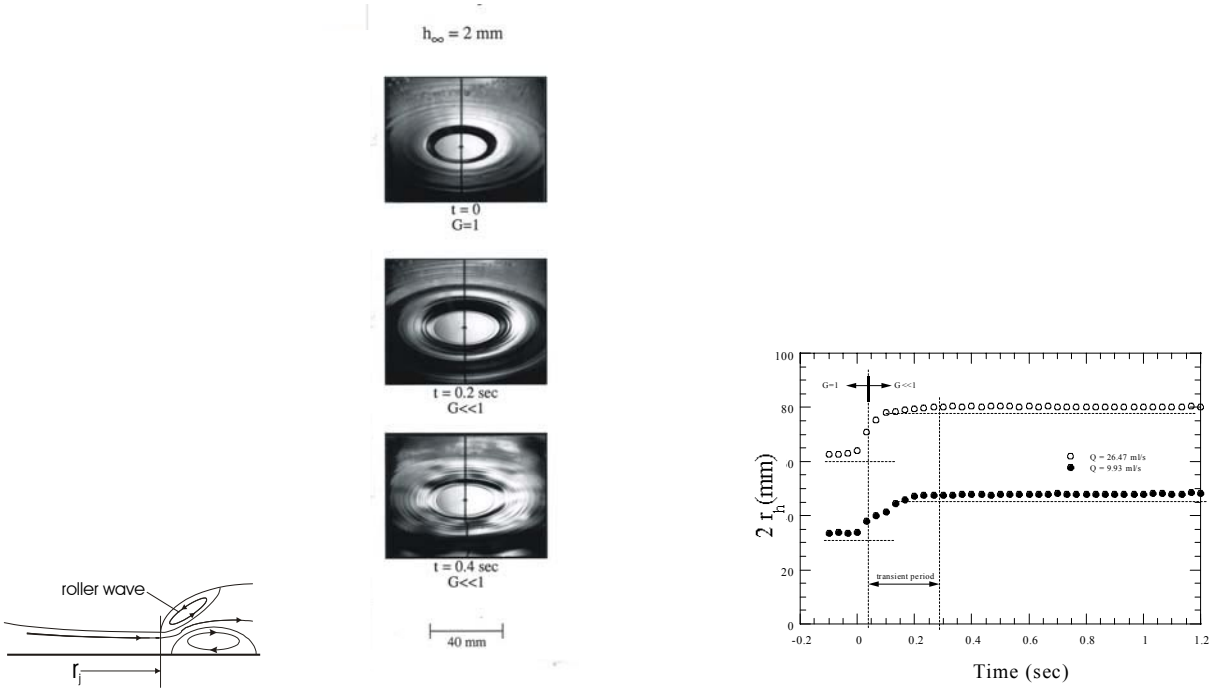

a) b) c)

Figure 2: a) hydraulic jump showing surface rollers; b) water jump during transition from normal (G=1) to microgravity (G<<1); c) measurements of the circular jump radius during transition from normal to microgravity.

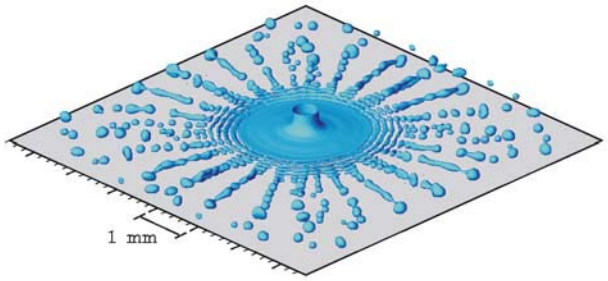

l

Figure 3: Simulation of the impact of a 0.45 mm diameter water jet with a velocity of 8 m/s on a flat surface 0.70ms after the jet contacts the surface. For the imposed boundary conditions, the liquid film becomes unstable and breaks up into droplets and a hydraulic jump does not form.

EFFECT OF MICROGRAVITY ON MAMMALIAN LYMPHOCYTES.

H.Banerjee,M.Blackshear,K.Mahaffey,C.Knight.A.A.Khan
Dept.of Biology,
Elizabethcity State University,
Elizabethcity,
NC-27909.
And L.Delucas,CBSE,University of Alabama at Birmingham,
Birmingham-35294

The effect of microgravity on mammalian system is an important and interesting topic for scientific investigation, since NASA's objective is to send manned flights to planets like Mars and eventual human colonization.The Astronauts will be exposed to microgravity environment for a long duration of time during these flights.Our objective of research is to conduct in vitro studies for the effect of microgravity on mammalian immune system.We did our preliminary investigations by exposing mammalian lymphocytes to a microgravity simulator cell bioreactor designed by NASA and manufactured at Synthecon Inc (USA).Our initial results showed no significant change in cytokine expression in these cells for a time period of forty eight hours exposure.Our future experiments will involve exposure for a longer period of time.

INTRODUCTION

During space flight the function of the immune system changes significantly. Several papers reported that postflight the number and the proportion of circulating lymphocytes in astronauts are modified (Uchakin et.al 2002), the in vitro mitogen induced T cell activation is depressed (Cogoli et al. 2002 Konstantinova et al. 1993) and there are detectable differences in cytokine production . Lymphocytes as well (Chapes et al. 1992). One of the possible modifying forces is the microgravity condition itself. Our aim was to analyse mechanisms responsible for changing lymphocyte functions in low gravity environment. For terrestrial simulation of microgravity we used a Rotary Cell Culture System (RCCS) developed by NASA.

In this experiment we exposed mouse B Lymphocyte cells to microgravity conditions and then analyzed the cells for cytokine expression.We exposed the cells to different time periods,however,our initial results failed to show any significant changes in cytokine expression under microgravity conditions.

MATERIALS AND METHOD

Mouse B Lymphocyte cells were purchased from ATCC,VA,USA and cultured in L-15 medium at 37°C in a cell culture incubator. Cells were exposed to microgravity conditions in a Rotary Cell Culture System (RCCS) developed by NASA for 24 hours,48 hours and 72 hours with proper control. After exposure cells were collected, lysed by antigen lysis buffer and cytokine expression(TGF-beta1 and IL-6) was determined by standard ELISA technique according to manufacturers instructions.

RESULTS

No significant changes in any cytokine expression tested was found during that particular exposure period under microgravity simulations.

DISCUSSION

Several attempts have been made to investigate the effects of microgravity on the growth and function of animal cells. Cellular activation of immune T lymphocytes is greatly affected by microgravity. On the other hand, little is known about the effects of microgravity on B lymphocytes.Thus,we attempted to study the effect of microgravity simulation on mouse B lymphocytes.

Our current experiment did not show any significant change in cytokine expression in microgravity exposed immune cells.We look forward to do experiments with longer exposure time,since astronauts are exposed to microgravity conditions for months and years.Several researchers have reported alteration of the immune system due to microgravity conditions(Uchakin et.al 2002). However, we did not notice any significant change in cytokine expression in any of our experiments done for shorter intervals of time ie,24 hours ,48 hours and 72 hours.

ACKNOWLEDGEMENT

This research is supported by NIH-EARDA Grant,NASA/ONR grant#NAG 5-1254 and NSF-EPSCOR University of Alabama subcontract# DTD42501.We are very grateful to Mr.James Harrington of NASA for his continous support.

BIBLIOGRAPHY

1) Meloni MA, Galleri G, Carta S, Negri R, Costanzo G, De Sanctis V, Cogoli A, Pippia P. Preliminary study of gene expression levels in human T-cells exposed to cosmic radiations.J Gravit Physiol. 2002 Jul;9(1):P291-2.

2) Chapes SK, Simske SJ, Forsman AD, Bateman TA, Zimmerman RJ.Effects of space flight and IGF-1 on immune function.Adv Space Res. 1999;23(12):1955-64.

3) Cogoli A. From cell biology to biotechnology in space. Korean J Biol Sci. 2000 Sep;4(3):195-200.

4) Konstantinova NA, Matveeva NA, Sirko IV, Firsov NN. The influence of cryoglobulins on the temperature-dependent erythrocyte backscattering nephelometry.Clin Hemorheol Microcirc. 2004;30(1):25-32.

5)Uchakin PN, Tobin BW, Morukov BV, Larina IV, Cubbage ML.Type 1 vs. type 2 cytokine secretion in vitro and its regulation by hydrocortisone in humans subjected to 120-day anti-orthostatic bed-rest regime.J Gravit Physiol. 2002 Dec;9(2):71-82.

TRANSITION FROM FORWARD SMOLDERING TO FLAMING IN SMALL POLYURETHANE FOAM SAMPLES

A. Bar-Ilan, O. Putzeys, G. Rein, and A.C. Fernandez-Pello

Experimental observations are presented of the effect of the flow velocity and oxygen concentration, and of a thermal radiant flux, on the transition from smoldering to flaming in forward smoldering of small samples of polyurethane foam with a gas/solid interface. The experiments are part of a project studying the transition from smolder to flaming under conditions encountered in spacecraft facilities, i.e., microgravity, low velocity variable oxygen concentration flows. Because the microgravity experiments are planned for the International Space Station, the foam samples had to be limited in size for safety and launch mass reasons. The feasible sample size is too small for smolder to self propagate because of heat losses to the surrounding environment. Thus, the smolder propagation and the transition to flaming had to be assisted by reducing the heat losses to the surroundings and increasing the oxygen concentration. The experiments are conducted with small parallelepiped samples vertically placed in a wind tunnel. Three of the sample lateral-sides are maintained at elevated temperature and the fourth side is exposed to an upward flow and to a radiant flux. It is found that decreasing the flow velocity and increasing its oxygen concentration, and/or increasing the radiant flux enhances the transition to flaming, and reduces the delay time to transition. Limiting external ambient conditions for the transition to flaming are reported for the present experimental set-up. The results show that smolder propagation and the transition to flaming can occur in relatively small fuel samples if the external conditions are appropriate. The results also indicate that transition to flaming occurs in the char left behind by the smolder reaction, and it has the characteristics of a gas-phase ignition induced by the smolder reaction, which acts as the source of both gaseous fuel and heat.

SPATIALLY HETEROGENEOUS DYNAMICS AND THE EARLY STAGES OF CRYSTAL NUCLEATION AND GROWTH IN METASTABLE LIQUIDS AND COLLOIDS

M. Bergroth, T. Solomon, Y. Gebremichael, A.S. Keys, M. Vogel, M.J. Solomon and S.C. Glotzer
Department of Chemical Engineering, University of Michigan, Ann Arbor, MI 48109-2136

Controlling the behavior of metastable liquids leading to solidification is essential to controlling the ultimate properties and behavior of these liquids and the materials made from them. Although a great deal is known about the behavior of bulk crystals and glasses, considerably less is known about the atomistic scale processes that control either vitrification or the earliest stages of nucleation and growth of the crystal phase. This situation is due largely to the difficulty in directly visualizing small and critical nuclei in metastable liquids and the local processes that inhibit their formation and promote the formation of macroscopic amorphous materials like bulk metallic glasses.

We are carrying out research pertinent to the earliest stages of nucleation and growth of crystals in metastable liquids via a coordinated simulation-experimental program. One aspect of our studies is concerned with mapping the local dynamics in a computer model of a homogeneous metastable liquid, relating the spatial heterogeneity of the dynamics to aspects of the local liquid structure, and in turn relating features of both the local dynamics and structure to nucleation processes. In the so-called Dzugutov liquid, crystallization is temporarily suppressed by introducing frustration through the interaction potential, rather than through size polydispersity as is typically done in colloids. Through comparison of the simulation results with confocal laser scanning microscopy (CLSM) experiments on colloids of varying degrees of polydispersity, we are ascertaining the role of SHD in nucleation and the effects of polydispersity and interactions on the suppression of crystallization. We expect that our work will provide new insight into controlling solidification processes in materials, with strategic relevance for both high-strength structural materials such as bulk metallic glass and for advanced food technologies for long-term storage and preservation.

In this poster, we show that particle motion in simulated supercooled, metastable liquids is highly coordinated and that particles move primarily along one-dimensional, string-like paths[1,2]. We further show the tendency for particles in the metastable liquid to form clusters in which the particles are arranged in icosahedra, and we show how strings emanate from and wrap around these clusters[3]. We show that particle motion is dynamically facilitated, supporting recent theoretical predictions[3]. We further show how the degree of facilitation and cooperative particle motion increases with the degree of undercooling[3]. Finally, we present preliminary results on the early stages of nucleation in the deeply supercooled liquid.

Experimentally, we study analogous properties in colloidal suspensions by direct visualization with CLSM. The colloidal model system is composed of monodisperse, sterically stabilized silica colloids of diameter approximately 1 micron dispersed in a density and refractive

index matched solvent mixture. The initially amorphous, high volume fraction suspensions exhibit glass-like dynamics. By means of CLSM, we observe the three-dimensional ordering of suspensions under quiescent conditions and as they are subjected to oscillatory shear flow. Qualitatively, we find that shear flow induces nucleation and growth of colloidal crystals in the initially amorphous suspensions. The pair correlation function and local bond orientation parameters are extracted from the CLSM image volumes by means of quantitative image processing. The strain rate and amplitude dependence of these measures of local ordering are quantified.

PI: Sharon C. Glotzer, Department of Chemical Engineering, University of Michigan, 3406 G.G. Brown Bldg., 2300 Hayward Street, Ann Arbot, MI 48109-2136. Email: sglotzer@umich.edu. Fax: 734.764.0459. Phone: 734.615.6296.

[1] Y. Gebremichael, M. Vogel and S.C. Glotzer, "Formation of transient clusters on nanoscopic length scales in a simulated one-component liquid," Mol. Simulation **30**(5), 281-287 (2004).

[2] Y. Gebremichael, M. Vogel and S.C. Glotzer, "Particle dynamics and the development of string-like motion in a mono-atomic, supercooled liquid," J. Chem. Phys., **120** (9): 4415-4427 (2004).

[3] M. Bergroth, Y. Gebremichael, A.S. Keys, M. Vogel and S.C. Glotzer, manuscript in preparation.

FLAMMABILITY MAP FOR MICROGRAVITY FLAME SPREAD

SUBRATA BHATTACHARJEE
CHRIS PAOLINI
San Diego State University, San Diego, California, subrata@thermo.sdsu.edu

KAZUNORI WAKAI and **SHUHEI TAKAHASHI**
Gifu University, Gifu, Japan

Recently[1], a simplified theory has been advanced to predict radiative extinction in a quiescent environment. It has been shown that steady flame spread over a fuel with a thickness greater than a critical thickness is impossible in a microgravity environment, irrespective of any ambient or fuel parameters. Building upon this result, we have extended this analysis[2] to a general case of microgravity flame spread at low opposing velocity over fuels of any thickness - thermally thin or thick. Spread rate expressions, similar to de Ris formulas[3] have been developed by including surface radiation as a representative loss mechanismin the surface energy balance, which are:

Thin Limit: $$\eta_{f,\text{thin}} \sim \frac{1-\eta_g}{2} + \frac{1}{2}\sqrt{\left(1+\eta_g\right)^2 - 4\Re_0} \tag{1}$$

Thick Limit: $$\eta_{f,\text{thick}} \sim \frac{F^2}{\Omega^2}\eta_g\left(1-\frac{\Re_0}{\eta_g}\right)^2 \tag{2}$$

where, $\eta_g \equiv \dfrac{V_g}{V_{f,\text{ thermal, thin}}}$, $\eta_f \equiv \dfrac{V_f}{V_{f,\text{ thermal, thin}}}$, and $\Omega \equiv \sqrt{\dfrac{\lambda_s \rho_s c_s}{\lambda_g \rho_g c_g}}$ (3)

and , $\Re_0 \equiv \dfrac{1}{F^2}\dfrac{\rho_s c_s}{\rho_g c_g}\dfrac{\varepsilon\sigma\tau}{\lambda_g}\left(\dfrac{T_v^4 - T_\infty^4}{T_v - T_\infty}\right)$ and $\Omega \equiv \sqrt{\dfrac{\lambda_s \rho_s c_s}{\lambda_g \rho_g c_g}}$ (4)

For small value of the radiation parameter $\Re_0$ or for large value of opposing flow velocity η_g de Ris expressions are recovered. In fact in the thermal regime, where radiation can be neglected, the thin and thick limit expressions can be combined.

$$\eta_{f,\text{thermal}} \sim \max\left(1, \frac{F^2}{\Omega^2}\eta_g\right) \tag{5}$$

The thermally thick solution is applicable when $\frac{F^2}{\Omega^2}\eta_g \geq 1$; therefore, the criterion for a fuel to be considered thermally thick in the thermal regime can be written as

$$\eta_g \geq \frac{\Omega^2}{F^2};\ \text{or},\ \tau \geq \tau_{\text{cr},1};\ \text{where},\ \tau_{\text{cr},1} = \frac{\lambda_s}{\rho_g c_g V_g F}; \tag{6}$$

Equations (1) and (2) have been found to reproduce experimental trends remarkably well for both thin PMMA[4] and thin cellulosic fuels[5]. for the flame spread rates in a microgravity environment. The formulas above can also be used for determining when a steady flame is impossible in a microgravity environment. By setting η_f to zero, conditions for flame extinguishment can be obtained.

References:

[1] Bhattacharjee, S., Takahashi, S., and Wakai, K., Comb. Flame, Vol. 132, pp. 523-532, (2003).

[2] Bhattacharjee, S., Ayala, R., Takahashi, S., and Wakai, K., Proceedings of the Combustion Institute, Vol. 30, (2004).

[3] de Ris, J.N., Proceedings of the Combustion Institute, 12:241 (1969)

[4] Takahashi, S., Wakai, K., and Bhattacharjee, S., Proceedings of the Combustion Institute, Vol. 29, (2002).

[5] Olson, S.L., Kashiwagi, T., Fujita, O, Kikuchi, M., and Ito, K., Comb. Flame, Vol. 125, pp. 852-864, (2001).

LIQUID MICRO-JET IMPINGEMENT COOLING OF A POWER CONVERSION MODULE

Avijit Bhunia[1, 2], Sriram Chandrasekaran[1] and Chung-Lung Chen[1]
[1] Rockwell Scientific Company, 1049 Camino Dos Rios, Thousand Oaks, CA 91360
[2] Corresponding Author, Tel: (805) – 373 – 4348, e-mail: abhunia@rwsc.com

The Power Management and Distribution (PMAD) system for NASA's long duration HEDS program is envisioned to distribute up to megawatt levels of electric power. The future military directed energy, surveillance and communication missions also demand electric power of similar magnitude with sophisticated power conditioning systems. As a result the power dissipation is projected to grow multifold in coming years, e.g., ~200W/cm^2 for silicon devices and >1000W/cm^2 for wide bandgap semiconductor (silicon carbide, gallium nitride) devices. With traditional heat spreading and air-cooling techniques, the thermal management system will be bulky, if not insufficient. In this article we demonstrate that liquid impingement and subsequent phase change, has the potential to make thermal management compact, and thus reduce weight and launch costs.

We present liquid (DI water) micro-jet array impingement cooling of a commercial power module (Figure 1a). The silicon devices (six IGBTs and Diodes) are placed on a packaging and isolation layer (DBC), which in turn is mounted on a base plate. At a switching frequency of 22KHz, the module converts DC input power to 3-phase AC output to drive a 50HP motor (Figure 1b). We implement base plate level micro-jet (D_j = 200μm) impingement targeted at the heater footprint location (Figure 1c). The jet impingement cooling chamber and the overall closed loop system are shown in Figure 2a and b respectively.

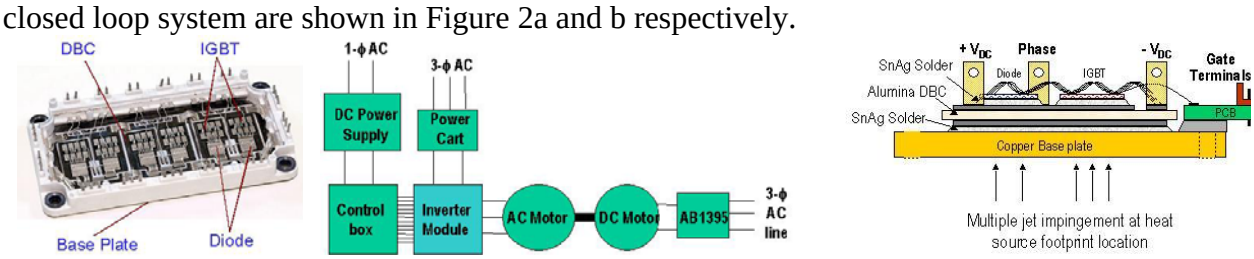

(a) (b) (c)

Figure 1: (a) 1200V-150A Power module from EUPEC (BSM100GD120DN2), (b) Schematic of the inverter module driving a 3-phase motor, (c) Schematic of the devices, packaging layers and base plate level liquid micro-jet array impingement.

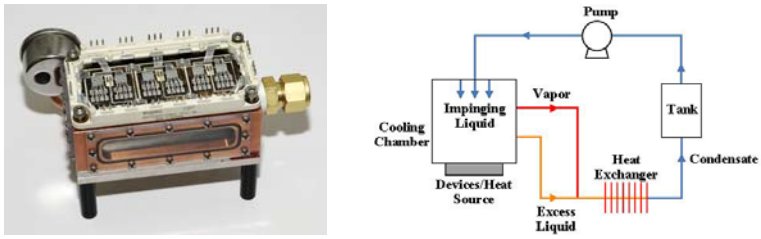

Figure 2: (a) Power module and liquid impingement cooling chamber. (b) Schematic of closed loop cooling system.

The high heat transfer coefficient associated with impingement and the simple orifice design lead to a cooling chamber conformal to the module. The resulting high volumetric power density (P_{VD} = heat

dissipated/cooling chamber volume) and the convenience of placing the heat exchanger at any desired remote location make the overall thermal management scheme compact.

Figure 3 shows a performance comparison of liquid micro-jet impingement, cold plate and air-cooling. The input power for cooling (to fan for air-cooling and to pump for liquid impingement and cold plate) is held constant at ~40W. The module operates at ~95% efficiency. Temperatures are measured at the base plate (T_{bp}) underneath each device. Figure 3a suggests that at module input power P_{in} = 13KW, liquid impingement lowers the maximum T_{bp} by 32°C compared to air-cooling (2X reduction) and by 18°C compared to cold plate (1.6X reduction). Figure 3b shows that at P_{in} = 13KW, the non-uniformity between T_{bp} values is reduced from 6°C in air-cooling to 4°C in cold-plate to <1°C for impingement cooling. From a system standpoint better the uniformity, higher is the module reliability. The diverging trend of the curves suggests that the payoff will be significantly more at higher power.

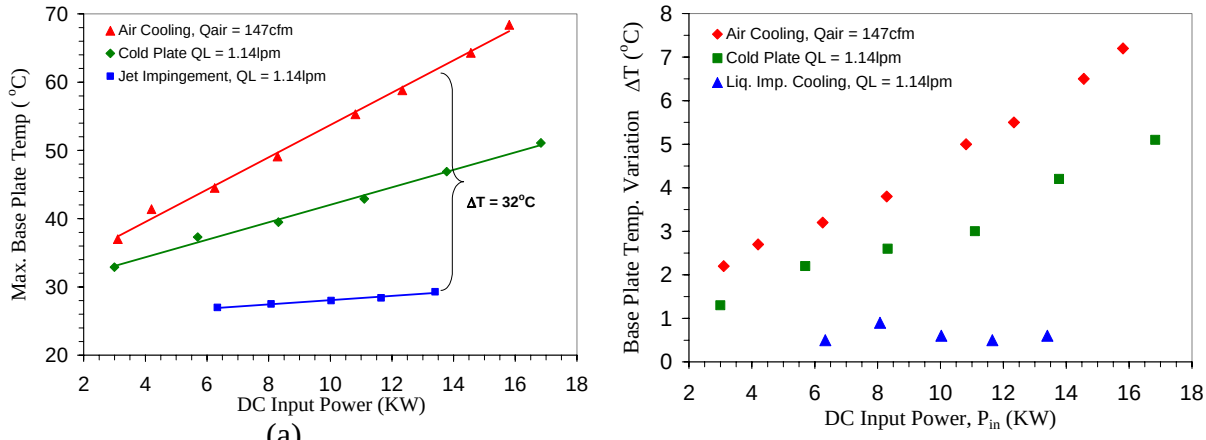

(a) (b)

Figure 3: Comparison of performance between various cooling techniques. (a) Maximum base plate temperature, (b) Non-uniformity in base plate temperature.

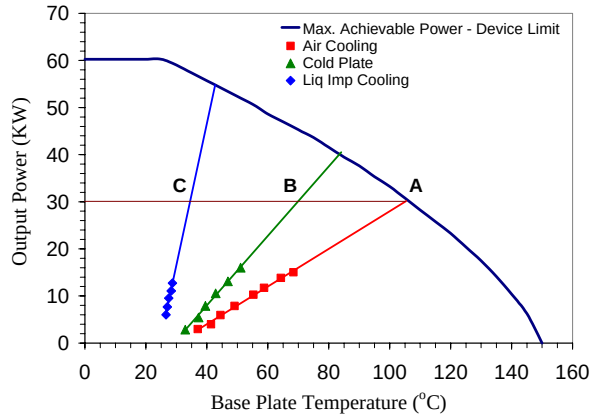

Figure 4: Comparison of cooling performance with reference to device limit.

Further comparison of the cooling techniques in light of the current carrying capability limit of the device (maximum achievable power from the module) is shown in Figure 4. With liquid impingement cooling, the module can deliver a maximum output power (P_{out}) of 55KW, compared to 40KW for cold-plate and 30KW for air-cooling. The corresponding P_{DV} values are 6.4, 6.7 and 1.2MW/m^3 respectively. P_{DV} for jet impingement cooling can be improved further by reducing the cooling chamber volume. Furthermore, at P_{out} = 30KW, T_{bp} and thus T_j can be reduced ~70°C compared to air-cooling (Points A-C) and ~35°C compared to cold plate (Points B-C).

The present results show that the liquid micro-jet impingement cooling far outperforms the conventional techniques. It is suitable for compact thermal management in space-based systems, especially with wide bandgap devices (such as silicon carbide) having dissipation densities >1000W/cm^2.

MODELING AND ANALYSIS OF CO-CURRENT FLAME SPREAD APPLIED TO THE UPWARD BURNING OF PMMA

Steven G. Buckley*, Ali S. Rangwala
Department of Mechanical and Aerospace Engineering, University of California, San Diego
9500 Gilman Drive, MS 0411; La Jolla, CA 92093-0411
buckley@ucsd.edu; 858-534-5681 / 858-534-5354 (F)

Jose L. Torero
School of Engineering and Electronics, University of Edinburgh, Scotland, United Kingdom

NASA uses tests involving upward flame spread as a flammability criterion to evaluate materials that could be potentially used in manned spacecraft. However, such tests remain an ON/OFF criterion, and no real translation of the ground based results to a micro-gravity environment has been proposed so far. The traditional 2-D solution proposed in 1956 by Emmons with extensions by Kodson, Williams and Buman (1968), Pagni and Shih (1978), and Annamalai and Sibulkin (1979) provides a baseline model for the Upward Flame Spread Test. Within this framework, measurements of the flame stand-off distance could be compared to predicted values obtained through this theory and used to establish a mass transfer number (B). The mass transfer number could then be used as a flammability criterion.

Recent experiments in upward burning flame spread over PMMA have shown the importance of lateral entrainment in the dynamics of the flame evolution, challenging the validity of 2-D boundary layer assumptions used to obtain the analytical solution. In this work we have tested the application of the classical 2-D model with an experimental setup modeled after the Upward Flame Spread Test. Analysis of video images allowed the extraction of the stand-off distance of the flame as a function of time, and an effective mass transfer number B is determined from these stand-off distances. When B is plotted as a function of streamwise distance x normalized by the pyrolysis length x_p, as in Figure 1, the data should collapse to a single curve. The failure of the data to collapse indicates the insufficiency of the classical model to fully describe this flow.

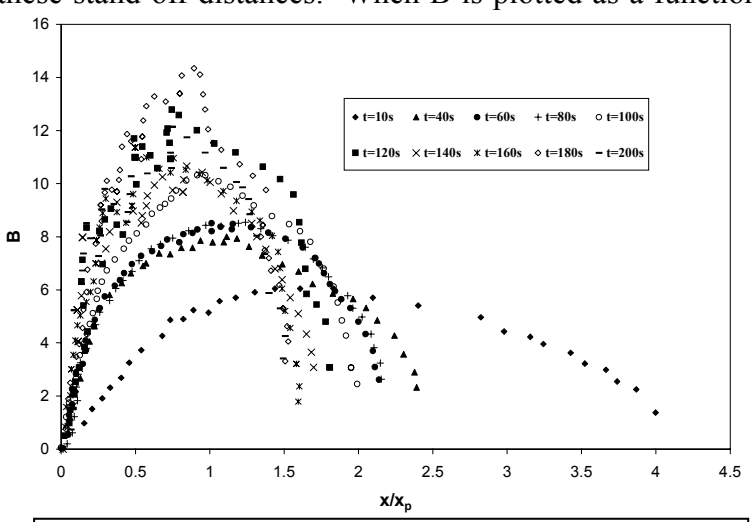

Figure 1: Evolution of empirical B number with time, from classical theory applied to experiments.

Experiments applied particle image velocimetry to ascertain the magnitude of lateral (side) entrainment suspected of diminishing the applicability of the 2-D analytical solution. Measurements of lateral entrainment were compared to 3-D predictions from the Fire Dynamic Simulator (FDS) code developed by NIST, as described by McGratten et

al. (2001). The simulations of upward-burning flame spread in several configurations showed good agreement with the experimentally measured the lateral entrainment. The results of these and further experiments are compared with measured experimental data for flame length and pyrolysis length. The agreement between experiments and the FDS model suggests that FDS could be used to obtain the stand-off distance and to extract the B number for solid fuels. Such application would allow the determination of a flammability criterion from the normal gravity tests and suggests possible extrapolation of these results to micro-gravity through the ability of the numerical code to remove the gravity term.

Beyond the observed agreement of FDS and experimental results, it is vital to validate the fundamental assumption of the proportionality of mass burning rate and shear stress inherent in traditional analytical solutions. Central to the approach of Emmons is the assumption that $\dot{m}'' \propto \partial u/\partial y$ in the 2-D flow, which propagates through later analytical solutions referenced above, but the validity of this has never been directly tested in this flame configuration. Testing of this assumption provides evidence of whether the insufficiency of the two-dimensional boundary layer solution is due to an inadequacy in the modeling approach, or merely to the need for an accounting of mass and/or heat transfer in the third dimension. Using the large eddy simulation model in FDS we provide data (Figure 2) to indicate that, while the two-dimensional boundary layer approach does not agree with experimental values, at steady state and in the plane of symmetry the assumption $\dot{m}'' \propto \partial u/\partial y$ holds, and hence the boundary condition imposed by Emmons appears to be valid. The verification of this assumption, in concert with the agreement of the numerical results and experimental data, allows us to conclude that predictions the stand-off distance using the FDS code are consistent with models incorporating a B-number type boundary condition, and thus it should be valid to extract a B number from such model outputs.

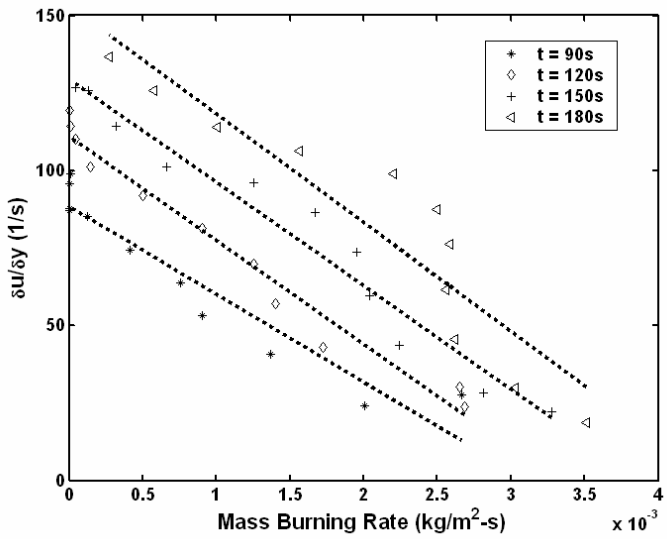

Figure 2: Proportionality of mass burning rate and strain rate du/dy predicted by FDS.

REFERENCES

H. Emmons, Z. angew. Math. Mech. 36 (1-2) (1956) 60-71.

F.J. Kosdon, F.A. Williams and C. Buman, Proc. Combust. Inst. 12 (1969) 253-264.

P.J. Pagni and T.M. Shih, Proc. Combust. Inst. 16 (1978) 1329-1343.

K. Annamalai and M. Sibulkin, Combust. Sci. Tech. 19 (1979) 167-183.

K.B. McGrattan, H.R. Baum, R.G. Rehm, A. Hamins, G.P. Forney and J.E. Floyd, Fire Dynamics Simulator - Technical Reference Guide (Version 2) National Institute of Standards and Technology (2001)

TESTS OF FLAMMABILITY OF COTTON FABRICS AND EXPECTED SKIN BURNS IN MICROGRAVITY

Jane M. Cavanagh, David A. Torvi,[1] and Kamiel S. Gabriel
Department of Mechanical Engineering
University of Saskatchewan
Saskatoon, SK

Gary A. Ruff
NASA Glenn Research Center
Cleveland, OH

During a shuttle launch and other portions of space flight, astronauts wear specialized flame resistant clothing. However during most of their missions on board the Space Shuttle or International Space Station, astronauts wear ordinary clothing, such as cotton shirts and pants. As the behaviour of flames is considerably different in microgravity than under earth's gravity, fabrics are expected to burn in a different fashion in microgravity than when tested on earth. There is interest in determining how this change in burning behaviour may affect times to second and third degree burn of human skin, and how the results of standard fabric flammability tests conducted under earth's gravity correlate with the expected fire behaviour of textiles in microgravity.

A new experimental apparatus was developed to fit into the Spacecraft Fire Safety Facility (SFSF), which is used on NASA's KC-135 low gravity aircraft. The new apparatus was designed to be similar to the apparatus used in standard vertical flammability tests of fabrics. However, rather than using a laboratory burner, the apparatus uses a hot wire system to ignite 200 mm high by 80 mm wide fabric specimens. Fabric temperatures are measured using thermocouples and/or an infrared imaging system, while flame spread rates are measured using real time observations or video. Heat flux gauges are placed between 7 and 13 mm away from the fabric specimen, so that heat fluxes from the burning fabric to the skin can be estimated, along with predicted times required to produce skin burns.

In November of 2003, this new apparatus was used on the KC-135 aircraft to test cotton and cotton/polyester blend fabric specimens in microgravity. These materials were also been tested using the same apparatus in 1-g, and using a standard vertical flammability test that utilizes a flame. In this presentation, the design of the test apparatus will be briefly described. Examples of results from the KC-135 tests will be provided, including heat fluxes and skin burn predictions. These results will be compared with results from 1-g tests using the same apparatus and a standard fabric flammability test apparatus. Recommendations for future microgravity fabric flammability tests will also be discussed.

[1] Corresponding Author: Phone (306) 966-5493, Fax (306) 966-5427,
Email: David.Torvi@usask.ca

EPS (ELECTRIC PARTICULATE SUSPENSION) MICROGRAVITY TECHNOLOGY PROVIDES NASA WITH NEW TOOLS

Gerald M. Colver,* Nate Greene, and Hua Xu
Department of Mechanical Engineering
Iowa State University
Ames, IA 50011
*gmc@iastate.edu
Ph. 515-294-7572

EPS (Electric Particulate Suspension) microgravity technology provides NASA with new tools:

- A portable diagnostic tool for **fire safety**
- Small scale utility for **combustion testing** of powders on International Space Station and (Mars) Rovers.
- Device for **burning/testing magnesium in CO_2** atmosphere of Mars
- Control of **heat transfer** in vacuum and gas enclosures in space environments

The Electric Particulate Suspension is a fire safety ignition test system being developed at **Iowa State University** with **NASA support** for evaluating combustion properties of powders, powder-gas mixtures, and pure gases in microgravity and gravitational atmospheres (quenching distance, ignition energy, flammability limits). A separate application is the use of EPS technology to control heat transfer in vacuum and space environment enclosures. In combustion testing, ignitable powders (aluminum, magnesium) are introduced in the EPS test cell and ignited by spark, while the addition of inert particles act as quenching media.

As a combustion research tool, the EPS method has potential as a benchmark design for quenching powder flames that would provide NASA with a new fire safety standard for powder ignition testing. The EPS method also supports combustion modeling by providing accurate measurement of flame-quenching distance as an important parameter in laminar flame theory since it is closely related to characteristic flame thickness and flame structure.

In heat transfer applications, inert powder suspensions (copper, steel) driven by electric fields regulate heat flow between adjacent surfaces enclosures both in vacuum (or gas) and microgravity. This simple E-field control can be particularly useful in space environments where physical separation is a requirement between heat exchange surfaces.

LUNAR SURFACE ENVIRONMENT LABORATORY

Joshua E. Colwell, Mihály Horányi, Scott Robertson, Stein Sture, Susan Batiste, and Zoltan Sternovsky
LASP, University of Colorado, Boulder CO 80309-0392, josh.colwell@lasp.colorado.edu, 303-492-6805, Fax: 303-492-6946

The lunar surface is covered with a layer of fine dust, or lunar regolith, that is produced by the continuous bombardment of the surface by the interplanetary micrometeoroid flux. The dust on the lunar mare is an angular, basaltic material with a mean particle size of about 100 μm and a broad size distribution extending down to at least 1 μm. The relatively low lunar gravity makes it easy for small disturbances to the surface to kick up large amounts of dust which travel higher and farther than in terrestrial gravity. In addition, the airless lunar surface leads to a plasma sheath on the night side due to solar wind ions and a photoelectron sheath on the day side due to photoemission of electrons by the solar UV flux. The dust on the lunar surface charges in this plasma environment and levitates and moves across the surface (Figs. 1-2). Any mission to the surface of the Moon, manned or unmanned, operates in this contaminating environment.

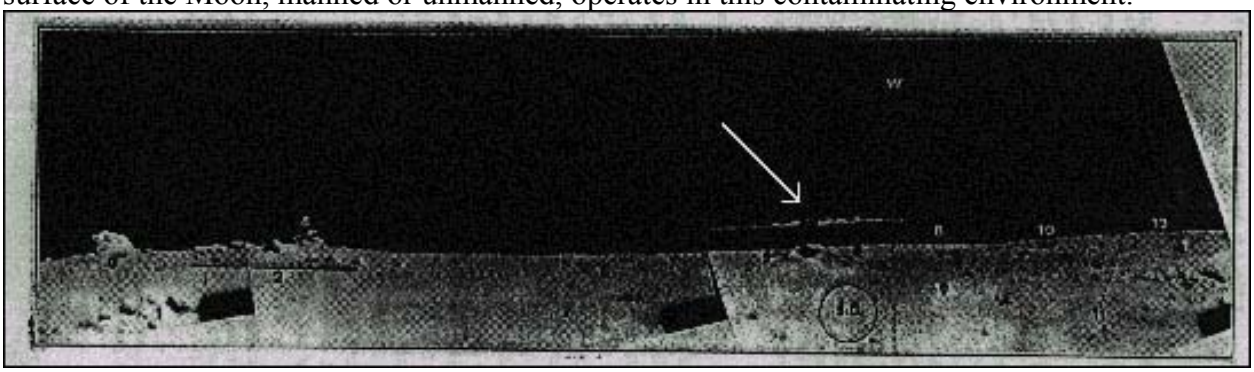

Figure 1: Surveyor photograph of the lunar horizon showing a cloud of small particles suspended 1 m above the surface (indicated by arrow). The circle labeled "S.D." indicates the apparent size and direction to the Sun [1]. NASA photo.

We have studied the charging, levitation, and transport of dust over planetary surfaces both experimentally and numerically [2-4]. We have reproduced the stably levitating dust clouds seen on the Moon (Fig. 1) in our laboratory experiments. We have also studied the response of planetary regolith to gentle impacts in a reduced gravity environment [5, 6].

In addition to dust contamination the charged particle environment at the lunar surface represents a potential hazard to astronauts. The night side of the Moon has a very different plasma environment than the day side due to the return flow of solar wind ions to the negatively charged surface. This results in a plasma sheath near the surface which can lead to even stronger electric fields near the surface than the dayside photoelectron sheath. As the Moon passes through the Earth's magnetotail there are additional charged particle fluences at the lunar surface. Characterization of this charged particle environment should precede extended astronaut stays on the Moon.

In situ resource utilization, including radiation and micro-meteorite shielding of human-outposts, will require excavation of the lunar surface. The unique angular nature of regolith

grains which become interlocked and densified by the lunar quakes complicates soil-movement techniques. Implementing vibrating excavating tools to loosen and dilate regolith for construction purposes will provide an efficient method to achieve regolith movement [7].

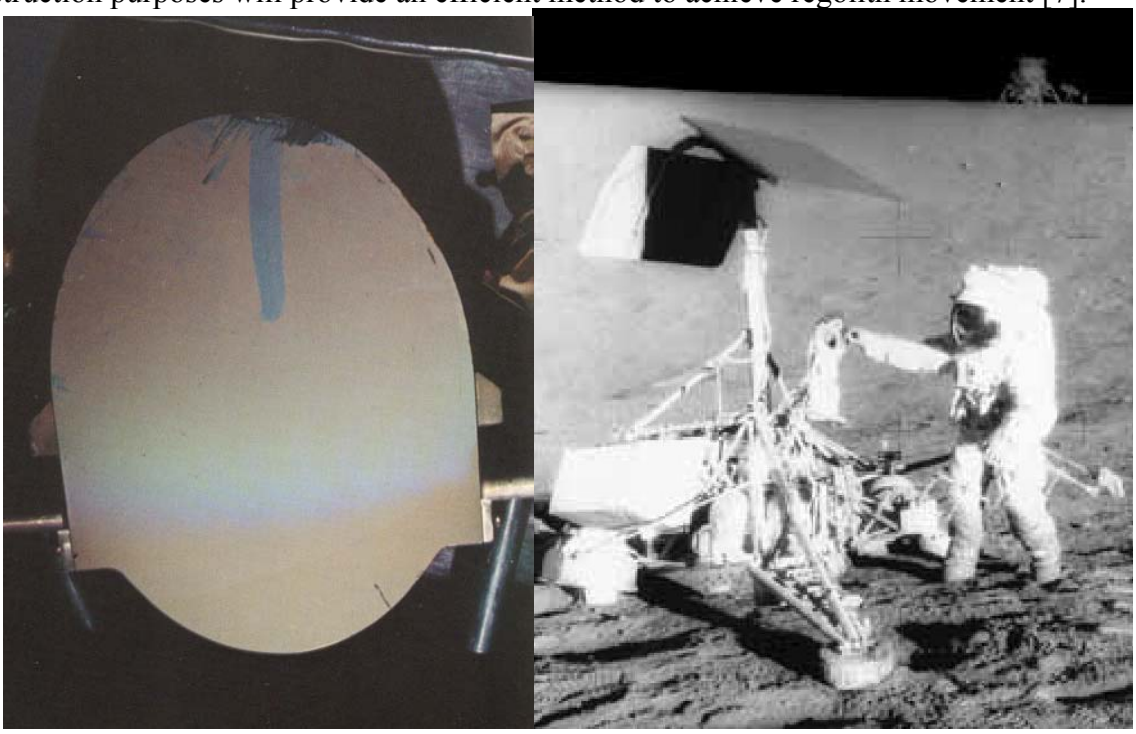

Figure 2: (left) An astronaut's glove print on the camera mirror of Surveyor 3 reveals the amount of dust that accumulated on the mirror after 31 months on the lunar surface; (right) an astronaut's spacesuit is coated with lunar dust up to the knees as he works at the Surveyor 3 spacecraft with the Apollo 12 LM in the background. NASA photos.

A lunar lander with instrumentation to measure near-surface plasma properties, regolith properties, and active experiments to study the response of surface dust to spacecraft activity in a variety of conditions and to test dust mitigation technologies would resolve many of the open questions surrounding the lunar surface environment, facilitating future manned and unmanned missions and surface experiments.

REFERENCES

[1] Rennilson, J. J., and D. R. Criswell, *The Moon*, **10**, 121-142 (1974).

[2] Sickafoose, A. A., J. E. Colwell, M. Horányi, and S. Robertson, *J. Geophys. Res.*, **107**, 1408 (2002).

[3] Sternovsky, Z., A. A. Sickafoose, J. E. Colwell, S. Robertson, and M. Horányi, *J. Geophys. Res.*, **107**, 5105 (2002).

[4] Robertson, S., A. A. Sickafoose, J. E. Colwell,and M. Horányi, *Physics of Plasmas*, **10**, 3874 (2003).

[5] Colwell, J. E., and M. Taylor, *Icarus*, **138**, 241 (1999).

[6] Colwell, J. E., *Icarus*, **164**, doi: 10.1016/S0019-1035(03)00083-6 (2003).

[7] Klosky, J. L., S. Sture, H. Ko, and F. Barnes, "Vibratory Excavation and Anchoring Tools for the Lunar Surface," *Space '96: The 5th International Conference and Exposition on Engineering, Construction and Operations in Space*, ASCE (1996).

CRITICAL VELOCITIES IN OPEN CAPILLARY CHANNEL FLOWS (CCF)

Michael E. Dreyer, Uwe Rosendahl, Antje Ohlhoff

Center of Applied Space Technology and Microgravity (ZARM)
University of Bremen, Am Fallturm, D-28359 Bremen, Germany
e-mail: dreyer@zarm.uni-bremen.de, Fax: +49-421 218-2521, Phone: +49-421 218-4038

ABSTRACT

We consider a forced liquid flow in an open capillary channel with free liquid surfaces under low gravity conditions. The channel consists of two parallel plates as shown in Figure 1. The gap distance, the width of the plates and the length of the channel are denoted with a, b and l, respectively. The liquid flows along the x-axis and forms free surfaces at the sides between the plates. The flow is maintained by external pumps and the free surface deforms according to the pressure along the flow path. In case of steady flow the capillary pressure of the free surface balances the differential pressure between the liquid and the ambient constant pressure gas phase. A maximum flow rate is achieved when the adjusted volumetric flow rate exceeds a certain limit leading to a collapse of the free surfaces. The aim of the considerations is to determine the profile of the gas/liquid interface, the maximum flow rate of the steady flow and the corresponding critical flow velocity. The maximum flow rate depends on the geometry of the channel and the properties of the liquid, specified by three dimensionless parameters, the OHNESORGE number $\mathrm{Oh} = \sqrt{\rho\nu^2/(2\sigma a)}$, the aspect ratio $\Lambda = b/a$ and the dimensionless length $\tilde{l} = \mathrm{Oh}\,l/(4a)$ (ρ is the density, ν the kinematic viscosity and σ the surface tension of the fluid).

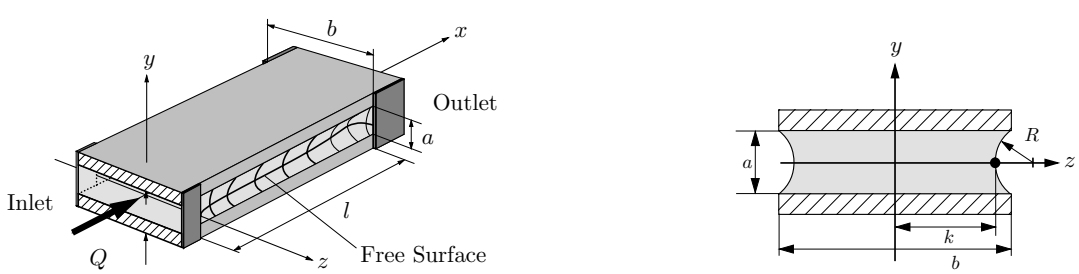

Figure 1: Schematic drawing of the flow through a capillary channel consisting of two parallel plates (left). The cross section area A perpendicular to the flow direction x (right).

We expect that the flow rate limitation occurs due to choking, which is known from compressible gas flows and open channel flows under normal gravity. The theory of choked flow predicts a limiting velocity corresponding to a characteristic signal velocity of the flow. Once that this critical velocity is reached the mass flow is maximum and cannot be increased further. Analogous to these phenomena we introduce the capillary SPEED INDEX $S_{ca} = v/v_{ca}$ where v is the mean liquid velocity and v_{ca} the speed of longitudinal small amplitude waves in open capillary channels. The maximal flow rate Q_{crit} is expected for $S_{ca} = 1$.

The experimental investigations were performed in the drop tower Bremen [1,3] and aboard the sounding rocket TEXUS-37. During the TEXUS experiment the flow rate was increased in small steps up to the critical value and the surface collapse was observed by

video cameras. The data evaluation yields the contour line of the liquid surfaces $k(x)$ as defined from Fig. 1 and the maximum flow rate of the steady flow which are well predicted by numerical model computations [2,4]. Furthermore a good agreement between the

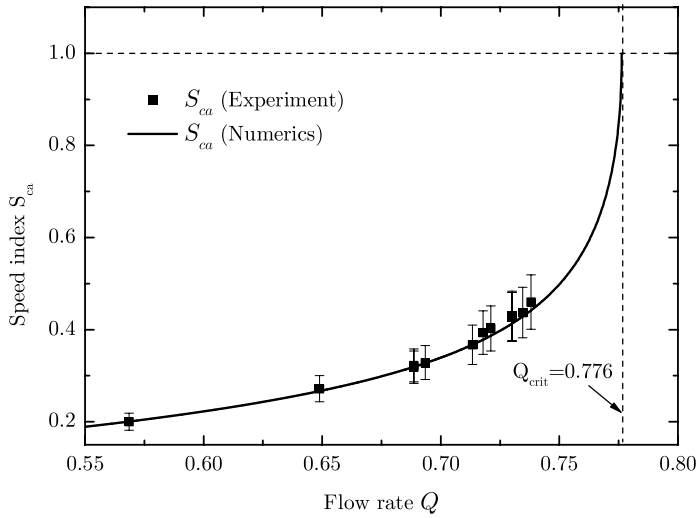

Figure 2: Capillary SPEED INDEX S_{ca} at the smallest cross section of the flow as function of the adjusted flow rate Q for the TEXUS experiment.

experimental data and numerical calculation of S_{ca} were found as depicted in Fig. 2. The numerical S_{ca} tends exactly towards unity for the numerical maximum flow rate, $Q_{crit}^{num} = 0.776$, which confirms the influence of the SPEED INDEX on the flow limitation. Experimentally, a maximum flow rate of $Q \simeq 0.95\, Q_{crit}^{num}$ was reached. A closer approach to the limit might be difficult from the experimental point of view since a small variation of Q leads to a large variation of S_{ca}. The final 5 % of flow rate changes S_{ca} by 50 %. Close to the limit very small increments in Q are required to increase the flow in quasi-static manner avoiding strong non-steady effects.

The experiment has been selected (94 NRA-7) to be conducted in the Microgravity Science Glovebox aboard the ISS. The Science Concept Review has been passed in 2002 and a feasability study (A) was conducted in 2003. A breadboard phase (B0) is currently underway testing detailed technical solutions with respect to the fluid handling, the video observation and the experiment control. The predefinition phase (B) is planned for this year. The experiment should be ready for flight in 2007. The funding of this work by means of the German Federal Ministry for Education and Research (BMBF) through the German Aerospace Center DLR under contract 50 WM 0241 is greatfully acknowledged.

1 M. E. Dreyer, U. Rosendahl, H. J. Rath, Experimental Investigation on Flow Rate Limitations in Open Capillary Vanes, AIAA 98–3165, 1998

2 U. Rosendahl, B. Motil, A. Ohlhoff, M. E. Dreyer, H. J. Rath, Critical Velocity in Open Capillary Channel Flows, AIAA-2001–5021, 2001

3 U. Rosendahl, A. Ohlhoff, M. E. Dreyer, H. J. Rath, Investigation of Forced Liquid Flows in Open Capillary Channels, Microgravity Science and Technology XIII/4, 2002

4 U. Rosendahl, A. Ohlhoff, M. E. Dreyer, Choked flows in open capillary channels: theory, experiment and computations, submitted to: Journal of Fluid Mechanics (JFM)

WIND-DRIVEN RIVULET BREAK-OFF IN CONDITIONS RANGING FROM 0G TO 1G

R. Ettema, J.S. Marshall, and G. McAlister
IIHR—Hydroscience and Engineering
University of Iowa
Iowa City IA 52242

A study has been performed of the wind-driven breakup of rivulets on a horizontal plate subject to different normal gravitational states, ranging from zero-gravity to terrestrial gravity conditions (1g), and also including some data for partial gravity conditions (between 0.1g and 0.38g). The experiments were conducted both in our laboratory at the University of Iowa and on board the NASA KC-135, parabolic-flight aircraft. The wind-driven rivulets exhibit a break-off phenomenon over a broad range of flow rates, in which a "head" at the tip of the rivulet breaks off periodically to form a droplet that advects down the plate. The rivulet break-off phenomena is found to be sensitive to the normal gravitational force acting on the plate. For instance, the frequency of rivulet break-off is nearly an order of magnitude greater in the 0g condition than it is for the same flow in the 1g condition. During the rivulet break-off event, a droplet detaches from the end of the rivulet and advects downstream on the plate. The detached droplet shape and behavior are observed to be quite different between the 0g and 1g cases. It is furthermore found in all cases examined that wind-driven rivulet and droplet flows are markedly different from gravitationally-driven flows (e.g., flow down an inclined plate). These differences arise primarily from the role of form drag on the droplets and on the raised ridge of the rivulet head near the moving contact line.

MELTING AND SOLIDIFICATION IN A RECTANGULAR CAVITY UNDER ELECTROMAGNETICALLY SIMULATED LOW GRAVITY

M. Faghri
Department of Mechanical Engineering
University of Rhode Island
Kingston, Rhode Island, USA

M. Charmchi
Department of Mechanical Engineering
University of Massachusetts
Lowell, Massachusetts, USA

A low gravity environment has been simulated numerically and experimentally, via an electromagnetic field, by studying the transport phenomena associated with the melting and solidification of an electrically conducting phase change material (gallium) inside a three-dimensional rectangular enclosure. Both transverse electric and magnetic fields are used to generate a Lorentz force, which is used to counteract the effects of gravity and thus simulate low-gravity environment. The problem is formulated as one-domain by employing an enthalpy-based transformation of the energy equation. The governing equations are then discretized using a control-volume-based finite difference scheme. Experimentally, the solid thickness is measured via ultrasonic techniques and the solid/melt interface is mapped using florescent light shadowgraphy through a transparent window. The experimental data consist of temperature history, ultrasonic detection of the interface, florescent light shadowgraphy and solid phase volume fraction. The experimental results show the presence of the magnetic filed had a marked effect on melting and natural convection whereas phase change convection was noticeable in the solidification. The numerical results show that the application of an electromagnetic filed can be used to simulate key melting characteristics found for actual low gravity. However, the resulting three-dimensional flow field in the melted region differs from actual low gravity. The application of an electromagnetic field creates a flow reversal phenomenon not found in actual low gravity. Flow distortions exist when an electromagnetic field is applied but their intensity is significantly lower than the distortions found when only a magnetic filed is applied.

TRANSITION FROM FORWARD SMOLDERING TO FLAMING IN SMALL POLYURETHANE FOAM SAMPLES

A.C. Fernandez-Pello, A. Bar-Ilan, O.M. Putzeys, and G. Rein
Department of Mechanical Engineering
University of California, Berkeley
Berkeley CA 94720

D.L. Urban
NASA Glenn Research Center
Cleveland, OH 44135

Experiments are also conducted on the effect of the flow velocity and oxygen concentration, and of a thermal radiant flux, on the transition from smoldering to flaming in forward smoldering of small parallelepiped samples of polyurethane foam with a gas/solid interface. Because the microgravity experiments are planned for the International Space Station, the foam samples had to be limited to a sample size that is too small for smolder to self propagate because of heat losses to the surrounding environment. Thus, the smolder propagation and the transition to flaming had to be assisted by reducing the heat losses to the surroundings and increasing the oxygen concentration in a range of 30% - 40% by volume. The former is attained by maintaining three of the sample lateral-sides at elevated temperature, and exposing the fourth side to an upward flow and to a radiant flux. It is found that decreasing the flow velocity and increasing its oxygen concentration, and/or increasing the external radiant flux enhances the transition to flaming, and reduces the delay time to transition. Below an oxygen mole fraction of 0.35, no transition is observed for any duct flow velocity. At an oxygen mole fraction of 0.35, transition is observed only for duct flow velocities of 0.25 m/s, while at an oxygen mole fraction of 0.40, transition is observed for all duct flow velocities below 2.0 m/s. Similarly, for a radiant heat flux of 7.25 kW/m^2, transition is only observed at a duct flow velocity of 0.25 m/s. However at a radiant heat flux of 8.75 kW/m^2 transition is observed for all duct flow velocities below 2.0 m/s. The results show that smolder propagation and the transition to flaming can occur in relatively small fuel samples if the external conditions are appropriate. Combined with observations from high speed video and schlieren photography, the results also indicate that transition to flaming occurs in the char left behind by the smolder reaction, and it has the characteristics of a gas-phase ignition induced by the smolder reaction, which acts as the source of both gaseous fuel and heat. A simplified energy balance analysis on the smolder front region is able to predict the boundaries between the transition/no transition regions, as shown in Fig 1.

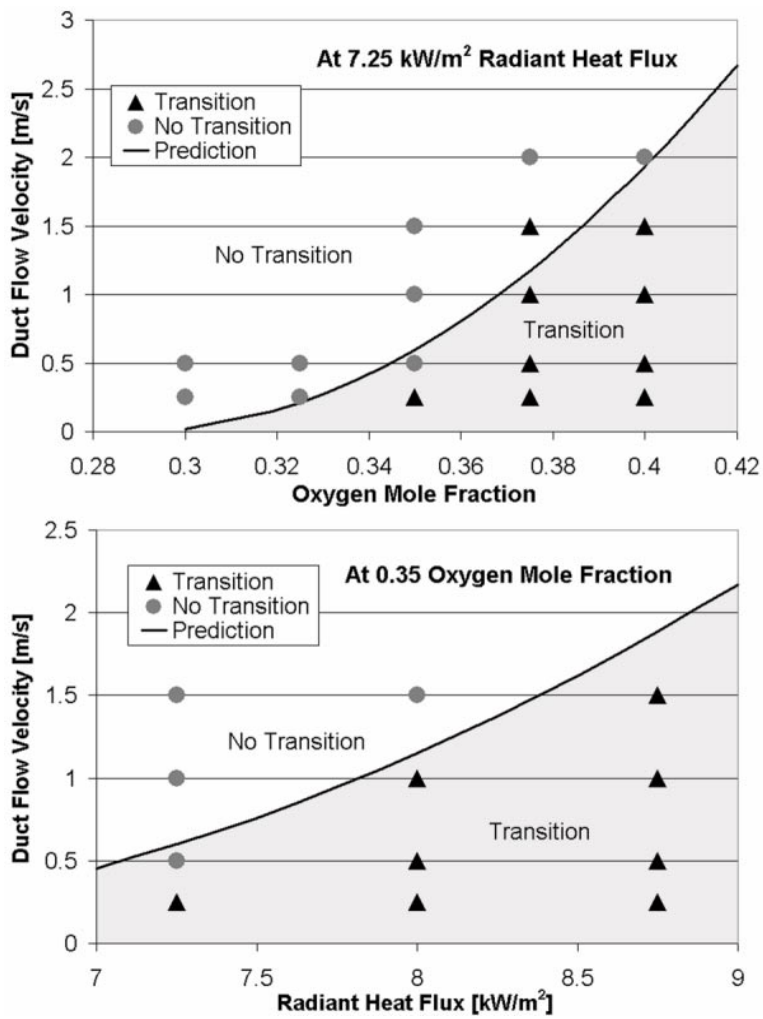

Fig 1. Comparison of experimental results with the energy balance analysis predictions of transition/no transition regions as a function of (a) oxygen mole fraction. (b) radiant heat flux.

PI contact information**:**
Prof. A. Carlos Fernandez-Pello
Department of Mechanical Engineering
6105A Etcheverry Hall
University of California
Berkeley, CA 94720-1740
Phone: (510) 642-6554
Fax: (510) 642-6163
Email: ferpello@me.berkeley.edu

PROGRESS ON ACOUSTIC MEASUREMENTS OF THE BULK VISCOSITY OF NEAR-CRITICAL XENON (BVX)

Keith A. Gillis, Iosif I. Shinder, and Michael R. Moldover
Process Measurements Division, National Institute of Standards and Technology,
Gaithersburg, MD 20899-8360

We plan to determine the bulk viscosity of xenon 10 times closer [in reduced temperature $\tau = (T-T_c)/T_c$] to its liquid-vapor critical point than ever before. (T_c is the critical temperature.) To do so, we must measure the dispersion and attenuation of sound at frequencies 1/100 of those used previously. In general, sound attenuation has contributions from the bulk viscosity acting throughout the volume of the xenon as well as contributions from the thermal conductivity and the shear viscosity acting within thin thermoacoustic boundary layers at the interface between the xenon and the solid walls of the resonator. Thus, we can determine the bulk viscosity only when the boundary layer attenuation is small and well understood. We present a comparison of calculations and measurements of sound attenuation in the acoustic boundary layer of xenon near its liquid-vapor critical point.

We used a novel, compact, acoustic resonator designed specifically for these measurements (Fig. 1). We measured the frequency response of this resonator filled with xenon at its critical density ρ_c in the reduced temperature range $10^{-3} < \tau < 10^{-1}$. From the frequency-response data, we obtained the resonance frequency and the attenuation for six resonant modes in the range 0.10 kHz $< f <$ 7.5 kHz. Using the known thermo-physical properties of xenon, we predict that the attenuation at the boundary first increases and then saturates when the effusivity of the xenon exceeds that of the solid. [The effusivity is $\varepsilon \equiv (\rho C_P \lambda_T)^{1/2}$, where C_P is the isobaric specific heat and λ_T is the thermal conductivity.] The model correctly predicts (±1.0 %) the quality factors Q of resonances measured in a steel resonator (ε_{ss} = 6400 kg·K^{-1}·s$^{-5/2}$); it also predicts the observed increase of the Q, by up to a factor of 8, when the resonator is coated with a polymer (ε_{pr} = 370 kg·K^{-1}·s$^{-5/2}$). The measured acoustic dissipation in near-critical xenon shows a prominent plateau for the Helmholtz mode and, to a lesser extent, for the longitudinal modes (Fig. 2). These results are the first direct

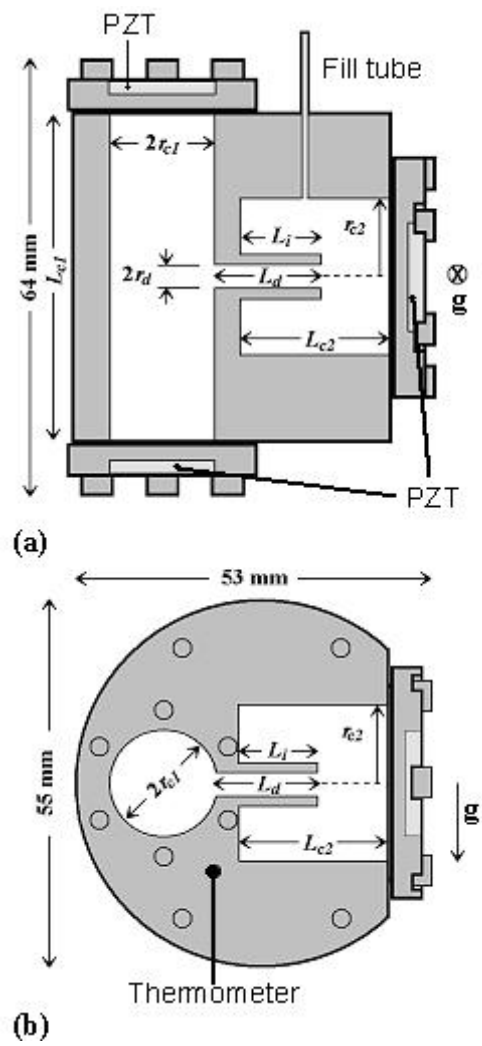

Figure 1. Acoustic resonator

evidence of thermal boundary dissipation being limited by the thermophysical properties of the solid wall.

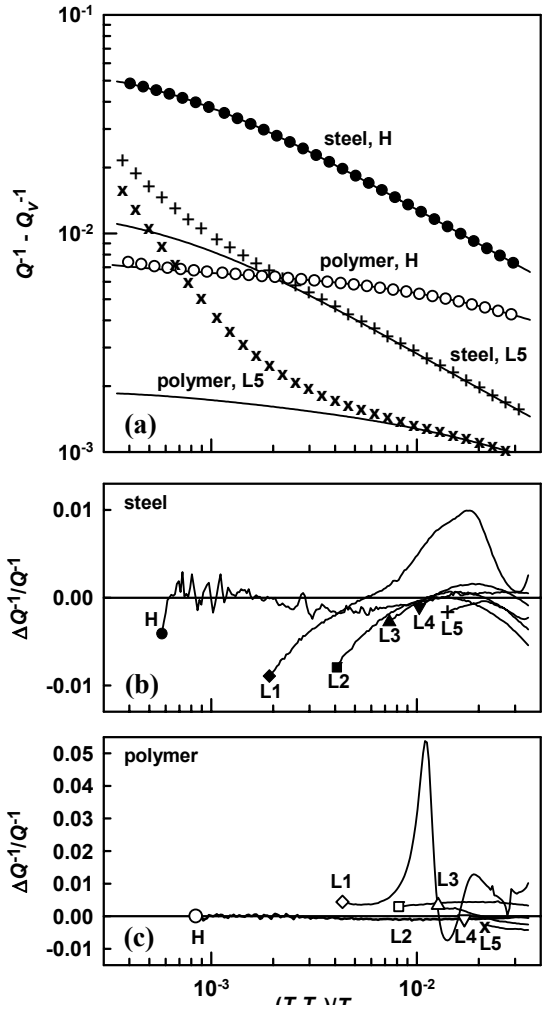

Figure 2. (a) Dissipation due to bulk viscosity and the thermal boundary layer versus reduced temperature. Theory for thermal boundary dissipation (———). The fractional deviations of the measured dissipation from theory versus reduced temperature for all the modes in the steel (b) and polymer-coated (c) resonators. Only data for which the dissipation from bulk viscosity was less than 0.8 % of the total dissipation is shown.

We observed an 8-fold reduction in the thermal boundary dissipation (as predicted) after coating a steel resonator with a low-effusivity polymer. (See Fig. 2a.) Such a reduction in thermal dissipation will be necessary in order to measure the low-frequency dissipation from bulk viscosity close to the critical point in future experiments.

To analyze the data, we formulated a theory for acoustic dissipation in a fluid that is bounded by a rigid wall with the condition that the temperature and heat flux across the boundary be continuous. The theory is valid both near to and far from the critical point; it includes volume and surface dissipation from thermal conduction, shear viscosity, and bulk viscosity.

We measured the speed of sound in xenon as a function of reduced temperature in the range $0.0006 < \tau < 0.03$. Using the measured sound speed and attenuation, the isothermal susceptibility from Ref. [1], and $(\partial P/\partial T)_\rho$ from Ref. [2], we derived C_V, C_P, and the background terms for the thermal conductivity. These derived properties were used to determine the amplitude $A^+ = 18.01$ for the singular part of C_V (with $\alpha = 0.110$) and the correlation length amplitude $\xi_0^+ = 0.1866$ nm. Although the data do not extend far into the asymptotic region, the agreement with other values is remarkable.

The onset of bulk viscosity is evident from the excess dissipation (over the thermal and viscous dissipation) indicated by the upturn at low τ of the measured dissipation shown in Fig. 2a. It is also evident that the dissipation from the bulk viscosity increases as the frequency increases in qualitative agreement with theory. The onset of bulk viscosity is more evident in the polymer-coated resonator because the thermal dissipation is smaller than it is in the bare-steel resonator.

[1] H. Güttinger and D.S. Cannell, Phys. Rev. A **24**, 3188-3201 (1981).
[2] H.L. Swinney and D.L. Henry, Phys Rev A **8**, 2566-2617 (1973).

Studying Biological Rhythms of Person's Skin-Galvanic Reaction and Dynamics of Light Transmission by Isomeric Substance in Space Flight Conditions

e-mail: vladimir.v@nt-ftlg.com
vladimir.p@nt-ftlg.com
Phone: (919) 942-9241
Fax: (919) 942-9241

General substantiation

1. State of the Question. Novelty and Practical Value of the Research.

Intensity and amplitude of human functional systems and human most important organs are wavelike, rhythmic by nature. These waves have constant periodicity, phase and amplitude. The mentioned characteristics can vary, however their variations have a pronounced reiteration in the course of time. This indicates a hashing of several wave processes and their interference. Stochastic changes in wave processes characteristics of a human organism are explained either by "pulsations" associated with hashing (superposition) of several wave processes and their interference, or by single influence of environmental physical factors on a human organism.

Human beings have respectively periods of higher and lower efficiency, state of health and so on, depending not only of environmental factors, but also of "internal" rhythmic factor. Sometimes peaks and falls periodicity of some or other characteristics is broken. Disturbance of steady-state biological rhythms is usually accompanied by reduction of activity steadiness of the most important systems of a human organism. In its turn this has an effect on organism's adaptation to changing living conditions as well as on general condition and efficiency of a human being. The latter factor is very important for space medicine.

Biological rhythmology is a special branch of biology and medicine, it studies rhythmic activity mechanisms of organs, their systems, individuals and species. Appropriate researches were also carried out in space medicine.

Some or other rhythmical processes are attributable to all living substances of our planet. Such processes are observed in all organisms –from unicellular algae to human organism – concerning both the whole organism as well as its separate cells. The majority of biological rhythms is probably not conditioned by periodic environmental effects, but it is subjected to some unknown biological clock. This rhythm mechanism does not simply respond to external stimulations, but it adapts itself to the external environment in a finer and more expanded manner, since necessary preparatory reactions take place in living organism before changing of external conditions, for example before it gets dark. Synchronization of a great number 400 of human organism's functional parameters changing rhythmically during one circadian period can be only explained by existence of such biological clock. However, the biological clock was not found both in organisms of all levels and in its separate cells. There is another striking fact – biological rhythms of hundreds millions of cornfield spikelets are strictly synchronized with each other. This field is not though an entire organism. Striking accuracy of observed rhythms gives an idea that there is nevertheless some periodically changing geophysical or cosmic environmental factor, which constantly "informs" plants and animals about the course of time.

In 1973-1974 V.P.Glushko advanced a hypothesis that if such factor existed, it could be found out through its influence on a lifeless inert matter. Such factor was discovered during synchronous

experiments with plants and isomer solutions. It was indicated by high coefficient of correlation between 24 hours' light absorption by lamina of a living plant and dynamics of light transmission through an isomer solution. Such factor turned to be a gravitational field, namely – gravitational perturbations (waves) going from the center of our Galaxy. The report on this work was given at "Problems of Plants Photo Energy" All-Union Conference held in Almaty in 1974 and at "Magnetic Fields in Medicine and Biology" International Conference held in Kaliningrad in 1975.

Authors' group V.P.Glushko, R.A.Gareev and A.N.Startsev gave a report on profound correlation between 24 hours' dynamics of person's psychophysiologic state and 24 hours' dynamics of light dispersion through isomer solutions, at the first Worldwide Aerospace Congress held in Moscow in 1995. It was there stated a hypothesis that a psychophysiologic state of an astronaut situated at a space station depends not only on already known space flight factors, such as zero-gravity, smells, sounds, electromagnetic noise of equipment, psychological and other so-called "internal" space flight factors, but it depends also on external factors such as gravity waves frequency variation resulted by Doppler effect, i.e. waves initiating biological rhythms. Initiating signal's frequency variation "disturbs" a biological rhythm of the organism and this has to influence on the whole astronaut's organism. Frequency variation of the signal initiating biological rhythm cannot be in principle simulated at the planet's surface, but this occurs naturally during space flight.

"*Tangr – 2"* space experiment held in 1998 and elicited the fact that T.Musabayev, an astronaut showed biological rhythms of skin-galvanic reaction shortened in time by 5-8% in comparison with similar rhythms registered on the Earth. **Mathematical processing of results of measurements was done by "Institute of theoretical and applied mathematics of the Ministry of a science - academy of sciences of Republic Kazakhstan».** The above said researches (3 experiments, each lasting for 3 hours with registration at intervals of a minute) were carried out after astronauts of 25-th expedition had spent about 3 or 4 months at "*Mir"* orbital station; i.e. after the period of critical adaptation to zero gravity and specific living environment existed at the orbital station. **Results of work are published in the collective monography «Space researches in Kazakhstan», under edition of academician M.M.Sultangazin, Almaty, year 2002. Section 5.12, «The Medical and biologic researches connected to flights of the Kazakhstan cosmonauts», page 446 - 460. And as in the collection of works the 2-nd international scientific - practical conference «The Science and education at the present stage of development of a society». Almaty, year 2003, page 72 - 73. Authors: Gareyev R.A., Fajzulina S.R., Glushko V.P., of the name: «The Psychophysical condition of the cosmonaut to KGR parameter during the period after-flight's rehabilitations».**

New Technologies of Physicotechnical Laboratory "GLUSHKO" will congregate to continue the begun researches. It is supposed to study out dynamics variation of "rhythms" of optical properties of isomer solutions situated both in space flight, as well as on the planet's surface. This will greatly contribute to resolving question about biological rhythms mechanism and its properties. If we evolve the hypothesis about a space factor initiating biological rhythms, it will be clear that there is not life as such outside the spatial region where this factor operates. This work is topical for pilot cosmonautics not only in view of the above-mentioned, but also in view of the knowledge about degree of dependence of biological clock's "course speed" on spacecraft's traverse speed after signal frequency has varied as a result of Doppler effect, as well as the knowledge about possibility of their disalignment.

ELECTROSTATIC RELEASE OF FINE PARTICLES ADHERED TO SURFACES ON THE MOON OR MARS

John Goree
Department of Physics and Astronomy
The University of Iowa
Iowa City, IA 52246
Phone: 319-335-1843; Fax: 319-335-1753

The adhesion of fine particles to surfaces is a concern for human exploration of the Moon and Mars. Airlocks, EVA suits, and photovoltaic cells have surfaces where dust can be an unwanted contaminant. When a particle rests on a surface, it is held in place by a van-der-Waals attraction, but this adhesion can be overcome by several mechanisms. One such mechanism for the Moon and Mars environments is the application of electrostatic forces. These forces occur spontaneously on the Moon. They could also be applied deliberately for the purpose of cleaning surfaces on the Moon or Mars.

The Moon, unlike Mars, has no atmosphere. Instead, it is immersed in interplanetary plasma, which consists of free electrons and protons at a low number density. The Moon disturbs this plasma, so that there is an electric field perpendicular to the Moon's surface. This electric field applies a vertical force to any electrically-charged fine particle.

Particles are known to become charged and levitated on the Moon. This was discovered in Apollo missions, where a thin cloud of dust was seen floating above the lunar horizon. Particles can be charged either photoelectrically by exposure to solar UV, or by collection of free electrons and ions from the surrounding plasma. This can lead to levitation, if the particle can first overcome van-der-Waals adhesion to surfaces such as a rock, a photovoltaic cell, or another dust particle.

Laboratory experiments have demonstrated that one mechanism for overcoming adhesion is an electrostatic force. Dielectric particles on a surface are charged due to exposure to plasma, or UV. In a pile of particles, two neighboring particles can acquire charges of the same polarity, thereby applying an interparticle repulsion sufficient to overcome the adhesion. This particle release occurs with a surprising speed that remains unexplained.

On Mars, there is an atmosphere of neutral gas instead of a natural plasma. However, it is possible to purposefully produce a localized plasma by ionizing the thin Martian atmosphere. This can be done by applying a voltage to an antenna or electrode. It is worth studying whether such a plasma could be used for cleaning surfaces. A similar method has been developed previously for the semiconductor industry to clean particulate contaminants from semiconductor wafer surfaces.

Another application for these principles is ion thruster technology. Fine particles can flake from interior surfaces of an ion-thruster's plasma source. When these particles overcome adhesion from the surface, they move about and become lodged in the grids that accelerate ions, causing a malfunction by shorting the grids. For this reason, it is of interest to study the plasma-generated electrostatic forces that overcome adhesion of particles to surfaces.

It is proposed to carry out laboratory experiments and possibly parabolic flights with lunar gravity conditions, to study these electrostatic mechanisms, using plasma sources and a UV lamp.

BUOYANCY EFFECTS IN STRONGLY-PULSED, TURBULENT DIFFUSION FLAMES

J.C. Hermanson
University of Washington, Box 352400, Seattle, WA 98195
Ph: (206)616-2310 Fax: (206)543-0217 email jherm@aa.washington.edu

H. Johari and E. Ghaem-Maghami
Worcester Polytechnic Institute,
Worcester MA 01609

D.P. Stocker and U. G. Hegde
NASA Glenn Research Center,
Cleveland, OH 44135

The objective of this experiment is to better understand the combustion behavior of pulsed, turbulent diffusion flames by conducting experiments in microgravity. The fuel jet is fully-modulated (i.e., completely shut off between pulses) by an externally controlled valve system leading to enhanced fuel/air mixing compared to acoustically excited or partially-modulated jets[1].

Experiments are conducted both in laboratories at UW and WPI and in the GRC 2.2s Drop Tower. A single fuel nozzle with diameter d = 2 mm is centered in a combustor 20 Δ 20 cm in cross section and 67 cm in height. The gaseous fuel flow (ethylene or a 50/50 ethylene/nitrogen mixture by volume) is fully-modulated by a fast-response solenoid valve with injection times from ϑ= 4 to ϑ= 300 ms. The nominal Reynolds number based on the fuel velocity during injection, U_{jet}, is 5,000. A slow oxidizer co-flow properly ventilates the flame[2] and an electrically heated wire loop serves as a continuous ignition source. Diagnostic techniques include video imaging, fine-wire thermocouples and thermopile radiometers, and gas sampling and standard emissions instruments (the last in the laboratory only).

The normalized flame lengths of fully-modulated diffusion flames consisting of isolated, non-interacting structures at low duty cycle, ζ (i.e., low jet-on fraction) are shown in Fig. 1. The flame length scales well with the parameter $P(1+..)^{1/3}$, where $P\ \Sigma(U_{jet}\vartheta d)^{1/3}$ and …is the stoichiometric air/fuel ratio[1]. The linear scaling persists to $P- 8$ where a transition from compact puffs to elongated flame structures begins. The visually-observed celerity of flame puffs near burn-out is generally less in microgravity than in normal gravity and the flame puffs in microgravity generally take a longer time to burn out. These two effects appear to be offsetting, with the result that the flame length of isolated, compact puffs in the linear scaling region is insensitive to buoyancy. By contrast, the mean length of flames with elongated, isolated structures ($P > 8$) does increase as buoyancy is removed.

The flame length in fully-modulated diffusion flames can also be significantly impacted by the off-time (or duty cycle) as shown in Fig. 2. Decreasing the off-time causes the discrete fuel puffs to give way to more closely-packed, interacting flame structures, which lead in turn to a longer flame length. This effect is greatest for the most compact puffs with the shortest injection time (lowest values of P). An example of a microgravity flame at a duty cycle sufficiently high to result in significant structure-structure interaction is shown in Fig. 3.

The combination of increasing flame puff size and decreasing puff celerity with downstream distance changes the separation between puffs, effectively increasing the duty cycle locally. This effect is greater in microgravity than in normal gravity due to the lower celerity in the former case, suggesting that the change in flame length with increasing injection duty cycle is correspondingly greater in microgravity. This is in qualitative agreement with the experiments.

Buoyancy appears to have a strong effect on the thermal characteristics of fully-modulated turbulent diffusion flames[3]. The cycle-averaged centerline temperatures are generally higher in the microgravity flames than in normal gravity, especially at the flame tip where the difference was as much as 200 K. The highest average centerline temperature (Fig. 4) appears to decrease, then to become roughly constant as P is increased. The transition occurs at $P - 8$ (similar to value for the transition in flame length mentioned previously).

The highest emission indices of CO and unburned hydrocarbons (UHC) were found for compact, isolated puffs and were roughly an order of magnitude higher than emissions from elongated flames[4]. The levels of CO, UHC, and NOx for all fully-modulated flames approached the low, steady-flame values for a duty cycle of approximately $\zeta \varnothing 0.4$, with a flame length significantly shorter than that of the steady flame. All emissions data were acquired in 1-g; the emissions levels of flames in microgravity have not yet been investigated.

This work is sponsored by NASA Glenn Research Center under Agreements NCC3-673 and NNC04AA37A.

References

[1] Hermanson, J.C., Dugnani, R., and Johari, H., *Comb. Sci. Tech.* **155**, 203-225, 2000.
[2] Hermanson, J.C., Usowicz, J., Johari, H., and Sangras, R., *AIAA Journal* **40** (7), 2002.
[3] Page, K.L., Stocker, D.P, Hegde, U.G., Hermanson, J.C. and Johari, H., *Third Joint Meeting of the U.S. Sections of The Combustion Institute*, Chicago, IL, March, 2003.
[4] Johari, H., Ghaem-Maghami, E., and Hermanson, J.C., *Combustion Science and Technology,* in press, 2004.

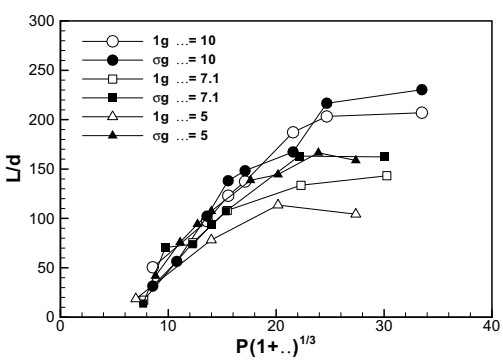

Fig. 1 Normalized flame length for fully-modulated flames.

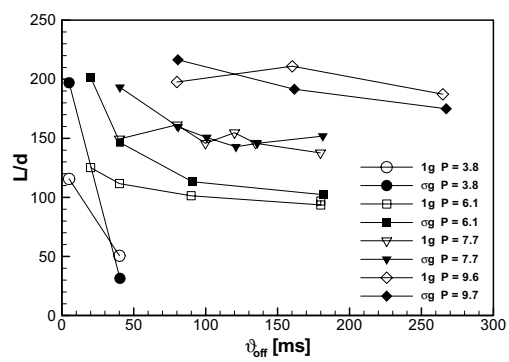

Fig. 2 Effect of injection off-time on normalized flame length for fully-modulated flames for …= 10.

Fig. 3 Sequence of fully-modulated flames in microgravity showing the merging of large-scale turbulent structures. $P = 7.6$, $\zeta = 0.5$.

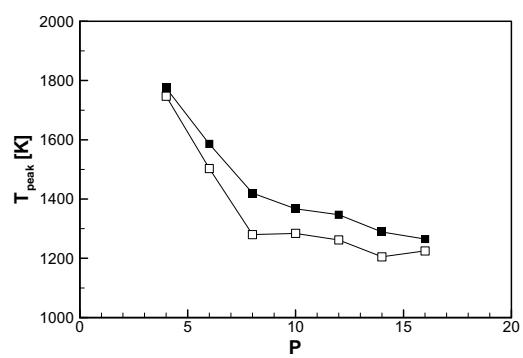

Fig. 4 Highest values of the average centerline temperature.

TWO-FLUID MODEL AND INTERFACIAL AREA TRANSPORT IN MICROGRAVITY CONDITION

Mamoru Ishii♣, Xiaodong Sun, and Shilp Vasavada
School of Nuclear Engineering, Purdue University, West Lafayette, Indiana

The objective of the present study is to develop a two-fluid model formulation with interfacial area transport equation applicable for microgravity conditions. The new model is expected to make a leapfrog improvement by furnishing the constitutive relations for the interfacial interaction terms with the interfacial area transport equation, which can dynamically model the changes of the interfacial structures. In the first year of this three-year project supported by the U.S. NASA, Office of Biological and Physics Research, the primary focus is to design and construct a ground-based, microgravity two-phase flow simulation facility, in which two immiscible fluids with close density will be used.

In predicting the two-phase flow behaviors in any two-phase flow system, the interfacial transfer terms are among the most essential factors in the modeling. These interfacial transfer terms in a two-fluid model specify the rate of phase change, momentum exchange, and energy transfer at the interface between the two phases. For the two-phase flow under the microgravity condition, the stability of the fluid particle interface and the interfacial structures are quite different from those under normal gravity condition. The flow structure may not reach an equilibrium condition and the two fluids may be loosely coupled such that the inertia terms of each fluid should be considered separately by use of the two-fluid model. Previous studies indicated that, unless phase-interaction terms are accurately modeled in the two-fluid model, the complex modeling does not necessarily warrant an accurate solution.

Traditionally, the interfacial area concentration, one of the parameters characterizing the interfacial structure, is specified by empirical correlations that are based on the two-phase flow regimes and regime transition criteria. In view of this, the focus of many studies for the microgravity two-phase flow was on identifying the flow regime transition or transition criteria. However, this approach has the following shortcomings:

1. The flow regime transition criteria are algebraic relations for steady-state fully-developed flows. They do not fully reflect the true dynamic nature of changes in interfacial structures. Hence the effects of the entrance and developing flow cannot be taken into account correctly, nor the gradual transition between the flow regimes. Under the microgravity conditions, the flow structure may not reach an equilibrium configuration. Therefore, the flow regime dependent constitutive relations developed for the steady-state fully-developed two-phase flow are not suitable.
2. The method based on the flow regime transition criteria is a two-step method, which requires the flow regime transition criteria and the regime dependent closure relations for the interfacial area.

♣ PI: School of Nuclear Engineering, 400 Central Drive, Purdue University, West Lafayette, IN 47907; email: ishii@ecn.purdue.edu; Tel: 765-494-4587; Fax: 765-494-9570.

3. The flow regime dependent correlations and criteria may be valid only in limited parameter ranges for certain specific operational conditions. When applied to the microgravity two-phase flow conditions, these models may cause significant discrepancies and artificial discontinuities.

To better represent the effects of the interfacial structure and the flow regime transition, the use of the dynamic equation to characterize the interfacial area transport has been proposed and is currently being pursued. Based on the current developments in the normal gravity two-phase flow, the interfacial area transport equation can be considered a rational choice in providing a closure relation for the interfacial area concentration for the microgravity two-phase flow. Through mechanistic modeling of various fluid particle interactions, the interfacial area transport equation can closely model the two-phase flow evolution across the flow regime transition boundaries, and thus prevent artificial discontinuities. Furthermore, the recent studies suggest the significance of investigation on particle interaction mechanisms in the evolution of two-phase structures (Colin et al., 1991; Hewitt, 1996; Takamasa et al., 2002). It is expected that the interfacial area transport equation can significantly improve the current capability of the two-fluid model from both scientific and practical viewpoints.

To benchmark the theoretical model, ground-based tests by employing two immiscible fluids with similar density is being performed to simulate the microgravity condition in the first phase of this research. A detailed scaling analysis is being performed to closely simulate the gas-liquid two-phase flow in the microgravity condition. Both the global and local two-phase flow parameters will be acquired by the state-of-the-art instrumentation, namely, multi-sensor conductivity probes, multi-sensor void-meter, and LDA system, along with detailed flow visualization and image analysis. Following the first stage experiment, the second stage experiment is to be performed with the gas-liquid two-phase flow in the in-flight or drop-tower microgravity facilities.

Currently, the design of the test facility has been basically completed. Through a detailed preliminary study, water and Therminol 59, which has a density of 971 kg/m^3 at 20°C, have been chosen as the two fluids to simulate microgravity environment on ground. Round pipes with 25.4 and 304.8 mm internal diameter have been selected as the test sections. The construction of the facility is expected to be completed and tested by the end of September 2004.

REFERENCES

Colin, C., Fabre, J. and Dukler, A.E., 1991, "Gas-liquid Flow at Microgravity Conditions-1. Dispersed Bubble and Slug Flow," *Int. J. Multiphase Flow*, 17, pp. 533-544.

Hewitt, G.F., 1996, "Multiphase Flow: The Gravity of the Situation," *NASA-CP-3338*, Proc. of the Third Microgravity Fluid Physics Conf., July 13-15, 1996, pp. 3-23.

Takamasa, T., Iguchi, T., Hazuku, T., Hibiki, T. and Ishii, M., 2002, "Interfacial Area Transport of Bubbly Flow under Microgravity Environment," To be published in *Int. J. Multiphase Flow*.

Aeolian sand transport with collisional suspension

James T. Jenkins,[1] José Miguel Pasini,[1] and Alexandre Valance[2]

[1] *Department of Theoretical and Applied Mechanics, Cornell University, Ithaca, NY 14853*
[2] *Groupe Matière Condensée et Matériaux, Université Rennes1, Campus Beaulieu-Bât11A, 35042 Rennes cedex*

Aeolian transport is an important mechanism for the transport of sand on Earth and on Mars. Dust and sand storms are common occurrences on Mars and windblown sand is responsible for many of the observed surface features, such as dune fields. A better understanding of Aeolian transport could also lead to improvements in pneumatic conveying of materials to be mined for life support on the surface of the Moon and Mars.

The usual view of aeolian sand transport is that for mild winds, saltation is the dominant mechanism, with particles in the bed being dislodged by the impact of other saltating particles, but without in-flight collisions. As the wind becomes stronger, turbulent suspension keeps the particles in the air, allowing much longer trajectories, with the corresponding increase in transport rate. We show here that an important regime exists between these two extremes: for strong winds, but before turbulent suspension becomes dominant, there is a regime in which in-flight collisions dominate over turbulence as a suspension mechanism, yielding transport rates much higher than those for saltation. The theory presented is based on granular kinetic theory, and includes both turbulent suspension and particle-particle collisions. The wind strengths for which the calculated transport rates are relevant are beyond the published strengths of current wind tunnel experiments, so these theoretical results are an invitation to do experiments in the strong-wind regime.

In order to make a connection between the regime of saltation and the regime of collisional suspension, it is necessary to better understand the interaction between the bed and the particles that collide with it. This interaction depends on the agitation of the particles of the bed. In mild winds, collisions with the bed are relatively infrequent and the local disturbance associated with a collision can relax before the next nearby collision. However, as the wind speed increases, collision become more frequent and the agitation need not decay completely. In the regime of collisional suspension, the particles near the surface of the bed are assumed to be in a state of constant agitation. We indicate the conditions at the bed corresponding to the limits of saltation and collisional suspension and outline experiments, simulations, and modeling that have been undertaken to bridge these limits.

TWO DIMENSIONAL TURBULENCE IN PRESENCE OF POLYMER

Yonggun Jun, Jie Zhang, and Xiao-Lun Wu
Department of Physics and Astronomy
University of Pittsburgh
Pittsburgh, Pennsylvania 15260

The phenomenon of drag reduction by adding a small amount of long-chain polymers to turbulent flow has been studied for a long time but is not fully understood. We investigated the effect of the dilute polymer concentration and the energy injection rate upon the drag reduction and the turbulent structures in fully-developed 2D turbulent flow. Our measurements were performed in a freely suspended soap film. The Particle Imaging Velocimetry (PIV) is used to determine the velocity field and the local topological structures. The local topology is characterized by the Jacobian determinant $\Lambda(x, y) = (\omega^2 - \sigma^2)/4$, where $\omega(x,y)$ is the local vorticity, and $\sigma(x,y)$ is the local strain rate. We found that large coherent structures were suppressed by polymers and the energy dissipation due to polymer suddenly increased around polymer concentration 10 wppm. The shape of the PDF of the local topology $P(\Lambda)$ is changed for higher polymer concentrations.

TRANSITION FROM IGNITION TO FLAME GROWTH UNDER EXTERNAL RADIATION IN THREE DIMENSIONS (TIGER-3D)

Takashi Kashiwagi, Yuji Nakamura, Sandra L. Olson, and William Mell

This study focuses on localized ignition by external radiant flux and subsequent flame growth over thin polymeric materials (plastic and paper) in microgravity. Two transition stages were observed. The first transition stage covers the period from the onset of ignition to the formation of stabilized flame near the ignited area. This is followed by the second transition of the flame growth stage from the initial stabilized flame to sustained fire growth away from the ignited area. For the first stage, ignition experiments of thin PMMA sheets were conducted using a CO_2 laser as an external source in the 10 s drop tower. The results of front side surface ignition and of backside surface ignition were observed. The effects of imposed flow velocity, sample thickness, and ambient oxygen concentration on ignition are obtained. Numerical study was conducted to investigate to understand and predict ignition behavior observed in the experiments. For the second stage, numerical study is being conducted to describe the effects of gravity on heat release rate of a PMMA sheet. The gravity level was varied from zero to normal gravity. The preliminary results show that the maximum heat release occurs at around 0.02 g.

ISOLATED LIQUID DROPLET COMBUSTION: INHIBITION AND EXTINCTION STUDIES

A. Kazakov, K.G. Kroenlein, and F.L. Dryer
Princeton University, Princeton, NJ

F.A. Williams
University of California, San Diego, CA

V. Nayagam
National Center for Microgravity Research, Cleveland, OH

NASA's new space exploration initiative calls for an expansion of human presence into space, and many of the technologies envisioned for these efforts involve fire risks including oxygen generating systems, power-generation equipment, propellant production systems, and waste-management technology and other essentials for life support. The flammability characteristics of materials and methods of sensing the imminence of fires, as well as mitigating those fires which might occur all require detailed information as to how flammability and extinction processes are affected by reduced gravitational body forces and ambient environments that can be significantly different that those on earth. The effects of these differences have not been fully characterized under conditions that supply sufficient results to determine the best means of optimizing fire safety related issues. Both experiments and modeling results can provide insights to developing optimal approaches and to defining fire safety related materials criteria and sensing/control methodologies.

Liquid flammables produce particular fire safety problems when liquids under pressure are released (formation of aerosols) and/or spills occur accidentally into inhabitable environments on earth as well as under reduced gravity conditions. Methodologies involving the inert dilution of the atmosphere to reduce oxygen index beyond what will support combustion (without precluding biological activity), addition of flame and ignition inhibitors to the liquid phase, and/or addition of flame and ignition inhibitors to the gas phase are individually, and in concert, techniques for enhancing fire safety on earth. Investigations in earth's gravitational field have shown that the effectiveness of a particular methodology is at least locally coupled with natural convective effects produced by the ignition and combustion event. The variation of this coupling in reduced gravity conditions can change the relative effectiveness of various approaches, in some cases eliminating their consideration.

A simple example from our earlier work is that in drop tower investigations, we found that isolated droplets of n-heptane would continue to burn at reduced oxygen indices created by nitrogen dilution that were much lower than the limiting value in earth's gravity field. In fact, the limiting value under microgravity conditions appeared to be below that necessary to sustain biological activity. This critical result has not been completely investigated, nor has similar research on limiting oxygen index ever been conducted (either experimentally or numerically) using isolated droplet combustion under reduced gravity in combination with the use of inhibiting additives and other inerts such as helium. The combination of helium with inhibiting additives either in the liquid or gas phase, appears to have promise for reducing the fire potential in inhabitable environments during human exploration endeavors. Experiments such as these are easily accommodated within the range of parameters available in the Multi-Droplet Combustion Apparatus (MDCA) being readied for use on the International Space Station (ISS). Experimental measurements permit assessment of ignition, burning rate, flame characteristics, and

extinction against which the other more complex geometric configurations can be compared. Indeed MDCA facilities and methodologies could also be adapted to investigate spherical solid material combustion properties. It has also been well established that slow convective flows under reduced gravitational environments can drastically alter the combustion and extinction characteristics of liquid droplets, and sphero-symmetric modeling studies are presently being expanded to consider two dimensional steady convection field conditions surrounding an isolated burning droplet.

To preliminarily assess the feasibility and potential mechanisms of fire suppression by CO_2 in non-buoyant systems, we recently conducted a series of numerical experiments involving CO_2 dilution. A 2-mm n-heptane droplet was ignited under normal ambient conditions (air at 1 atm) and was computed for sufficient times to establish an initial flame structure (~10 ms). After that, the simulation was restarted with different far-field gas compositions, composed of varying amounts of CO_2 and air. As expected, at elevated levels of CO_2 in the far field, burning rate decreased, and at high levels of CO_2, flame extinction was observed. The extinction event correlated with flame-zone concentrations of CO_2 near 27% and appears to result from reduced temperature and chemical rates within the flame structure as a result of an increase in local heat capacity. As CO_2 delivery to the flame zone controls the system dynamics, the absolute location of the computationally-defined "far-field" dominates the overall system response in terms of the necessary characteristic time associated with CO_2 diffusion into the flame structure. The implication is that highly-localized delivery mechanisms may be required to extinguish an isolated heterogeneous combustion event. The suppression of flame propagation, on the other hand, is a more feasible use of introducing high heat capacity diluents. In low gravity environments, forced convection may have significant influence on the effectiveness of diluents on extinction processes.

Isolated droplet combustion experiments and modeling with and without relative gas phase convection can be utilized to evaluate the influence of convection of the effectiveness of various fire suppression methodologies. Future efforts using isolated droplet burning experiments and numerical modeling tools can:

1. Map flammability boundaries including Limiting Oxygen Index (LOI) for well-characterized combustion events under varying gravitational accelerations.
2. Measure the effects of inert-substituted environments on the burning rates, flame structure, and extinction conditions, as functions of gas phase composition, including substituted diluents, dilution by increased diluent addition, and the presence of additives that may chemically inhibit combustion.
3. Experimentally investigate fuel additives that could lead to fire-safe fuels while operating as efficient propulsion source.
4. Investigate the effects of slow convection on the above characterizations.
5. Develop predictive numerical codes and chemical kinetic schemes to model flammability boundaries as a function effective gravitational acceleration and the unique ambient conditions encountered in space exploration applications.

ELECTRIC-FIELD-DRIVEN PHENOMENA FOR MANIPULATING PARTICLES IN MICRO-DEVICES

Boris Khusid
New Jersey Institute of Technology
University Heights, Newark, NJ 07102
Phone: 973-596-3316; Email; khusid@adm.njit.edu

Andreas Acrivos
The City College of New York
140th Street & Convent Avenue
New York, NY 10031
Phone: 212-650-8159; Email: acrivos@scisun.sci.ccny.cuny.edu

Compared to other available methods, ac dielectrophoresis is particularly well-suited for the manipulation of minute particles in micro- and nano-fluidics. The essential advantage of this technique is that an ac field at a sufficiently high frequency suppresses unwanted electric effects in a liquid. To date very little has been achieved towards understanding the micro-scale field-and shear driven behavior of a suspension in that, the concepts currently favored for the design and operation of dielectrophoretic micro-devices adopt the approach used for macro-scale electric filters. This strategy considers the trend of the field-induced particle motions by computing the spatial distribution of the field strength over a channel as if it were filled only with a liquid and then evaluating the direction of the dielectrophoretic force, exerted on a single particle placed in the liquid. However, the exposure of suspended particles to a field generates not only the dielectrophoretic force acting on each of these particles, but also the dipolar interactions of the particles due to their polarization. Furthermore, the field-driven motion of the particles is accompanied by their hydrodynamic interactions. We present the results of our experimental and theoretical studies which indicate that, under certain conditions, these long-range electrical and hydrodynamic interparticle interactions drastically affect the suspension behavior in a micro-channel due to its small dimensions.

A STUDY OF COLLOIDAL CRYSTALLIZATION

Wesley M. Kopacka, Andrew D. Hollingsworth, and William B. Russel
Department of Chemical Engineering, Princeton University 08544

Paul M. Chaikin
Department of Physics, Princeton University 08544

One of the still open problems in condensed matter physics today is that of crystallization.[1] The ability to accurately study atomic or molecular crystallization is hindered by the incredibly small length and time scales involved compared to many of the experimental techniques available today. On the biological front, determining the structure of the more than 80,000 proteins in the human body is limited by our inability to crystallize proteins effectively. As a result, only 4000 human protein structures have been solved. Nanotechnologies such as photonic band gap materials and photothermal nanosecond light-switches rely heavily on being able to control crystallization to achieve particular packing structures, spacings, and sizes. A firm understanding of the thermodynamic and kinetic driving forces is therefore essential in fabricating products with specific properties. Model systems to study the physics behind the phase behavior, structure, and dynamics of crystallization are needed to shed light to the various applications being studied today.

Colloidal suspensions may be considered ideal model systems because of the significant amount of knowledge and advances that have occurred in colloid science. In addition, colloidal length and time scales can be easily explored with many common instruments used today. Colloids are already being used to model protein crystallization and are the precursors for most nano-devices being developed. However, current research on the crystallization of high-density model colloidal suspensions has yet to produce definitive conclusions on the kinetics for nucleation and growth mechanisms in the various phases. Results for different "model" systems often differ, raising questions as to whether the system is actually a well-defined "model", experimental techniques are inaccurate, or assumptions are incorrect. Recently, microgravity experiments on colloidal crystallization[2,3] revealed dendrites in the coexistence regime and crystallization in the usually "glassy" region of the hard sphere phase diagram, both of which were never before observed in ground-based experiments. This posed yet another question as to the role that gravity plays in crystallization. Although it would be ideal to perform these experiments in a microgravity environment where the effects of convection and buoyancy are not present, a suitable alternative is to index- and density-match the particles and solvent to which the equivalence of a milligravity environment is achieved. The presence of crystals well into the glass regime has been observed recently in a ground-based experiment in which index and density matching was utilized to simulate milligravity.[4] Performing experiments in these conditions will also provide insight and direction for studies using the PCS+ (Physics of Colloids in Space+) aboard the International space station in 2005.

My research details a thorough, quantitative analysis of the kinetics of hard sphere colloidal crystallization, reducing the effect of gravity by density-matching the particles and solvent. The primary tool is the PHaSE (Physics of Hard Spheres Experiment) multi-functional light scattering apparatus flown on board two MSL-1 (Microgravity Science Laboratory-1) missions

in 1997, STS-83 and STS-94, which now resides in the Princeton Materials Institute at Princeton University. Recently, experiments have also been performed using the PCS+ instrument, an upgraded version of the PHaSE instrument that will be used for the mission currently scheduled to fly at the end of 2005. Nucleation and growth can be followed accurately over long periods of time with the PHaSE/PCS+ instruments and index/density-matched suspensions. The following phenomena are being studied: (1) the growth mechanisms in the coexistence regime, (2) the formation of dendrites near freezing, and (3) the crystallization of "glassy" samples. The exhaustive quantitative studies of these phenomena under milligravity conditions fill an important void in the scope of crystallization behavior previously studied under normal gravity and future micro-gravity data from the PCS+ mission.

---

[1] Cheng, "Colloidal hard sphere crystallization and glass transition," Thesis, **1998**.
[2] Zhu, Li, Rogers, Meyer, Ottewill, STS-73 Space Shuttle Crew, Russel, & Chaikin, *Nature*, 387: 883-885, **1997**.
[3] Cheng, Zhu, Russel, Meyer, & Chaikin, *Applied Optics*, 40(24): 4146-4151, **2001**.
[4] Kegel, *Langmuir*, 16: 939-941, **2000**.

CONTACT INFORMATION

Mr. Wesley M. Kopacka
Graduate Student

Princeton University
Department of Chemical Engineering
A-217 Engineering Quadrangle
Princeton, NJ 08544

wkopacka@princeton.edu
609-258-2123 (office)
609-258-6878 (fax)

POSITIONING OF SIMULATED VAPOR BUBBLES IN MICROGRAVITY BY THE KELVIN FORCE

John Kuhlman[+], Donald D. Gray[*], Shannon Glaspell[#], Paul Kreitzer[#], Charlie Battleson[#], Michelle Lechliter[#], Michael Campanelli[#], Nicholas Fredrick[#], Christopher Sunderlin[#], Brianne Williams[#]
West Virginia University, Morgantown, WV 26506

[+]Professor, and [#]Undergraduate Student, Department of Mechanical and Aerospace Engineering
[*]Professor, Department of Civil and Environmental Engineering

INTRODUCTION

Experiments were performed in July 2003 in the NASA "Weightless Wonder" KC-135 aircraft through the Reduced Gravity Student Flight Opportunities Program, to study the influence of the magnetic Kelvin force on the behavior of air bubbles in a paramagnetic liquid in microgravity (μ-g). This aircraft, which flies through a series of parabolic arcs providing about 20 seconds of μ-g per parabola, allowed a unique environment in which to study the resultant phenomena. The experiment was conceived, designed, constructed, and performed by the WVU student team and their advisors.

When there is no dominant body force such as gravity to produce a buoyant force, vapor bubbles that form may remain adjacent to heat rejection surfaces, rather than be driven away due to buoyancy. This reduces the heat exchange rates and can cause burnout or damage the surface that needs to be cooled. The experiment modeled one possible method for repelling the vapor bubbles on a heat rejection surface in μ-g. In the presence of a non-uniform magnetic field, a body force, known as the Kelvin force, is exerted on all magnetically permeable materials. Diamagnetic and paramagnetic fluids are repelled from and attracted to magnetic fields, respectively. The Kelvin force is approximately three orders of magnitude larger for liquids than for gases, leading to a magnetic buoyancy force on bubbles in a liquid.

HYPOTHESIS

This experiment used the Kelvin force to control the position of air bubbles in a 4.9 molar solution of manganese chloride $MnCl_2$ (simulated coolant), which is a paramagnetic liquid. Air bubbles were injected into the bottom of two geometrically identical tanks, one fitted with a 2,000 gauss permanent magnet at the bottom of the tank, and one without a magnet. The Kelvin force exerted on the liquid has been estimated to be approximately 0.28 g. The resulting bubble formation, detachment, and motion were video taped for both tanks under identical gravitational accelerations. In μ-g, it was expected that the Kelvin force would attract the liquid towards the magnet located at the bottom of the tank, thereby driving the air bubbles (simulated vapor bubbles) away from the bottom of the tank.

RESULTS

Results indicated that air bubbles within the magnet tank could be repelled from the magnet surface through the use of the Kelvin force to attract the liquid to the surface. This conclusion was valid for all parabolas for which the free surface of the $MnCl_2$ solution did not invert in the tanks due to small negative-g conditions, and for which the air flow rate was large enough to cause bubbles to flow into both tanks during the microgravity portion of each parabola. Several types of flows were observed during the course of the experiment due to variations in gravity levels onboard the KC-135, as well as variations in air flow from the syringe pump.

For the first type of flow that was recorded, it was observed that as the air bubbles flowed into the geometrically identical tanks at identical flow rates, the control tank (no magnet) allowed the bubbles to become relatively large (~1 cm) before breaking away from the bottom surface of the tank and slowly floating toward the free surface. In the magnet tank, however, the air bubbles were observed to remain smaller (~2-3 mm) and to be more numerous, to detach from the bottom of the tank, and to be forced toward the free surface much more quickly. Sample captured video images of this flow type are shown in Fig. 1 (Day 1, Parabola 33, 8 mm camera) and Fig. 2 (Day 1 Parabola 33, NAC HSV-500C high speed camera at 500 fps).

The second type of flow that was observed also supported the general conclusion that the Kelvin force could repel the air bubbles from the surface of the magnet. However, for this flow situation, bubbles were not pushed completely to the free surface in the magnet tank. Instead, bubbles were forced away from the magnet surface and remained within the fluid at some distance from the magnet surface. This was caused by negative fluctuations in gravity that reduced the momentum of the air bubbles moving toward the free surface, causing a change in direction. Often, in this circumstance, the control tank bubbles would rest on the tank bottom.

For several parabolas, there was a period of negative gravity. The free surface within the tanks would invert, preventing bubble formation. Sometimes, the negative gravity would "prime" the syringe pump, allowing the bubbles to more easily flow into the tanks once the liquid had returned to the bottoms of the tanks. The data collected from these parabolas was not discarded if there were periods of zero gravity either directly before or after the inversion, and bubbles were observed in both tanks once the period of inversion ended.

The double syringe pump used for the experiment was expected to function in microgravity similar to how it did with Earth gravity. However, once in flight, the lower flow rates (below approx. 1 mL/min) were found to be inadequate under microgravity conditions to drive out the liquid solution that entered the air supply tubes during the 1.8-g pull out portions of the parabolas. Generally, better results were obtained at the higher air flow rates (5-15 mL/min).

The recorded data from the WVU Crossbow model CXLO4LP3 three-axis accelerometer and on-board NASA accelerometers provided useful information as to the duration and variations of gravity levels experienced during the experiment. Fig. 3 shows an example of measured gravitational acceleration levels from the Crossbow accelerometer data (with a raw output voltage of 2.32-2.33 volts corresponding to zero-g; see voltage display in Fig. 2) for an entire parabola. Fig. 4 zooms in on a typical period of zero gravity; computed mean and RMS values are listed.

The apparatus functioned as designed for 28 of the 67 total zero-g parabolas flown over the 2-day period, where bubbles were observed simultaneously in both tanks and the liquid was not inverted. For these 28 parabolas, the Kelvin force successfully repelled the bubbles from the bottom of the tank for all but one, or possibly two cases. At least 18 other parabolas had bubbles in one tank or the other, with bubble size and motion consistent with the other 28 parabolas. The remaining 21 parabolas had syringe pump flow rates that were too low to generate air bubbles.

Fig. 1: Flow Type 1 (Day 1 Parabola 33, 8 mm camera).

Fig. 2: Flow Type 1 (Day 1 Parabola 33, high speed).

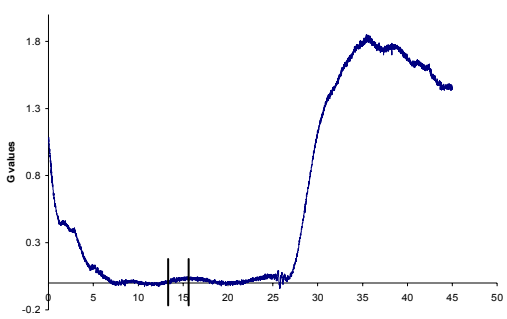

Fig. 3: Accelerometer Data (Day 1, Parabola 33).

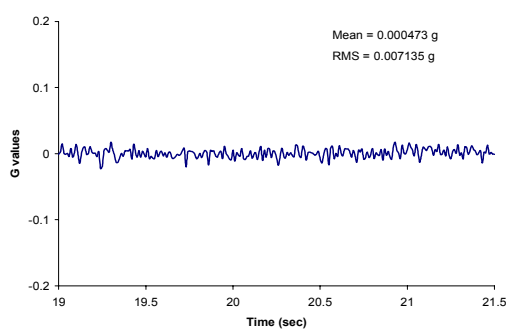

Fig. 4: Accelerometer Data (zoomed in on zero-g portion).

AC ELECTROKINETIC JETS AND SPRAYS FOR SPACE APPLICATIONS

Dmitri Lastochkin, Ping Wang, and Hsueh-Chia Chang
Department of Chemical and Biomolecular Engineering
University of Notre Dame
Notre Dame, IN 46556

New mechanisms for ejecting drops and bubbles using high-frequency AC electric fields are reported for: (i)-generating micron-sized liquid drops of electrolytes in air and (ii)-generating a micron-sized bubble jet in an electrolyte within a microfluidic device.

(i) AC Electro-sprays: The new AC electrospray ejects drops from a meniscus at the tip of a capillary filled with the liquid to be sprayed. A needle electrode is inserted into the capillary such that its tip is just behind the meniscus. The other electrode is on the air side a short distance beyond the meniscus. When a high voltage (1000 V to 2000 V) AC field is activated, a micro-jet forms intermittently at the meniscus and ejects drops. Unlike DC electro-sprays, these drops are larger and are electro-neutral. In contrast, DC electro-spray, which is widely used in the pharmaceutical industry in conjunction with a mass spectrometer for drug testing, generates only charged liquid drops. The electro-neutral drops generated by the current high-frequency AC electro-spray immediately extend the utility of electro-sprays to a much wider area of potential application. Its negligible current and wattage also imply that the spray can be driven by miniature and portable power packs and without consuming much power from the on-board power sources. DC electrosprays are currently used to position and stabilize space crafts. The larger drop size and the electro-neutral drops of the AC spray should allow more precise and yet stronger manipulation actions. Possible other space applications include dispensing contents of biochips and medical diagnostic chips into on-board analytical instrument.

(ii) Micro-bubble Jet Pump. A new micron-sized bubble jet in an electrolyte within a microfluidic device is reported. An intense (1000 V) AC high-frequency electric field is established between two orthogonal line electrodes (less than 25 microns in diameter) with a large peak-to-peak voltage drop. This intense field at the tip triggers a local electrolysis reaction that generates small bubbles at the tip at high speeds. The field also shapes each air bubble into a sharp cone and then pinches it off at high rates to form a jet consisting of a stream of fast-moving bubble train. These bubbles stream off the cone tip at velocities higher than 10 cm/second and drag the surrounding liquid with it. This produces a two-phase jet of bubble and liquid with a linear velocity in excess of 10 cm/second. The jet also drives a high-intensity vortex around it. The streaming bubbles are less than 10 microns in diameter and quickly dissolve into the electrolyte. The bubbles hence do not accumulate within the micro-fluidic device. The metal loss from the electrode due to reaction and the resulting contamination are also negligible. The jet can be used as a microfluidic pump to transport fluids in micro-heat exchangers, fuel cells, CPU cooling, biochips in space crafts and space stations. It functions well in micro-gravity environments and is hence ideal for space applications. It does not contaminate the liquid and requires only a miniature power source ideal for space application.

PHOTOREGULATED ELECTRON TRANSFER AT BIO-INORGANIC INTERFACES

Nikolai Lebedev[1,2], Scott A. Trammell[1] Anthony Spano[2]
[1]US Naval Research Laboratory, [2]University of Virginia

Efficient connection between bio- and inorganic materials is crucial for the development of new generation of photo-, chemo- and bio-sensors, power sources, information processing devices, and ultimately will lead to the construction of integrated bio-computer hybrids. The main problem in the construction of such bioinorganic devices is the electrical connection between biomolecules and semiconductors or metals, and viability of the protein after immobilization. In the present work using genetically engineered proteins and specifically synthesized organic linkers, we were able to construct self-assembling aligned biomolecular surfaces on various metals and semiconductors, including gold, ITO, glasses, porous SnO_2, carbon nanotubes, and in artificial lipid membranes. Using bacterial photosynthetic reaction centers (RCs) as an active protein, we were able to demonstrate that after immobilization on the surfaces this protein can operate as a photosensor, optical switch, or photovoltaic device for local power generation. Our experimental results have shown that after binding to an electrode, photosynthetic RCs are able to undergo efficient photoinduced charge separation, operate as a photorectifier and transfer current only in only one, protein orientation-dependent direction. Part of the protein (H-subunit) acts as an insulator and must be removed for substantial improvement of the protein performance. Electron transfer in the constructed devices follows a tunneling mechanism and can be described by integrated Marcus' formalism. It shows an exponential dependence of the rate of electron transfer on the distance between RC and electrode and demonstrates rather low reorganization energy.

Two ways of oriented binding of photosynthetic RC to electrode and the structure of the linkers

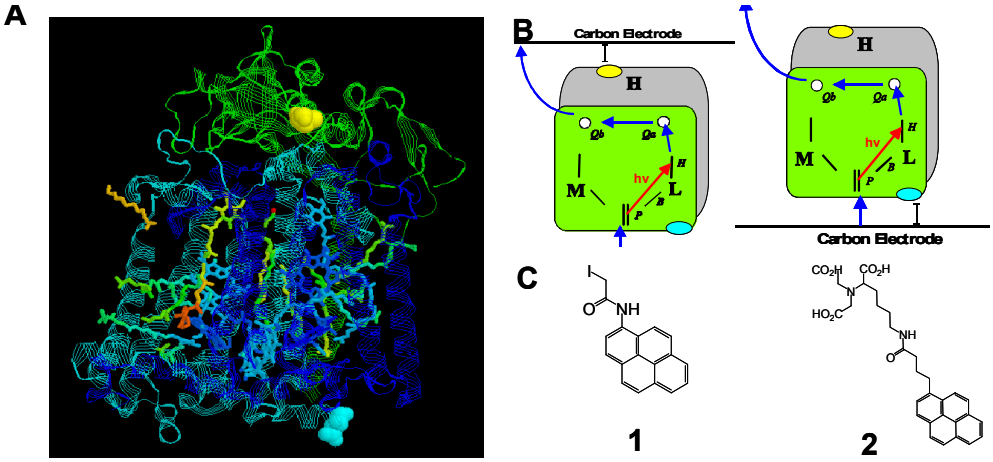

Effect of protein orientation on the efficiency and direction of photocurrent at the electrode:

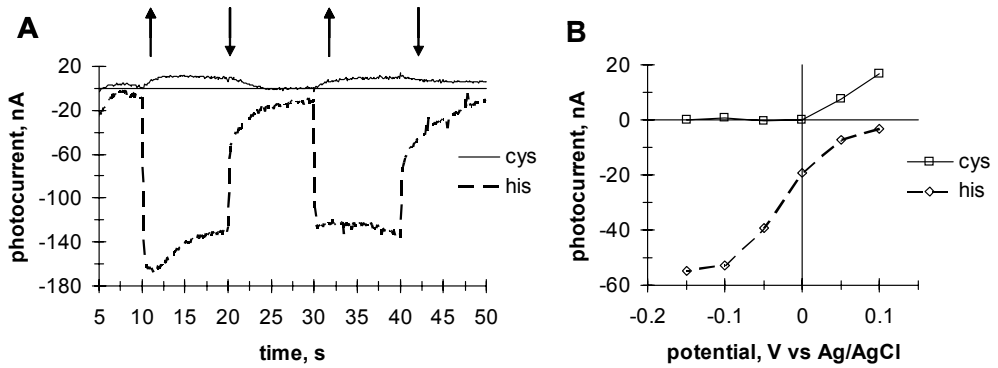

Effect of the distance and driving force on the efficiency of electron transfer between RC and the electrode:

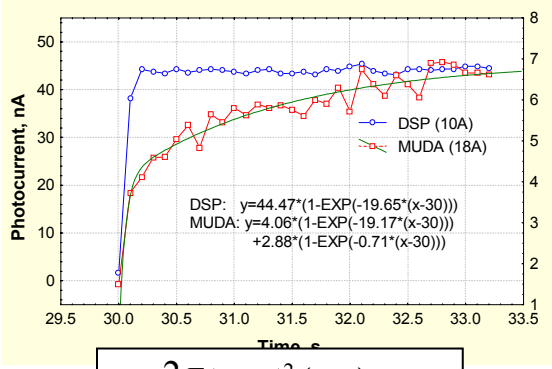

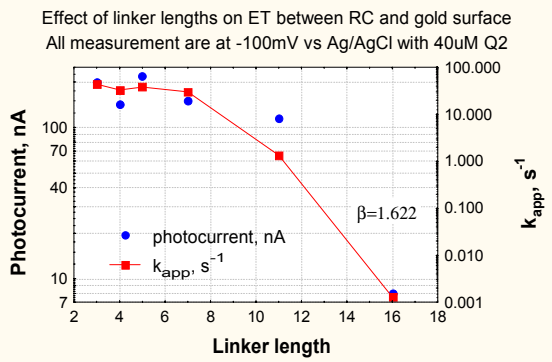

$$k = \frac{2\pi}{h}\left|H_{DA}\right|^2 (FC)$$

$$\left|H_{DA}\right|^2 \propto \exp\left[-\beta\left(R-Ro\right)\right]$$

$$FC \propto \exp\left[-\frac{(\lambda - \Delta Go)^2}{4\lambda RT}\right]$$

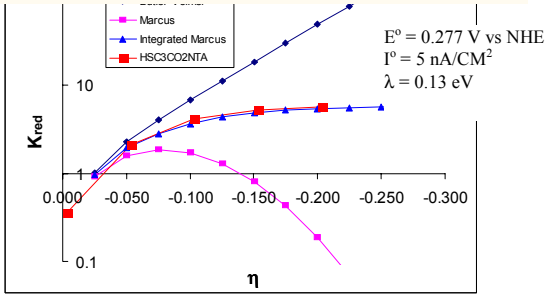

MIMICKING MICROGRAVITY IN BIO- AND NANO-COLLOIDAL SYSTEMS USING SUPERCRITICAL CARBON DIOXIDE

C. Ted Lee, Jr.
Department of Chemical Engineering, The University of Southern California
925 Bloom Walk, HED 207, Los Angeles, CA, 90089-1211
Phone: (213) 740-2066, Fax: (213) 740-8053, tedlee@usc.edu

Density modulation of highly-compressible supercritical carbon dioxide ($scCO_2$) will be used to minimize density differences in $scCO_2$-surfactant mixtures, thereby providing a simple, ground-based approach for approximating microgravity conditions in colloidal and interfacial systems. Density matching will allow investigation of the effects of microgravity on the surface phenomena of complex fluids, suspensions, and multiphase systems, with specific emphasis on interactions between nanometer-sized colloids and nanocolloidal aggregation. Recently, a variety of nanometer-scale surfactant morphologies have been discovered in $scCO_2$ – including spherical and cylindrical microemulsions. By adjusting the density of CO_2 to match that of the water/surfactant phase, the effects of gravity vanish, allowing an investigation of the impact of microgravity on the fluid dynamics and interfacial phenomena of colloidal systems. Specifically, the influence of effectively-reduced gravity on electrostatic and intermolecular interactions, colloidal aggregation, and the *microemulsion* critical point can be realized. It has been known since the early 20th century that gravity effects strongly couple with the critical phenomena of pure fluids, fluid mixtures, and colloidal systems – a result of large concentration (i.e., density) gradients that develop at the critical point due to molecular or colloidal aggregation. This proposal will allow critical phenomena to be studied independent of gravity in a ground-based experiment.

We have investigated the effect of mimicking microgravity in water-in-CO_2 microemulsions, as shown in Figure 1.

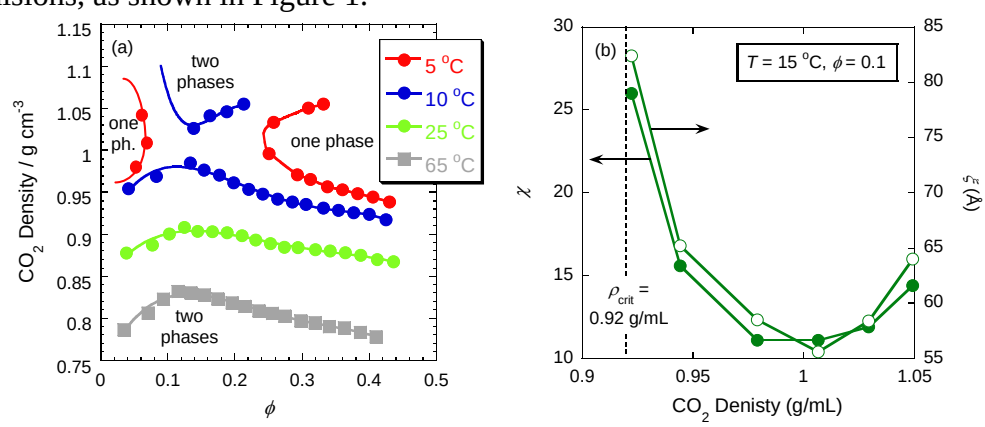

Figure 1. (a) Phase behavior of W/C microemulsions as a function of CO_2 density, temperature, and droplet volume fraction, ϕ, and (b) osmotic susceptibility χ and correlation length ξ determined from neutron scattering

Matching the density of CO_2 to that of water and, thereby, diminishing buoyancy effects has a profound influence on the microemulsion properties. For example, the microemulsion phase-behavior data demonstrate a rather unique phenomenon, namely the coupling of two *microemulsion critical points* to form a so-called "hourglass" cloud-point curve at a water-matched CO_2 density of approximately 1.0 g/mL and a temperature of 5 °C. Furthermore, the onset of nanodroplet clustering can been seen from the osmotic susceptibility (χ) and correlation length (ξ) determined from neutron scattering. As the microemulsion critical point is approached both χ and ξ diverge to large values. This well-known phenomenon can be understood by recalling that the correlation length is a measure of the average size of the aggregated droplet clusters. Thus, the cluster size diverges as the critical point is approached. Interesting, however, is the minima observed for both the osmotic susceptibility and correlation length at a CO_2 density of approximately 1.0 g/mL. These minima may be a result of coupling the effects of gravity with the critical phenomena, due to the large density gradients that develop with cluster formation. Under the influence of gravity, larger droplet clusters are expected to settle at faster rates, thus, sweeping past and incorporating smaller clusters, potentially resulting in an enhancement of the critical/clustering phenomena. Thus, the observed minima in the susceptibility (interaction strength) and correlation length (cluster size) likely results from diminished gravity effects under simulated (i.e., density matched) microgravity. Indeed, previous space-based studies have revealed that under microgravity conditions in the absence of sedimentation, unique colloidal ordering and crystallization – of which colloidal clustering is the first step – can be observed in systems that show no such abnormalities under earth gravity.

Knowledge of the microemulsion critical phenomena will serve as a gateway to allow study of colloidal critical phenomena under simulated microgravity in our laboratory. Furthermore, the discovery of the microemulsions phases mentioned above has laid the groundwork for the formation of more complex, liquid crystalline phases in surfactant-scCO_2 systems. These surfactant morphologies hold promise in ground-based studies of protein crystallization, where density matching to reduce buoyancy-driven convection will result in a process that is diffusion-dominated, thereby potentially producing large, high quality crystals of membrane proteins. It is important to point out that the phenomena of microemulsion criticality and protein crystallization both involve nanocolloidal aggregation, whether to form droplet fractals or protein crystals. Indeed, the fundamental similarly between these two seemingly-different processes points to the importance a ground-based technique for studying mimicking microgravity could have on future NASA missions, as well as for technological advancement here on Earth.

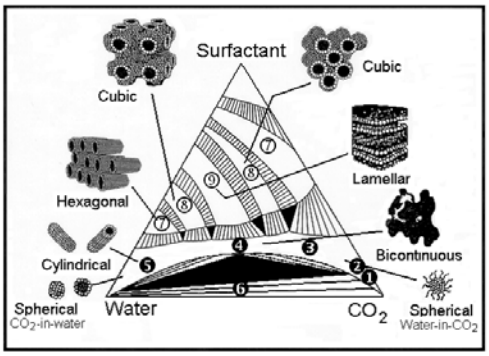

Figure 2. Schematic illustration of the various surfactant phases expected in surfactant/water/CO_2 systems that could be used to crystallize proteins under microgravity.

THERMOACOUSTIC CONVECTION AND TRANSPORT IN GASES AND NEAR-CRITICAL FLUIDS UNDER NORMAL AND MICRO-GRAVITY CONDITIONS

Yiqiang Lin, Zhiheng Lei, and Bakhtier Farouk*
Department of Mechanical Engineering and Mechanics, Drexel University, Philadelphia, PA.
*e-mail: bfarouk@coe.drexel.edu; fax: 215 895 1478; phone: 215 895 2287
Elaine S. Oran
Naval Research Laboratory, Washington, D.C

ABSTRACT

The recently initiated research project is aimed at studying thermoacoustic and buoyancy-driven transport in gases and near-critical fluids at normal and reduced gravity environments. Large-scale detailed computational models are being developed to simulate and understand the complex phenomena, and thereby analyze the heat and mass transport in gases and near-critical fluids under both microgravity and normal gravity conditions. Normal and reduced gravity experiments are being designed where careful measurements and visualization studies will be carried out to characterize thermoacoustic waves in gases and near-critical fluids. Ground-based reduced gravity experiments will be carried out in the 2.2 s drop tower at the Glenn Research Center.

When a compressible fluid is suddenly exposed to a localized heat flux, part of the fluid in the immediate vicinity of the boundary expands. This gives rise to a rapid increase in the local pressure, leading to the production of pressure waves called thermoacoustic waves. Thermal convection induced or augmented by acoustic waves is termed as 'thermoacoustic convection'. In real gases, the heat transfer and fluid dynamic effects of thermoacoustic waves are only significant when the heat addition is rapid and the gravitational effects are reduced. We shall investigate the thermoacoustic wave characteristics in different real gases in normal and reduced gravity environmnents. Preliminary solutions of two-dimensional thermoacoustic wave generation and propagation in a nitrogen-filled (at normal temperature and pressure conditions) squre enclosure is shown in Figures 1(a) - 1(d). The left wall was rapidly heated (with a linearly varying temperature profile along the vertical axis).

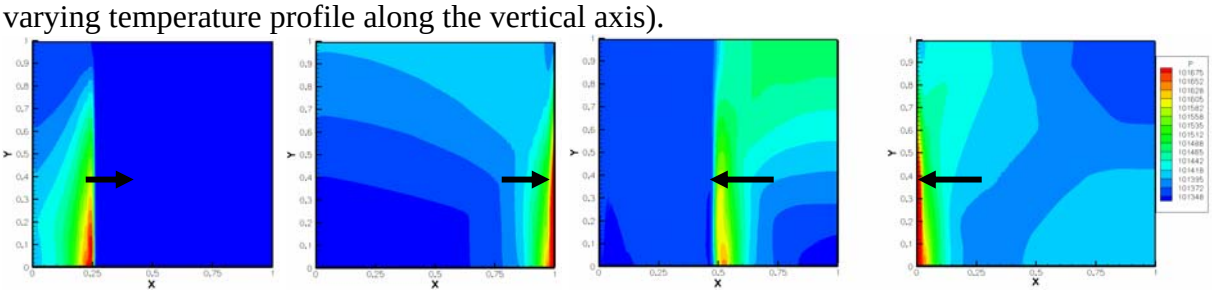

(a) (b) (c) (d)

Figure 1. Thermoacoustic wave propagation in nitrogen due to rapid heating of the left wall

In near-critical fluids, the highly compressible nature coupled with the high density significantly enhances heat and mass transfer due to any temperature perturbation and the resulting thermoacoustic wave. This effect is also known as the *Piston Effect.* This effect is difficult to study in normal gravity, as even very small temperature increase in supercritical fluid

gives rise to large buoyancy effects (high Rayleigh Number) due to the very small values of thermal diffusivity of near critical fluids. Interesting property variations of carbon dioxide near its critical point are shown in Figures 2(a) and 2(b).

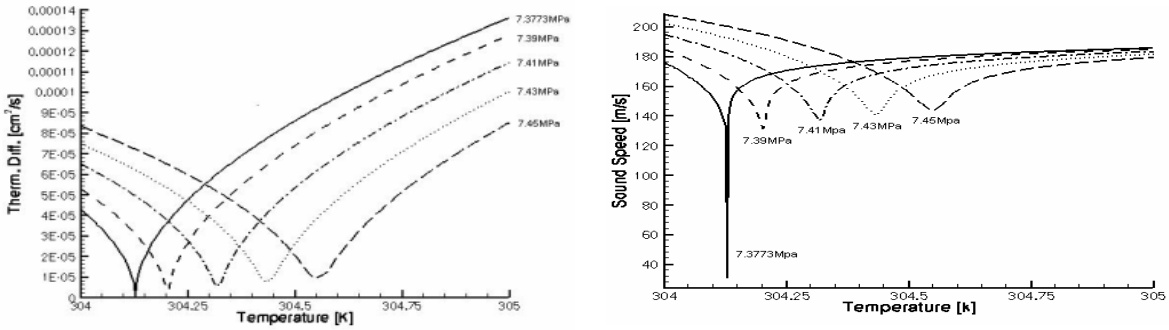

(a) (b)

Fig. 2 Thermal diffusivity and the sound speed of near-critical carbon dioxide[1]

Mildly supercritical fluids (at pressures and temperatures slightly above the critical point) exhibit specific behaviors that make them attractive for both fundamental science and industrial applications. The generation and propagation of thermoacoustic waves in slightly supercritical carbon dioxide will be investigated by solving the fully compressible form of the Navier-Stokes equations. The thermodynamic properties of the slightly supercritical carbon dioxide will be calculated using the NIST standard reference database 12[1].

A schematic of the proposed experimental set up for studying thermoacosutic waves in real gases is shown below in Figure 3. The thermoacoustic waves will be generated and propagated inside a cylinder. A resistance-capacitance circuit will be used to rapidly heat a thin foil that constitutes one end of the cylinder. By carefully choosing the foil, the capacitor and the discharge voltage, we can get different temperatures in the foil and different heating rates.

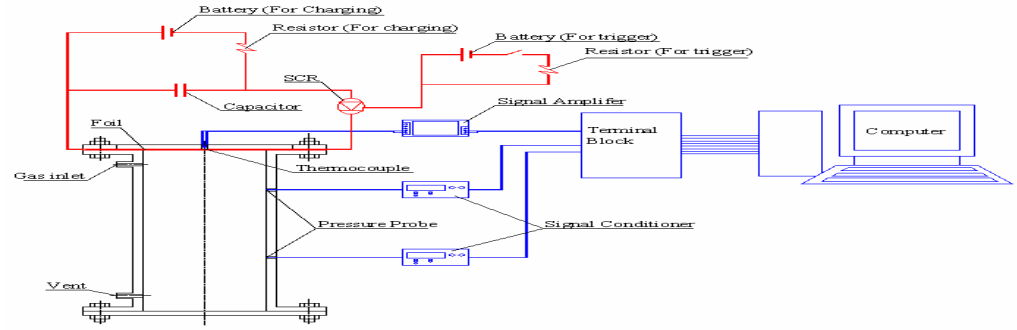

Fig. 3. Schematic of the experimental set up to study thermoacoustic waves in real gases

Experiments will be first carried out under normal gravity conditions. Similar experiments are also planned for enclosures filled with mildly super-critical carbon dioxide. For both real gases and super-critical fluids, experiments will be carried out at ground based reduced gravity experimental facilities.

References

1. Lemmon, E. W., Peskin, A. P., McLinden, M. O., and Friend, D. G. 2000. NIST Thermodynamic and Transport Properties of Pure Fluids, U.S. Department of Commerce, Gaithersburg, MD.

FLUID PHYSICS AND TRANSPORT PHENOMENA IN A SIMULATED REDUCED GRAVITY ENVIRONMENT

J. Lipa
Physics Department
Stanford University
Stanford, CA 94305

We describe a ground-based apparatus that allows the cancellation of gravity on a fluid using magnetic forces. The present system was designed for liquid oxygen studies over the range 0.001 - 5 g's. This fluid is an essential component of any flight mission using substantial amounts of liquid propellant, especially manned missions. The apparatus has been used to reduce the hydrostatic compression near the oxygen critical point and to demonstrate inverted phase separation. It could also be used to study pool boiling and two–phase heat transfer in Martian, Lunar or near-zero gravity, as well as phenomena such as Marangoni flow and convective instabilities. These studies would contribute directly to the reliability and optimization of the Moon and Mars flight programs.

PI name: John Lipa
Physics Department, Stanford University, Stanford CA 94305
e-mail address : jlipa@stanford.edu
phone number 650-723-4562

A CONTINUOUS MICROCULTURE DEVICE FOR MONITORING THE EFFECTS OF SPACE ENVIRONMENTS ON LIVING SYSTEMS

R. Martineau, M. Piccini, and B. Towe
Harrington Department of Bioengineering
Arizona State University
Tempe, AZ, USA

We report our development of a microculture device that continuously cultures genetically engineered bacterial cells and monitors their response to environmental/chemical stimuli. Responses include changes in culture turbidity, pH, production of fluorescent proteins, and bioluminescence. Cells are maintained in a 10µl glass capillary by infusing microliter quantities of media and reagents using novel, miniature pumps and valves. Metabolic wastes are removed and nutrients delivered through microdialysis. Microbore tubing (150 µm i.d.) forms the fluidic interconnects between components and optical monitoring is accomplished using light emitting diodes as excitation sources and photodiodes as detectors. The system is housed in conventionally machined acrylics with dimensions of 3.0 x 8.9 x 0.6 cm^3. On-board electronics support data acquisition, power delivery, microfluidic component driving, and computer interfacing. All microfluidic components and media are on-board. The device uses a single link to a computer and contains media for a few days.

Applications for the device include the testing of potentially stressful stimuli (microgravity, radiations, etc.) for effects on life as well as automated biological assays. Ultimately, we aim to create an array of cultures which contains cells that are selectively responsive to fundamental stressors and to fingerprint an environment by probing bacterial responses via reporter fusions to stress-response pathways.

EFFECT OF VARIED AIR FLOW ON FLAME STRUCTURE OF LAMINAR INVERSE DIFFUSION FLAMES

M. A. Mikofski*
University of California Berkeley, USA
mikofski@me.berkeley.edu

L. G. Blevins, T. C. Williams, and C. R. Shaddix
Sandia National Laboratories, USA

The structure of laminar inverse diffusion flames (IDFs) of methane and ethylene in air was studied using a cylindrical co-flowing burner. Inverse diffusion flames are similar to normal diffusion flames, except that the relative positions of the fuel and oxidizer are reversed. Several flames of the same fuel flow-rate yet various air flow-rates were examined. Flame heights were obtained using visible images and measurements of hydroxyl (OH) laser-induced fluorescence (LIF). Radiation from soot surrounding the IDF was found to mask the reaction zone in visible images. As a result, flame heights determined from visible images were overestimated. The height of the reaction zone as indicated by OH LIF was shown to be a more relevant measure of height. The concentration and position of polycyclic aromatic hydrocarbons (PAHs) and soot were observed using LIF and laser-induced incandescence (LII). PAH LIF and soot LII indicated that PAH and soot are present on the fuel side of the flame, and that soot is located closer to the reaction zone than PAH. Ethylene flames produced significantly higher PAH LIF and soot LII signals than methane flames, which is consistent with the sooting propensity of ethylene.

Photographs of ethylene IDFs, shown in Fig. 1, demonstrate that flame height scales with air flow-rate. Radiating soot almost entirely covers each ethylene flame, and only a small portion of the blue region is visible near the base of each flame. Fig. 2 shows OH and PAH LIF of ethylene IDFs. The upside-down U shape in each panel of Fig. 2 is OH LIF, which indicates the location of the reaction zone. PAHs are present on the outer (fuel) side of the reaction zone. Fig. 3 shows soot LII images for the ethylene IDFs. PAH LIF is vaguely present in the LII images. The soot and PAH are present on the fuel side of the reaction zone, but the soot is closer to the reaction zone than the PAH.

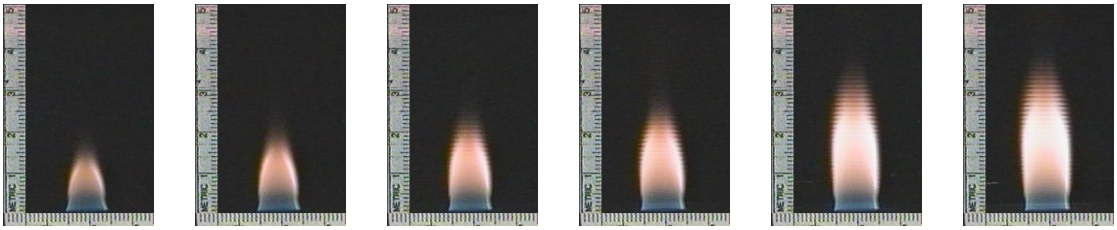

Q_{air} = 17 cc/s 20 cc/s 23 cc/s 27 cc/s 33 cc/s 37 cc/s

Figure 1. Visible images of ethylene IDFs.

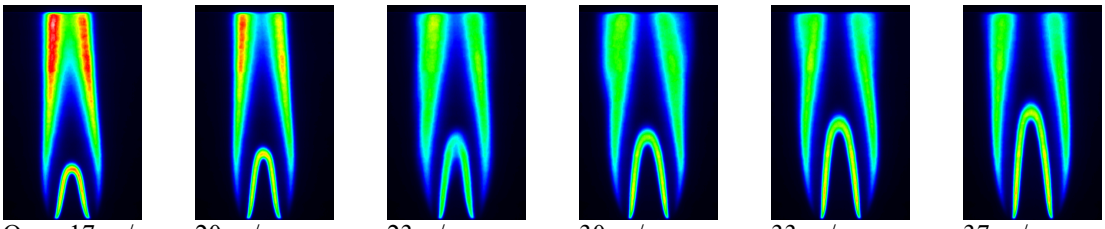

Q_{air} = 17 cc/s 20 cc/s 23cc/s 30 cc/s 33 cc/s 37 cc/s

Figure 2. OH and PAH LIF of ethylene IDFs.

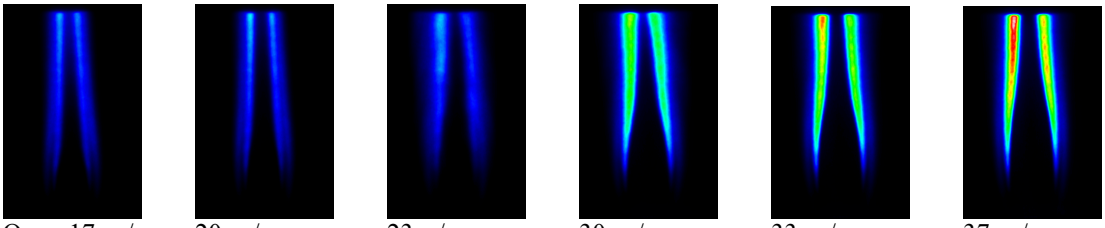

Q_{air} = 17 cc/s 20 cc/s 23cc/s 30 cc/s 33 cc/s 37 cc/s

Figure 3. PAH LIF and soot LII of ethylene IDFs.

LIGHT SCATTERING AND DIRECT VISUALIZATION STUDIES OF ANISOMETRIC COLLOIDAL AGGREGATES AND GELS

Ali Mohraz and Michael J. Solomon
Department of Chemical Engineering, University of Michigan, Ann Arbor, MI 48109-2136
(mjsolo@umich.edu)

ABSTRACT

Suspensions of anisometric colloids find widespread technological applications in areas such as the manufacturing of ceramics and the production of polymer/clay nanocomposites. Although often the functional properties of the final products rely on the anisometric shape of the colloids, the fundamental role of this parameter in mediating the microstructure and rheology of aggregated structures such as colloidal gels is poorly understood. To experimentally assess the effect of particle geometry on the morphology of such amorphous structures, colloidal boehmite rods of approximately monodisperse dimensions and aspect ratios in the range 5-30 have been synthesized. Aggregation is induced by the addition of electrolytes to aqueous suspensions and the structure of fractal aggregates in both the DLCA and RLCA regimes is characterized over three decades of the scattering vector by combined ultra-small, small, and wide-angle light scattering. The microstructure of rod aggregates in the DLCA regime shows an unexpected dependence on the geometry of primary particles [1], in contrast with the universal behavior of colloidal spheres. Monte Carlo simulations of rod aggregation corroborate this finding and the underlying mechanism for this unforeseen deviation is understood in light of the interaction of Brownian motion and anisotropic excluded volume of primary particles [1]. Furthermore, as the rod aspect ratio is increased, the structural distinction between the DLCA and RLCA aggregates is diminished. The implication of these structural anomalies in the internal dynamics of fractal networks is investigated by photon correlation spectroscopy.

Direct visualization of three-dimensional structure by confocal laser scanning microscopy (CLSM) provides a powerful means for investigating the effect of particle shape and orientation of the structure and dynamics of colloidal suspensions. Stable suspensions of fluorescent colloidal spherocylinders and ellipsoids in organic solvents have been prepared by the adaptation of literature methods. The sterically-stabilized polymeric colloids have been dispersed in density and refractive-index matching mixed organic solvents suitable for CLSM studies. Image processing algorithms for location of the centroid position and orientation angle of individual particles have been developed. By means of these methods, we investigate the distribution of rod orientations in suspensions and gels.

[1] Mohraz, A. D.B. Moler, R.F. Ziff and M.J. Solomon, "Effect of monomer geometry on the fractal structure of colloidal rod aggregates," *Physical Review Letters* **92**(15) 155503 1-4 (2004).

MECHANICAL PROPERTIES OF FINE PARTICLE ASSEMBLIES

Masami Nakagawa
Colorado School of Mines

We will present two in-house projects which will have direct relevance to in-situ space resources utilization. One of the aims of the first project is to measure mechanical properties of packed particles of different sizes and materials by measuring the wave velocity using piezoelectric sensors. Our results include preliminary measurements under microgravity environment using the NASA GRC drop tower facility. The second project is the feasibility study of mechanical properties of small scale assemblies of wet/cohesive granular materials by using micromanipulators. One of the driving questions for the second project is how to define mechanical properties of an assembly containing only a small number of particles but still behave as a collective solid. We can test the validity of extending our results of mesoscopic systems to predictions about macroscopic behavior, and so provide an alternative to bulk testing of precious extraterrestrial samples.

DIRECT NUMERICAL SIMULATION OF GAS-LIQUID SYSTEMS IN VARIABLE GRAVITY ENVIRONMENTS

Jean-Christophe Nave, Sanjoy Banerjee
Dept. of Mechanical Engineering, University of California, Santa Barbara, CA, USA, 93106
banerjee@engineering.ucsb.edu, phone: (805) 893-3456, fax: (805) 893-4731

Liquid films are present in many processes that occur in space applications. It is important to understand interfacial behavior as gravity becomes less important because, depending on the flow regime, interface motion may change dramatically. For instance, we observe enhancement of waves in film flow, when gravity decreases. An understanding of the influence of gravity as a controlling mechanism related to interface structure is important for both fundamental and design purposes. For instance, large topology changes of the gas liquid interface are responsible for enhancement of transfer processes. The types of problems studied here are of interest for condensers and evaporator performance in microgravity.

The numerical simulations presented here show different regimes in both gravity and micro-gravity environments where deformation of the gas/liquid interface is important. We use a finite difference method on a staggered grid, and the projection method to solve the Navier-Stokes equations. In order to deal with large density ratios, we use a ghost fluid method [1], This method allows for a sharp treatment of the interface and also, for first order accurate treatment of surface tension forces. Time integration is performed using a 3rd order Runge-Kutta TVD scheme. The numerical challenges associated with the problem of simulating gas/liquid systems are numerous. The aspect ratio of the waves demands that the physical domain be long, forcing us to use very fine nodalization. Also, the high density ratio between the gas phase and the liquid phase leads to poor convergence of the equations. We have developed a solution technique for the Poisson pressure equation that is quite efficient in this situation. We use a BiConjugate Gradient Stabilized method along with a Incomplete Lower/Upper preconditioner. Using periodic boundary conditions, we present two cases of a horizontal liquid film being driven by a pressure gradient, one with wall normal gravity, the other one with zero gravity.

The different simulations are performed in three-dimension and the interface is implicitly tracked using a level set method. Figure 1 shows interfacial waves on falling films at low Reynolds numbers (Re) that agree with experiments, providing validation of the methods. In order to illustrate the behavior of the physical system under different gravity conditions, some results, in which a high Re film on a shallow inclined plane (~0.25 degree) driven by gravity (Figure 2), are first shown. The interface stays quite flat while bulk vortices due to turbulence generated by wall shear, disrupt it. The effect of gravity in stabilizing the interface is apparent by comparison with Figure 3. Note that waves are steeper when the wall normal component of gravity is set to zero, as it is in this Figure.

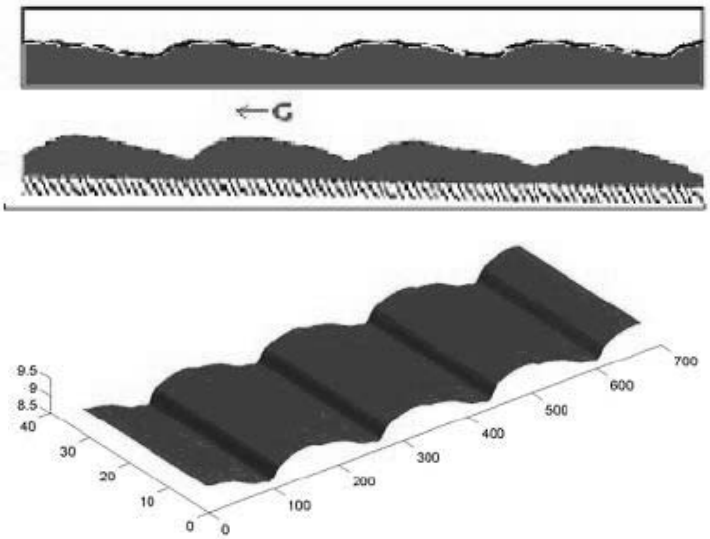

Figure 1: Comparison of simulation (top) and experiment (middle), and 3D view (Bottom)
Flow rate= 0.19 cm2/s, Wave Length= 0.85 cm, Wave velocity= 18.78 cm/s (Simulation)
Flow rate= 0.201 cm2/s, Wave Length= 0.8 cm, Wave velocity= 21.7 cm/s (Experiment)

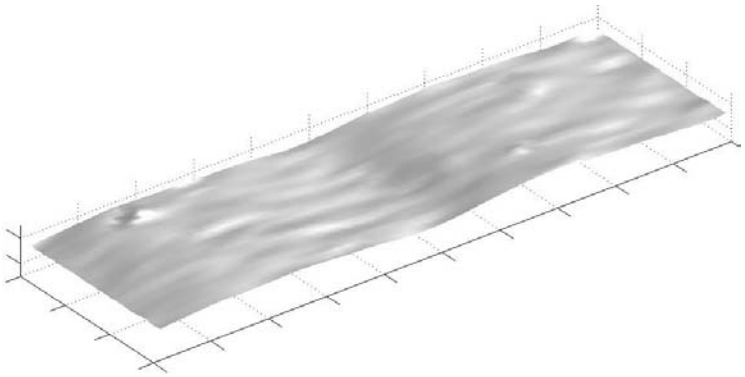

Figure 2: Interface deformations (bumps) from impinging coherent structures (looking at an angle from the top) at Re=1060.

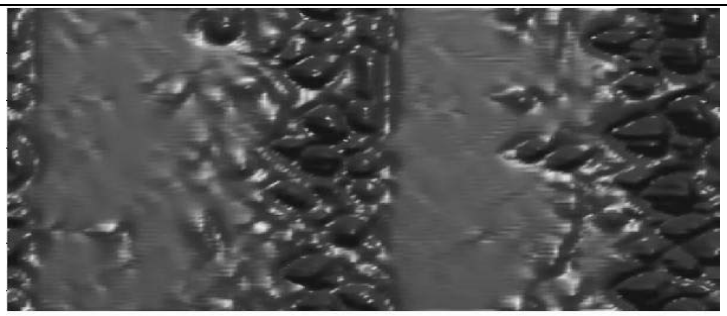

Figure 3: Interface deformation in absence of wall normal gravity at Re=1060 (looking down). Note 3D interfacial wave structure.

References

[1] Fedkiw, R. and Liu, X.-D.(1998), The Ghost Fluid Method for Viscous Flows, *Progress in Numerical Solutions of Partial Differential Equations*, Arachon, France, edited by M. Hafez

[2] P.L. Kapitza, 1945, "Experimental Study of Ondulatory Flow Conditions", D.Ter Haar, ed., Collected Papers of P.L. Kapitza, (Pergamon, Oxford, 1965).

A New Test Method For Material Flammability Assessment in Microgravity & Extraterrestrial Environments

S.L. Olson*, H. D. Beeson[+], J.P. Haas[+], and J.S. Baas[+]

**NASA Glenn Research Center, Cleveland, OH 44135*
[+] NASA White Sands Test Facility, Las Cruces, NM

The standard oxygen consumption (cone) calorimeter (described in ASTM E 1354 and NASA STD 6001 Test 2) is modified to provide a bench-scale test environment that simulates the low velocity buoyant or ventilation flow generated by or around a burning surface in a spacecraft or extraterrestrial gravity level. The Equivalent Low Stretch Apparatus (ELSA) uses an inverted cone geometry with the sample burning in a ceiling fire (stagnation flow) configuration.

For a fixed radiant flux, ignition delay times for characterization material PMMA are shown to decrease by a factor of three at low stretch, demonstrating that ignition delay times determined from normal cone tests significantly underestimate the risk in microgravity.

The critical heat flux for ignition is found to be lowered at low stretch as the convective cooling is reduced. At the limit of no stretch, any heat flux that exceeds the surface radiative loss at the surface ignition temperature is sufficient for ignition.

Regression rates for PMMA increase with heat flux and stretch rate, but regression rates are much more sensitive to heat flux at the low stretch rates, where a modest increase in heat flux of 25 kW/m^2 increases the burning rates by an order of magnitude.

The global equivalence ratio of these flames is very fuel rich, and the quantity of CO produced in this configuration is significantly higher than standard cone tests.

These results [2] demonstrate the ELSA apparatus allows us to conduct normal gravity experiments that accurately and quantifiably evaluate a material's flammability characteristics in the real-use environment of spacecraft or extra-terrestrial gravitational acceleration. These results also demonstrate that current NASA STD 6001 Test 2 (standard cone) is not conservative since it evaluates materials flammability with a much higher inherent buoyant convective flow.

A Better Test Method is Needed

NASA's current method of material screening determines fire resistance under conditions representing a worst-case for normal gravity flammability - the Upward Flame Propagation Test (Test 1[1]). The applicability of Test 1 to fires in microgravity and extraterrestrial environments, however, is uncertain because the relationship between this buoyancy-dominated test and actual extraterrestrial fire hazards is not understood.

Unlike Test 1, the NASA STD 6001 Test 2 [1] standard oxygen consumption (cone) calorimeter (also described in ASTM E 1354) provides quantitative data on ignition delay times and burning rates of materials. However, it currently lacks any pass-fail criteria. In addition, it too is buoyancy-dominated.

The objective of this research is to modify the well-instrumented standard cone configuration to provide a reproducible bench-scale test environment that simulates the buoyant or ventilation flow that would be generated by or around a burning surface in a spacecraft or

extraterrestrial gravity level. We will then develop a standard test method with pass-fail criteria for future use in spacecraft materials flammability screening. (For example, dripping of molten material will be an automatic fail.)

Scaling Arguments

The ELSA concept is based upon scaling analysis that demonstrates buoyant stretch and forced stretch can be equated. This means that through scaling we can burn materials over a wide range of gravity levels.

Equivalent stretch rates can be determined as a function of gravity, imposed flow, and geometry. For purely buoyant stagnation flow, the equivalent stretch rate is $a_b = [(\rho_e-\rho^*)/\rho_e][g/R]^{1/2}$ [6,7], where the density difference from the average flame temperature to ambient is used, g is gravity, and R is the radius of curvature of the sample. For purely forced flow, the equivalent stretch rate is characterized by either $a_f = 2\tilde{U}_\infty R$ for a cylinder[6], or $a_f = U_{jet}/d_{jet}$ for a jet impinging on a planar surface[9]. U_∞ is the velocity of the ambient stream or the jet, R is the radius of curvature of the cylinder, and d_{jet} is the diameter of the jet. A generalized expression for stretch rate which captures mixed convection includes both buoyant and forced stretch is defined[6] as $a_{equivalent} = a_f(1+ a_b^2/a_f^2)^{1/2}$. The inherent buoyant stretch for the current ELSA holder is ~4 s^{-1} based on a correlation of regression rates for cylinders and flat disks. This correlation also allows us to determine that the normal cone buoyant stretch rate is 33 s^{-1}] by extrapolating the correlation to the 'ideal' burning rate (heat flux from flame to surface only) for clear PMMA from [11].

The stretch rate is simply the velocity gradient as the flow decelerates toward the fuel surface. The velocity gradient for flame spread problems has been shown to be the important flow parameter [Wichman, 1983], and the flame is spreading deep within the boundary layer where the velocity gradient is almost constant. For forced flow velocities of up to 20 cm/s (spacecraft ventilation), the velocity gradient (stretch rate) is of the same order for small fires. Thus a test method which varies the velocity gradient (stretch rate) will capture the essential flammability behavior of flame spread as well as stagnation point fires.

To demonstrate this scaling with experimental results, the ignition delay results of FIST [4] at different flow rates, including natural convection, are added to the ignition delay –stretch plot by estimating the Blasius boundary layer velocity gradient at the surface for the free stream flow based on their experiment geometry. The correlation holds up very well over a wide range of velocity gradient in cm/s per cm (flame stretch rate, s^{-1}). While the normal cone flow field is not well characterized, the flame is stabilized near a surface with a cross flow (entrained air), and velocity gradients in a laminar boundary layer near the surface are constant. For a 5 cm surface (1/2 sample) with an average velocity gradient near the surface of 33 s^{-1}, the average entrained cross flow would be ~20 cm/s, which is reasonable.

References

1)D. Mulville, *Flammability, Odor, Offgassing, and Compatibility Requirements and Test Procedures for Materials in Environments that Support Combustion*, NASA-STD-6001, (1998).

2) Olson, S.L., Beeson, H.D., Haas, J.P., and Baas, J.S.; *An Earth-Based Equivalent Low Stretch Apparatus For Material Flammability Assessment in Microgravity & Extraterrestrial Environments*, Proceedings of the Combustion Institute, 30, to appear, (2004).

[3] Wichman, I.S., "*Flame Spread in an Opposed Flow with a Linear Velocity Gradient,*"Combustion and Flame, 50, 28 (1983).

[4] Roslon, Olenick, Walther, Torero, Ross, and Fernandez-Pello, *"Microgravity Ignition Delay of Solid Fuels in Low Velocity Flows"*, AIAA J., V. 39, No. 12, 2336-2342, (2001).

Most Probable Fire Scenarios in Spacecraft and Extraterrestrial Habitats - Why NASA's Current Test 1 Might Not Always Be Conservative

S.L. Olson, NASA Glenn Research Center

NASA's current method of material screening determines fire resistance under conditions representing a worst-case for normal gravity flammability - the Upward Flame Propagation Test (Test 1[1]). Its simple pass-fail criteria eliminates materials that burn for more than 12 inches from a standardized ignition source. In addition, if a material drips burning pieces that ignite a flammable fabric below, it fails.

The applicability of Test 1 to fires in microgravity and extraterrestrial environments, however, is uncertain because the relationship between this buoyancy-dominated test and actual extraterrestrial fire hazards is not understood. There is compelling evidence that the Test 1 may not be the worst case for spacecraft fires, and we don't have enough information to assess if it is adequate at Lunar or Martian gravity levels.

Microgravity Flames do Strange Things

Flames in microgravity are known to preferentially spread upwind (ie opposed flow) [2], not downwind (i.e. concurrent flow) as in the normal gravity upward flammability screening Test 1. Over most of the range of air ventilation rates (5-20 cm/s) comparable to spacecraft ventilation, upstream flame spread was the only viable flame. Only when the flow becomes strong enough (estimated to be ≥ 10 cm/s), will at least a partial downstream flame become viable. Numerical and experimental results [7] predict an upstream flame only at 5.0 cm/s, an upstream flame and two localized edge flames propagating downstream at 10.0 cm/s, and both an upstream and downstream flame at 20.0 cm/s.

This propensity to spread upwind does not only occur for thin materials, but also occurs for thicker materials and other shapes. For example, experiments were conducted aboard the Mir space station using plastic cylinders. The intent was to burn them with a concurrent flame spread similar to that of Test 1. However, rather than spread along the rod, the flame stabilized at the front tip of the rod and burned like a candle flame at the end of a fat wick [3,4] ,

Under the right flow conditions in space, things will burn that won't burn on Earth. This is most clearly demonstrated by a flammability map [5,6]. In the opposed flow flame spread flammability map for a cellulose fuel, the LOI, or limiting oxygen index on Earth in opposed flow is 16.5% O_2. However, if the flow is on the order of spacecraft ventilation (5-20 cm/s), flames can be sustained even at 14 % O_2. Thus a normal gravity measure of flammability does not guarantee that the material won't burn in space.

Some preliminary work on independent opposed and concurrent flame spread was conducted in a glovebox experiment [8]. The flame spread results in the cabin air (~21% O2) show that the quenching region spans from +0.5 to -2 cm/s, so even correcting for the small spread rate, the concurrent flame has a higher flow flammability boundary than the opposed flow flame.

On the Moon or Mars (0.17g and 0.38 g, respectively), where buoyant flows will be greater than 20 cm/s, the concurrent flame spread will be viable simultaneously with any opposed flow flame. Experiments conducted aboard the KC-135 [9] demonstrate the faster burning of concurrent flames in partial gravity environments. These higher flow test conditions are on the blowoff side of the flammability boundary.

If a fire is initiated, and the crew takes steps to extinguish it, the first line of defense is to turn off the flow. As demonstrated by the data above, the flame cannot survive indefinitely without a supply of fresh oxygen. Once the fire is out, the crew would reactivate the flow to clean up any residual smoke.

However, experiments have shown that even a very slight air flow of a fraction of a cm/s [4] is sufficient to allow the flame to survive. These flames can become almost undetectable (small, non-luminous) and yet persist for many minutes [10, 11] for a fingering flame spread observed under very weak ventilation. The tiny flamelet (~6 mm x 2mm) spread steadily, albeit slowly, for 80 seconds. When the flow was turned up 100-fold to 50 cm/s, the flame did not blow out as one would expect, but flared up into a much larger spreading flame. The fingering behavior is unique to low gravity. The formation of these different flame structures is due to changes in lateral diffusive flux of oxygen from the outer flow to the flame, convective flow patterns and oxygen shadow caused by oxygen consumption at the upstream flamelet. These types of behaviors must be known and understood so that the crew can watch for them.

References

1)D. Mulville, *Flammability, Odor, Offgassing, and Compatibility Requirements and Test Procedures for Materials in Environments that Support Combustion*, NASA-STD-6001, 1998.

2) K.B. McGrattan, T. Kashiwagi, H.R.Baum, and S.L. Olson, S.L.;.*Combust. Flame*, 106, (1996) 377-391.

3) Y.Halli, and J.S. T'ien, , NBS-GCR-86-507, 1986.

4) A.V. Ivanov, et. al, NASA Contract NAS3-97160 final report, Russian Space Agency, Keldysh Research Center, Moscow 1999, also NASA CP-1999-208917, pp. 47-50.

5) S.L. Olson,, *Comb. Science and Tech*. 76 (1991) 233-249.

6) T'ien, J.S., SIBAL Science Requirements Document, 2002.

7) Prasad, K., Olson, S.L., Nakamura, Y., and Kashiwagi, T.; "Effect of Wind Velocity on Flame Spread in Microgravity", the *Proceedings of the Combustion Institute, V. 29,* pp 2553-2560, July, 2002.

8) Olson, S.L., Kashiwagi, T., Fujita, O., Kikuchi, M., and Ito, K.; "Experimental Observations of Spot Radiative Ignition and Subsequent Three-Dimensional Flame Spread over Thin Cellulose Fuels", *Combustion and Flame*, V. 125, pp. 852-864, 2001.

9) Sacksteder, K.R., Ferkul, P.V., Feier, II, Kumar, A., and T'ien, J.S., "Upward and Downward Flame Spreading and Extinction in Partial Gravity Environments, Seventh International Workshop on Microgravity Combustion and Chemically Reacting Systems, NASA/CP-2003-212376/Rev1, pp141-144, 2003.

10) Wichman, I.S., ATHINA Science Requirements Document, 2004.

11) Olson, S.L., Baum, H.R., and Kashiwagi, T.; "Finger-like Smoldering over Thin Cellulosic Sheets in Microgravity", *Twenty-Seventh Symposium (International) on Combustion*, pp. 2525-2533, 1998.

INTERFACIAL INSTABILITIES DURING EVAPORATION

Ozgur Ozen
University of Florida

Interfacial instabilities in the presence of vapors have traditionally been investigated by others who have assumed that the vapor phase is infinitely deep and passive, i.e. vapor fluid dynamics has been ignored. However, when we look at many engineering processes, such as heat pipes and coating technologies where interfacial instabilities take place, we might imagine that the assumption of an infinitely deep vapor layer, or at least that of a passive vapor, is inappropriate.

We have looked at a variety of problems where a liquid is in contact with a gas (sometimes even its own vapor) and investigated the role of the active gas phase on the interfacial instability. We have especially focused on the evaporative instabilities where the instability mechanism is more complicated. In order to understand the physics of these instabilities, calculations were done employing the techniques of linear stability analysis and the dominant balance method. The theoretical results and interpretations are also backed by experiments in bilayer fluid systems using IR imaging for flow visualization.

MICROFLUIDIC BIOCHIP DESIGN

Charles Panzarella

As humans prepare for the exploration of our solar system, there is a growing need for miniaturized medical and environmental diagnostic devices for use on spacecrafts, especially during long-duration space missions where size and power requirements are critical. In recent years, the biochip (or Lab-on-a-Chip) has emerged as a technology that might be able to satisfy this need. In generic terms, a biochip is a miniaturized microfluidic device analogous to the electronic microchip that ushered in the digital age. It consists of tiny microfluidic channels, pumps and valves that transport small amounts of sample fluids to biosensors that can perform a variety of tests on those fluids in near real time. It has the obvious advantages of being small, lightweight, requiring less sample fluids and reagents and being more sensitive and efficient than larger devices currently in use. Some of the desired space-based applications would be to provide smaller, more robust devices for analyzing blood, saliva and urine and for testing water and food supplies for the presence of harmful contaminants and microorganisms. Our group has undertaken the goal of adapting as well as improving upon current biochip technology for use in long-duration microgravity environments.

In addition to developing computational models of the microfluidic channels, valves and pumps that form the basis of every biochip, we are also trying to identify potential problems that could arise in reduced gravity and develop solutions to these problems. One such problem is due to the prevalence of bubbly sample fluids in microgravity. A bubble trapped in a microfluidic channel could be detrimental to the operation of a biochip. Therefore, the process of bubble formation in microgravity needs to be studied, and a model of this process has been developed and used to understand how bubbles develop and move through biochip components. It is clear that some type of bubble filter would be necessary in Space, and several bubble filter designs are being evaluated.

Another area of current research is DNA hybridization on solid surfaces. In DNA hybridization, short single strands of DNA, called oligonucleotides (oligos), are bonded to a solid substrate such as glass, and then fluid containing unknown DNA flows over it. The bound DNA are called the probes, and the suspended DNA are called the targets. A fluorescent molecule is attached to each target DNA. If the target and probe DNA complement each other, they will hybridize (zip up), and then the fluorescent molecules will emit detectable light when stimulated by a laser. The intensity of the fluorescent signal relates to the degree of surface hybridization and can be used as a means of identifying the unknown DNA. This is the basis of many commercial DNA microarrays such as the GeneChip made by Affymetrix, which can contain hundreds of thousands of oligo spots and are used primarily for studying gene expression.

Another application of this technique currently under consideration is the identification of microorganisms from their unique genetic signature. This is particularly important to NASA because such a device could be used to test for contaminated food and water supplies onboard distant spacecraft or outposts. The basic principle would be to deposit an array of oligo spots that uniquely identify the organisms most commonly suspected for contamination. Then, the process of surface hybridization could be used to see if any of the DNA from the unknown samples match the known DNA. The exact details of this process have not yet been completely worked out, but a number of companies such as HealthSpex are working on prototype devices.

There are a number of problems that need to be solved before this process becomes practical. First, the list of desired microorganisms needs to be determined, and from the genome of every organism on that list,

short DNA sequences (oligos) need to be selected that are capable of uniquely identifying them. The DNA from the sample needs to be extracted, purified and possibly amplified before passing over the immobilized probes.

In order to make the device as small as possible, it would be desirable to integrate the sample preparation, transport and detection processes into a single miniaturized device. In the ideal device, microfluidic channels would transport small amounts of sample fluid over the probe sites, and optical sensors integrated directly into the microchip would detect the hybridization.

Current research efforts are focusing on the optimization of this type of biosensor. The critical question is whether the fluorescent signal itself can provide enough information to uniquely identify the unknown organisms. This depends first and foremost on the proper choice of the oligo probes. They must be unique enough to differentiate the unknown organism from any other organism. This depends on where in the genome the oligo is selected and how long it is. It is generally believed that a length of about 25-30 nucleotide pairs is a good choice for gene expression analysis, but it is not clear that this would be the optimal length for microbial identification.

One problem that arises is how to distinguish between perfect complementary hybridization and single-base-pair mismatch hybridization. Without this ability, it would be impossible to differentiate between closely related organisms. One way of alleviating this problem is to apply a temperature gradient along the substrate and exploit changes in the kinetics of the hybridization process with temperature. Each complementary oligo pair has a unique melting temperature (the temperature at which half the available oligos are paired), and the melting temperature between a perfect match and a single mismatch can often be as large as 10 degrees Celsius. The melting temperature depends on the composition of the oligo as well as its length. If the position of the oligo spot on the substrate corresponds to its melting temperature, then different surface hybridization patterns can be used to distinguish between complementary and non-complementary duplexes.

In order to examine all of these issues, a computational model of DNA hybridization in a microchannel has been developed. Assuming the kinetics of the hybridization process are known, it can be used to optimize the design of the detector to improve its sensitivity and specificity for the set of microorganisms under consideration. In addition to the choice of oligo, other factors that can be varied include the channel dimensions, flow rate, inlet concentrations, sensor area and temperature profile. This model is used to predict the degree of hybridization and the unique surface concentration pattern for each case. In order to help with the problem of oligo selection, software has been developed that can compute the thermodynamic properties of the oligos such as their entropy, enthalpy, Gibbs free energy and melting temperature from known empirical data. It is also able to calculate the changes in these properties due to mismatches. This software is integrated directly into the model.

DETECTION AND PREVENTION OF CARDIAC ARRHYTHMIAS DURING SPACE FLIGHT

Dilip Pillai and David S. Rosenbaum
MetroHealth Campus, Case Western Reserve University
2500 MetroHealth Drive
Cleveland, Ohio 44109
(216) 778-2273
dpillai@metrohealth.org

Kathy J. Liszka
The University of Akron

David W. York, Michael A. Mackin, and Michael J. Lichter
NASA Glenn Research Center

There have been reports suggesting that long-duration space flight might lead to an increased risk of potentially serious heart rhythm disturbances. If space flight does, in fact, significantly decrease cardiac electrical stability, the effects could be catastrophic, potentially leading to sudden cardiac death. It will be important to determine the mechanisms underlying this phenomenon in order to prepare for long-term manned lunar and interplanetary missions and to develop appropriate countermeasures.

Electrical alternans affecting the ST segment and T-wave have been demonstrated to be common among patients at increased risk for ventricular arrhythmias. Subtle electrical alternans on the ECG may serve as a noninvasive marker of vulnerability to ventricular arrhythmias. We are studying indices of electrical instability in the heart for long term space missions by non-invasively measuring microvolt level T-wave alternans in a reduced gravity environment. In this investigation we are using volunteer subjects on the KC-135 aircraft as an initial study of the effect of electrical adaptation of the heart to microgravity. T-wave alternans will be analyzed for heart rate variability and QT restitution curve plotting will be compared for statistical significance.

Our hypothesis is that prolonged exposure to microgravity will alter T wave alternans measurements, decrease heart rate variance, increase QT dispersion, decrease heart rate recovery and alter QT restitution curve. A recently published study has shown that long duration spaceflights prolong cardiac conduction and repolarization. They concluded that long duration flight is associated with QT interval prolongation and may increase arrhythmia susceptibility. We propose using computer technology as a noninvasive clinical tool to detect and study clinically significant TWA during standard exercise testing using electrode systems specifically adapted for the purpose of obtaining and measuring TWA.

The equipment we will use for this operational and follow-on biomedical testing is the FDA approved Cambridge Heart Heartwave Diagnostic System modified to use a laptop computer versus a desktop unit developed for a hospital lab setting. The unique features of this ECG unit are the microvolt sensitivity, the back lead which is used to derive 3D electrical vectors of the heart, and the proprietary Cambridge Heart analysis and display software. The unit measures microvolt T-wave alternans using seven proprietary micro-V alternans sensors and seven standard electrodes placed in the standard 12-lead configuration, as well as four Frank vector positions. The micro-V sensors reduce the effects of muscle noise and baseline wander when used in conjunction with specialized signal processing techniques.

Protocols will be observed for preflight, in-flight, postflight and KC-135 flight data collection. The KC-135 flights will help with early operational research testing techniques. The purpose of the operational experiment is to correlate cardiac parameters with blood pressure and gravity levels to determine how the data fits historical ground data. The complete experiment has both operational and biomedical research component. IRB approval of the study will be obtained. Informed consent will be obtained from the participants.

The T wave alternans test results can be positive, negative or indeterminate. The test has an excellent negative predictive value and therefore, those who test negative are at a low risk for sudden cardiac death. Those who test positive may be at risk of susceptibility to ventricular arrhythmias. A statistical analysis of the land-based, low gravity, Martian trajectory and Lunar trajectory environment measurements will be made and determined if there is any significant difference between the recordings.

A population of approximately 15 healthy men and 5 healthy women subjects, representative of the astronaut cohort will be asked to voluntarily participate in this study. Their blood pressure and ECG/TWA will be measured pre-flight and in-flight. Prior to flight, subjects will be asked to participate in an orientation session. Still photos will be taken of the skin where the conductive gel is used for the multi-segment sensors. Photos will be recorded preflight, immediately postflight, and several times during the proceeding week until it has been determined that any skin reaction has disappeared or that no rash is present and will not appear.

A Fast Fourier Transform (FFT) spectral analysis uses the vector magnitude ECG signal recorded from three orthogonal leads over a predetermined minimum number of ECG beats. The analysis yields two measurements: the alternans magnitude and alternans ratio. These are obtained using the Cambridge Heart CH2000 Cardiac Diagnostic System instrument. A positive T-Wave alternan test is the presence of sustained alternans with an amplitude at least 1.9 microvolt and alternans ratio of = 3.0. A quantitative analysis of this data will be performed and presented in a chart form listing each subject's (no name, just subject's number) systemic blood pressure and ECG for pre-flight and in-flight. This data will be compared with ground-based studies and used to develop further medical protocols and possible countermeasures.

The goal of this research is to perform operational testing in low gravity of an advanced ECG with microvolt resolution and 3D localized features to account for altered heart position associated with the low gravity environment of space. Once operational feasibility is proven medical protocols will be developed to determine if advanced ECG testing (including T-wave alterations and Q-T dispersions) can be performed in low gravity. The purpose of the operational experiment is to correlate cardiac parameters with blood pressure and gravity levels to determine how the data fits historical ground data. The complete experiment has both operational and biomedical research component. The first flight week, May 17, 2004, will be operational testing. A research plan will be developed for testing beginning on the August 2, 2004 flight week. An early operational and research objective will be to determine if a series of TWA tests of 20-40 seconds (30-60 beats) can be correlated to produce the same result as one consecutive 128 beat test.

THE EFFECT OF GRAVITY MODULATION ON FILTRATIONAL CONVECTION IN A HORIZONTAL LAYER

Natalya Popova
Department of Mathematics
University of Illinois at Chicago
Chicago, IL 60607
npopov1@uic.edu

The present paper examines the effect of vertical (transverse) harmonic oscillations of the frequency ω and the amplitude A on the onset of convection in an infinite horizontal layer of fluid saturating a porous medium. Constant temperature distribution is assigned on the rigid impermeable boundaries, so that there exists a vertical temperature gradient. The mathematical model is described by equations of filtrational convection [1,2] in the Darcy-Oberbeck-Boussinesq approximation, introduced in the coordinate system inflexibly fixed to the oscillating horizontal layer.

Mechanical quasi-equilibrium solution to the system is obtained. The linear stability analysis for this solution is performed by using Floquet theory. The system of equations for normal disturbances includes the following nondimensional parameters: the Prandtl number $Pr=\nu/\chi$, the wave number α, the gravitational Grashoff number $Gr=\beta Ch^2 g_0 K/\nu^2$, the vibrational Grashoff number $Gv=Gr\bullet\eta$. Here $\eta=A\omega^2/\varphi g_0$, g_0 is the steady gravity acceleration, φ is the porosity of the medium, ν is the kinematic viscosity of the fluid, χ is the thermal diffusivity, K is the intrinsic permeability of the medium, β is the coefficient of thermal expansion of the fluid, C is the quasi-equilibrium temperature gradient, h is the thickness of the layer. The vibrational Grashoff number does not depend on gravity and describes filtrational convection in weightlessness.

The system for the perturbed quantities is reduced to the single damped Mathieu equation for the temperature perturbations. The behavior of its solution is represented by a Fourier series in time. Employment of the method of continued fractions allows us to derive the dispersion equation for the Floquet exponent σ in the explicit form [3].

This equation is investigated with the focus on the following two problems. First, the Floquet spectrum, which describes the stability of the quasi-equilibrium state, is investigated analytically and numerically for different values of the parameters: frequency ω, amplitude A of oscillations, and the Rayleigh number $Ra=Gr\bullet Pr$. Second, the neutral curves $Gv(\alpha)$ and $Gr(\alpha)$ for the synchronous and subharmonic resonant modes are constructed for different values of ω and A. These curves define the regions of parametric instability. The conditions of weightlessness ($Gr=0$) and microgravity (Gr is small) are examined for each of the problems described above.

Also, for both of these problems, asymptotics are derived for large values of ω using the method of averaging and, for small values of ω, using the WKB method. The results obtained by using the method of continued fractions and the asymptotic methods are in a good agreement.

Analytical and numerical investigation of the problem proves that sufficiently intensive vertical (transverse) translational oscillations can delay or even completely suppress the onset of filtrational convection, i.e. stabilize the system. However, for some values of the vibration parameters, these oscillations can destabilize the system and even induce the convection in the stable system (for instance,

in the case of the negative temperature gradient). Therefore, by means of changing the parameters of vibration – the frequency and the amplitude - we can control convective instability in a layer of fluid saturating a porous medium.

References

1. Nield D., Bejan A., Convection in porous media, Springer-Verlag, New York, 1998.
2. Gershuni G., Zhukhovitskii E., Convective stability of incompressible fluid, "Nauka", Moskva, 1972.
3. Yudovich V., Zenkovskaya S., Novossiadliy V., Shleykel A., Parametric excitation of waves on a free boundary of a horizontal fluid layer, C.R. Mecanique 331, 2003.

MINIATURE TIME OF FLIGHT MASS SPECTROMETER

Richard S. Potember, Ph.D.
Applied Physics Laboratory
The Johns Hopkins University
Johns Hopkins Road
Laurel, MD 20723-6099
Phone: 240-228-6251 Fax: 240-228-6904 E-mail: Richard.Potember@jhjuapl.edu

We are developing and testing a small, efficient time-of-flight mass spectrometer to rapidly identify important biomarkers and countermeasures for human space exploration. We are using the time-of-flight mass spectrometer to evaluate critical biomarkers and countermeasures that are indicators of bone loss and repair associated with space travel. This miniature instrument will provide new capabilities in the area of sampling, sample preparation, rapid quantitation of biomarkers and it will allow us to apply our technology to other space based problems such as monitoring the spacecraft environment for chemical and biological contaminants.

Mass spectrometry is a technique for determining the masses of molecules and specific fragmentation products formed during vaporization and ionization. From detailed analysis of the mass distribution of the molecule and its fragments, molecular identification is accomplished. These molecular measurements can be carried out at the attomole (10-18 mole) level of material using specialized laboratory-based instruments. The combination of specific molecular identification and extreme sensitivity makes mass spectrometry one of the most powerful analytical laboratory tools yet developed for detection and identification of chemical and biological substances.

1. Muscle Alterations and Atrophy We have recorded full spectrum mass spectral signature of key target biomarker analytes using the MALDI technique at physiological concentrations found in urine. Sampling from urine has been chosen as a high priority for this project. Compounds investigated included: insulin-like growth factors (IGF-I), Urinary 3-methylhistidine, and estradiol. IGF-I is a potent anabolic factor that mimics most of the growth promoting actions of GH *in vivo*. IGF-1 has also been identified by the Bone Demineralization / Calcium Metabolism Team as an important biomarker.

Another biomarker is urinary 3-methylhistidine. It is a measure of myofibrillar protein degradation. 3-methylhistidine cannot be re-utilized by the body. It is rapidly and quantitatively excreted in the urine. Estradiol is a steroid hormone important for the maintenance of muscle mass and bone density. It is widely speculated that steroid hormones such as estradiol play a central role in the early stages of muscle atrophy and bone demineralization.

We have also used matrix-assisted laser desorption mass spectrometry as a tool to *quantitatively* measure 3-MH in biological fluids. The TOFMS team analyzed various concentrations of 3-methylhistidine in water and in urine to determine the relationship between analyte concentration and analyte molecular ion intensity. The concentrations used in this study were based on 3-methylhistidine concentration typically found in urine, i.e. 20pmole – 3.5nmole. The team examined the utility of two types of internal standards, histidine, a structural analogue, and d_3-3-methylhistidine, a stable-isotope labeled analogue. 3-Methylhistidine (3-MH) samples in water and urine were prepared ranging from 5uM – 10mM, keeping the (3MH)/(histidine) ratio constant at 1:10. Protonated molecular ions for 3MH and histidine could be identified in the corresponding MALDI spectra. A plot of the ratio of relative peak intensities of (3MH)/(d_3-3-MH) versus 3-MH concentration gave a linear response with a correlation coefficient, $R^2 = 0.9799$ and a relative standard deviation of the slope of 4.00%.

2. Bone Demineralization / Calcium Metabolism

We have completed initial laboratory studies with biomarkers specific to bone loss and metabolism. These biomarkers include trivalent hydroxypyridinium crosslinks and creatinine. Trivalent hydroxypyridinium crosslinks are released into the circulation during bone resorption and are excreted as free pyridinolines molecules. In bone and cartilage, the collagen is bound by pyridinoline or deoxypyridinoline crosslinks. Deoxypyridinoline is found exclusively in bone while pyridinoline is found in skin, joint and cartilage. Creatinine is used to extrapolate the status of bone remodeling activity in various metabolic bone conditions.

We have performed a mass spectral analysis of alendronate to determine the mass spectral pattern by MALDI and to add the compound to our library of critical biomarkers. Bisphosphonate administration to the hindlimb of suspended rats and limb immobilization studies in dogs suggest that this compound is an effective countermeasure to bone loss. Alendronate is a member of the bisphosphonate family of drugs used to treat/prevent osteoporosis. We analyzed a commercially available product, Fosamax.

3. Radiation in Space

The risks to personnel in space from the naturally occurring radiation are generally considered to be one of the most serious limitations to human space missions. The consequences of exposure to radiation in space are considered a major limiting factor for long-duration interplanetary space travel for humans. Radiation doses in space may be hundreds of times greater than those experienced on earth. These energetically charged particles can kill cells in the body or cause mutations that may lead to cancer, cataracts, central nervous system damage or other diseases.

We have evaluated three novel peptide cancer biomarkers to demonstrate the utility of MALDI-TOF as a tool for the early detection of carcinomas. The advantage in using it for detection over these other methods is the robust nature of the analyzer. MALDI-TOF mass spectrometry is rapid, sensitive, and tolerant of salts in biological samples.

This work was supported by a grant from the National Space Biomedical Research Association.

PARTIALLY PREMIXED FLAME (PPF) RESEARCH FOR FIRE SAFETY

Ishwar K. Puri*, **Suresh K. Aggarwal, Andrew J. Lock,** University of Illinois at Chicago
Uday Hegde, National Center for Microgravity Research

ABSTRACT

Incipient fires typically occur after the partial premixing of fuel and oxidizer. The mixing of product species into the fuel/oxidizer mixture influences flame stabilization and fire spread. Therefore, it is important to characterize the impact of different levels of fuel/oxidizer/product mixing on flame stabilization, liftoff and extinguishment under different gravity conditions. With regard to fire protection, the agent concentration required to achieve flame suppression is an important consideration. The initial stage of an unwanted fire in a microgravity environment will depend on the level of partial premixing and the local conditions such as air currents generated by the fire itself and any forced ventilation (that influence agent and product mixing into the fire). The motivation of our investigation is to characterize these impacts in a systematic and fundamental manner.

UIC-NASA PPF Drop Rig

(a) General Description

The UIC-NASA PPF drop rig includes equipment for performing normal- and reduced-gravity partially premixed flame experiments. The rig is equipped with two fuel storage tanks that have a volume of 0.5 L and can be filled to a maximum pressure of 250 psi. Various fuel, oxidizer, and diluent combinations can be stored in these tanks. For safety reasons, the mixtures utilized are outside the flammability limits. Both the inner and outer flows are supplied independently by using mixtures in two separate tanks. The gas flows are metered by on board MKS mass flow controllers that have a maximum range of 5 L/min for the inner flow and 20 L/min for the outer flow and are rated accurate within 1% of their maximum ranges. A variety of burners can be enclosed within a standard NASA supplied chamber. For normal atmospheric tests in the 2.2 Second Drop Tower, the chamber is not sealed.

(b) Diagnostics:

Several diagnostic techniques have been employed in the rig to examine partially premixed flame behavior: (i) A color CCD video camera is used to record the transient visible structure of the flames in normal and microgravity. (ii) Temperature measurements have been made using a thermocouple rake. (iii) Global radiation measurements through the use of a thermopile type radiometer have provided valuable heat loss information. Other diagnostics currently being developed for implementation during the next research phase (2004-2006) are: (i) A rainbow schlieren deflectometry (RSD) system for accurate nonintrusive temperature measurements, and (ii) Light intensity attenuation system for measuring soot loading in the flame.

Example Results

(a) Fundamental Research on Partially Premixed Flames

Our investigations have characterized the behavior of partially premixed flames in microgravity environments through observations of the transient flame structure, temperature profiles, and global radiation. These measurements have supplemented by detailed numerical simulations that have been extensively validated. The gravity-dependent behavior of the flames was characterized in terms of flow dilation, buoyancy, and radiation heat loss. These results will be published in the *Proceedings of the 30th International Symposium on Combustion* [1].

(b) Fire Safety Research

* PI: 842 W. Taylor(MC251),Chicago, IL 60607, ikpuri@uic.edu, Ph:312-355-3317 Fx:312-413-0447

Experiments are underway to investigate flame liftoff and blowout in normal- and microgravity from a fire safety perspective. The premixed fuel-air streams are diluted with nitrogen in order to simulate the entrainment of inert product species into a fire. Nitrogen addition is found to raise the Schmidt number sufficiently to allow for flame liftoff, i.e., that product diluted flames may in some cases detach and cause secondary fires at some distance from the reactant source. The effects of the reactant stoichiometry and flow conditions are being investigated for these lifted flames. In all cases, we find lifted flames to be much more stable in microgravity due to the removal of buoyancy-induced instabilities. In most cases the flame moves closer to the reactant source in microgravity relative to its normal gravity location clearly illustrating that normal gravity results are inadequate to describe microgravity flames and, therefore, fires. Moreover, different fuel/air concentrations have different effects on flame liftoff under the influence of gravity. Preliminary results on these aspects have been presented at the 42nd AIAA Aerospace Sciences Meeting and Exhibit, Reno, Nevada, Jan. 5-8, 2004 [2].

Our experiments also consider the influence of other diluents on these lifted flames, such as carbon dioxide and argon. These diluents are the primary components of non-halon gaseous fire extinguishing agents. The two inert species influence the flames differently. One reason arises from their differing heat capacities. They also inhibit the burning intensity, since they increase the third body concentrations and, therefore, influence the combustion chemistry. The diluents have differing radiation emission properties, which impact the heat losses from these flames. Differences between normal- and microgravity flame lift off and blow off may also be impacted by buoyancy driven instabilities and the contribution of diluent species properties to instability characteristics, such as their amplitude. Our investigation hopes to elucidate these issues in a fundamental manner to facilitate the appropriate fire safety strategies.

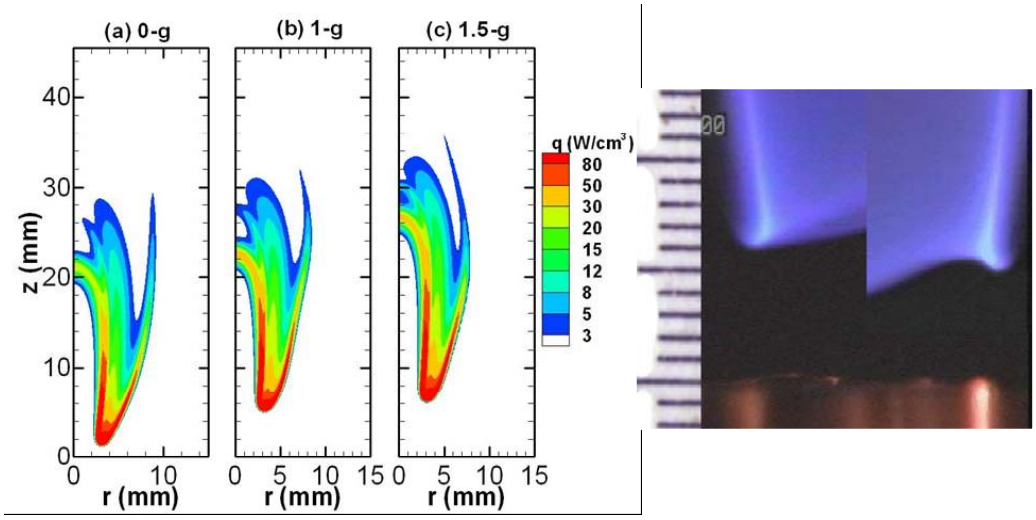

Figure 1: Influence of gravity on the liftoff height of a nonpremixed flame established on a coannular burner. Left: results of detailed numerical simulations. Right: normal- and microgravity experiments.

1 . Lock, A., Ganguly, R., Puri, I. K., Aggarwal, S. K., and Hegde, U., "Gravity Effects on Partially Premixed Flames: An Experimental-Numerical Investigation", to appear in *Proceedings of The Combustion Institute*, 30, 2004.

2. Lock, A., Qin, X., Ganguly, R., Puri, I. K., Aggarwal, S. K., and Hegde, U. "Lifted Partially Premixed Flames in Microgravity", *42nd Annual AIAA Aerospace Science Meeting and Exhibit*, Reno NV, January 2004

EFFECTS OF CHEMICALLY-PASSIVE SUPPRESSANTS ON LAMINAR PREMIXED HYDROGEN/AIR FLAMES

L. Qiao, C.H. Kim, and G.M. Faeth
Department of Aerospace Engineering
University of Michigan
Ann Arbor, Michigan, USA

Fundamental unstretched laminar burning velocities and flame response to stretch, as characterized by Markstein numbers, were considered experimentally and computationally for outwardly-propagating spherical laminar premixed flames. Experimental and computational conditions were as follows: fuel-equivalence ratios of 1.0 and 1.8; pressures of 0.5-1.0 atm; gaseous suppressant including argon, helium, nitrogen and carbon dioxide; and suppressant concentrations in the range of 0-40%, by volume. Predicted flame behavior was obtained from one-dimensional time-dependent numerical simulations treating variable property multi-component transport, with detailed hydrogen/oxygen chemical kinetics from Mueller et al. (1999). The present flames were sensitive to flame stretch, yielding values of unstretched-to-stretched laminar burning velocities in the range 0.5-1.5 for levels of flame stretch well below quenching conditions, e.g., for Karlovitz numbers less than 0.5. The present passive flame suppressants improved in performance in the following order: argon, helium, nitrogen, and carbon monoxide. This order reflects the capability of suppressants to promote quenching of the reaction zone by either increased specific heats or by enhanced conduction heat losses. Finally, the comparison between measurements and predictions was excellent for present conditions, which involved flames not too near quenching conditions where radiant heat losses were modest.

DYNAMIC WETTING OF ROOM TEMPERATURE POLYMER MELTS: DEVIATIONS FROM NEWTONIAN BEHAVIOR

Enrique Ramé
National Center for Microgravity Research

We examine the dynamic wetting of two simple, room temperature polymer melts, polystyrene and polyisobutylene, by observing the liquid-vapor interface formed on the outside of a silica surface forced into a bath of the test fluid at controlled rates. The dynamic interface shapes of these fluids deviate from the prediction of models that include only Newtonian flow behavior. Specifically, near the contact line the fluid interface curvature is enhanced compared to the Newtonian fluid having the same shear viscosity and static wetting behavior. This observation is surprising because neither elasticity nor any other non-Newtonian behavior is detected for these materials using standard rotational rheometry. To probe the cause of the deviation further, we observe the interface shape of analogous model fluids having measurable elasticity in the rheometer and show that elasticity causes qualitatively similar, although larger, deviations from Newtonian behavior. This study demonstrates that fluids which appear Newtonian in standard rheometric characterization may have wetting behavior which deviates from purely Newtonian. We may expect these deviations to appear not only in the interface shape near the moving contact line but also in such key properties as spontaneous spreading times and in flows which control coating processes.

STUDY OF CO-CURRENT AND COUNTER-CURRENT GAS-LIQUID TWO-PHASE FLOW THROUGH PACKED BED IN MICROGRAVITY

Shripad T. Revankar and Xiangcheng Kong
School of Nuclear Engineering, Purdue University, West Lafayette, IN 47907

ABSTRACT

The main goal of the project was to develop experiments to obtain data and develop models on the co-current and counter-current gas-liquid two-phase flow through a packed bed in microgravity and characterize the flow regime transition, pressure drop, void and interfacial area distribution, and liquid hold up.

An experimental and analytical modeling program for the study of co-current air-water two-phase down flow in a packed column was developed. A detailed survey of the literature was performed on two-phase flow in packed columns. The literature shows only one set of study from Glenn Research Center NASA is available on two-phase flow in packed bed under microgavity conditions. A large amount of effort was put in the development of instrumentation for the local and global measurement in the packed bed. A two point conductivity probe for the measurement of void fraction in the bed at pore level, a film thickness probe for the measurement of film thickness and drying characteristics of the packing, and a bed wise impedance meter for bed wise void measurement were developed. These probes were calibrated and plans were made for the installation of these probes in the packed bed. A packed bed test facility was designed and constructed. The bed is a cylindrical pipe of diameter 69 mm and height of 1.52m. the bed particles were glass spheres of diameter 6 mm. The bed porosity was 0.377.

Single phase flow characterization of the test loop was performed by flowing air and water in the bed and measuring bed pressure drop. From these measurements single phase constants in Ergun pressure drop equations were calculated.

Two Phase co-current down flow of air-water test were conducted. The flow regime in the bed was observed and recorded with high speed video camera. Flow regime map was developed. Five flow regimes were identified, trickling, wavy, transitional, pulsing and bubble flow. Pressure drop in the bed were also obtained for various flow regimes in the bed. An analytical model was developed for predicting flow regime transition from trickle to pulse mode using two-phase film model.

Packed bed reactors have potential space-based applications in bioregenerative food production, waste treatment, watering and nutrient transport in plant root systems, waste recovery, and extraction from planetary materials. The present research addresses the most important topic of HEDS-specific microgravity fluid physics research identified by NASA ‘s one of the strategic enterprises, OBPR Enterprise. The first two years are devoted to ground based flight definition experimental and modeling program. During the next two years microgravity flight tests are carried out using the ground-based parabolic flight research aircraft.

Reference

Charpentier, J. C., Favier M., 1975, Some liquid holdup experimental data in trickle-bed reactors for foaming and nonfoaming hydrocarbons, *AIChE J.*, Vol. **21**, pp. 1213-1218.Chou T. S., Worley

Jr. F.L., Luss D., 1977, Transition to pulsed flow in mixed-phase co-current downflow through a fixed bed, *Ind. And Eng. Chem., Proc. Design and Dev.*, Vol. **16**, pp. 424-429.
Drinkenberg A.A., Blok J. R., Varkevisser J., 1983, Transition to pulsing flow, holdup and pressure drop in packed columns with co-current gas-liquid downflow, *Chem. Eng. Sci.*, **38**, pp.687-699.
Sato Y., T. Hirose, 1973, Flow pattern and pulsation properties of cocurrent gas-liquid downflow in packed beds, *J. Chem. Eng. Jpn.*, **6**, pp. 315-319.

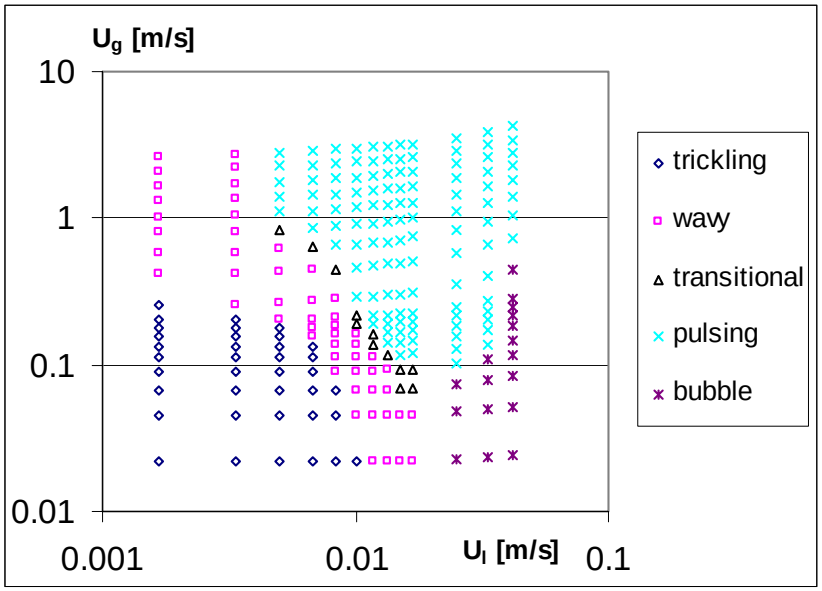

Figure 1 Flow regime map for packed bed of diameter 0.07 m and bed porosity 0.38, air-water co-current downward flow, spherical packing of diameter 6mm

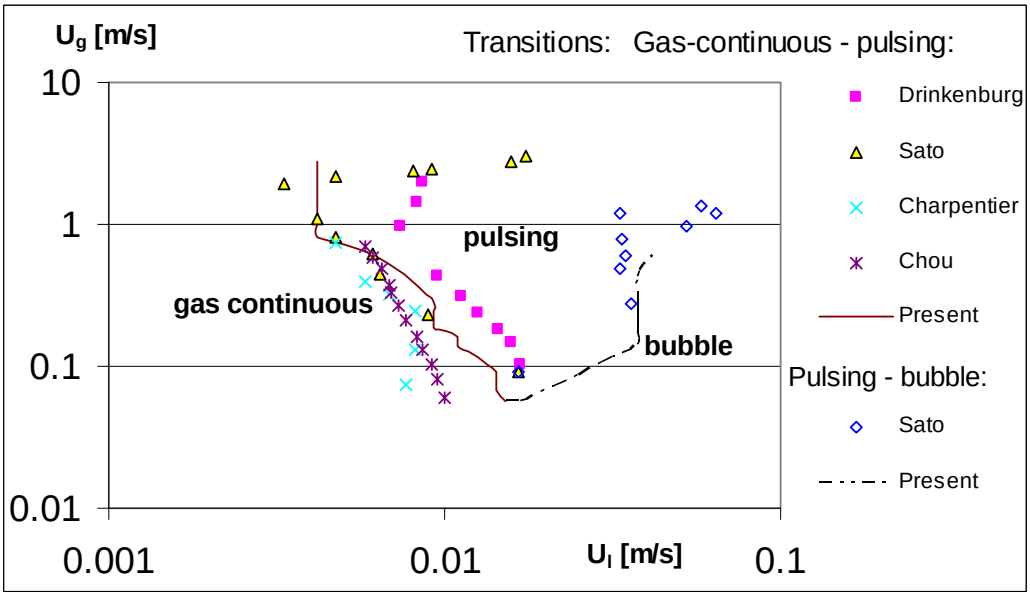

Figure 2. Comparison of flow regime map with data of Chou (1977), Drinckenburg (1983), Sato (1973) and Charpentier (1975).

EFFECTS OF HEAT FLUX, OXYGEN CONCENTRATION AND GLASS FIBER VOLUME FRACTION ON PYROLYSATE MASS FLUX FROM COMPOSITE SOLIDS

D.B. Rich,[1] C.W. Lautenberger,[1] Z. Yuan,[2] and A.C. Fernandez-Pello[1*]
[1]University of California, Department of Mechanical Engineering, Berkeley, 94720 CA USA
[2]NASA Glenn Research Center; Cleveland, OH, 44135 USA
*ferpello@me.berkeley.edu

Experimental work on the effects of heat flux, oxygen concentration and glass fiber volume fraction on pyrolysate mass flux from samples of polypropylene/glass fiber composite (PP/G) is underway. The research is conducted as part of a larger project to develop a test methodology for flammability of materials, particularly composites, in the microgravity and variable oxygen concentration environment of spacecraft and space structures. Samples of PP/G sized at 30x30x10 mm are flush mounted in a flow tunnel, which provides a flow of oxidizer over the surface of the samples at a fixed value of 1 m/s and oxygen concentrations varying between 18 and 30%. Each sample is exposed to a constant external radiant heat flux at a given value, which varies between tests from 10 to 24 kW/m^2. Continuous sample mass loss and surface temperature measurements are recorded for each test. Some tests are conducted with an igniter and some are not. In the former case, the research goal is to quantify the critical mass flux at ignition for the various environmental and material conditions described above. The later case generates a wider range of mass flux rates than those seen prior to ignition, providing an opportunity to examine the protective effects of blowing on oxidative pyrolysis and heating of the surface.

Graphs of surface temperature and sample mass loss vs. time for samples of 30% PPG at oxygen concentrations of 18 and 21% are presented in the figures below. These figures give a clear indication of the lower pyrolysis rate and extended time to ignition that accompany a lower oxygen concentration. Analysis of the mass flux rate at the time of ignition gives good repeatability but requires further work to provide a clear indication of mass flux trends accompanying changes in environmental and material properties.

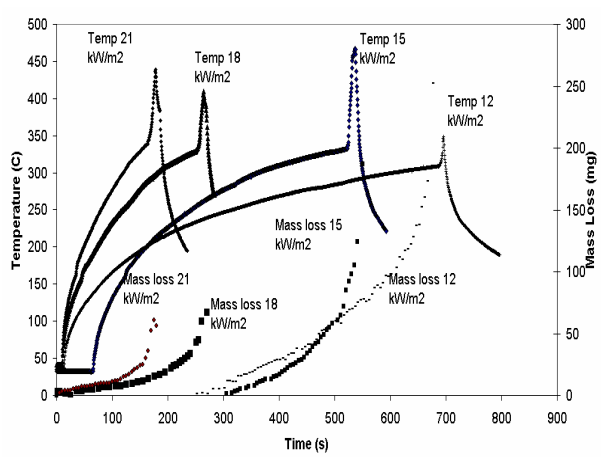

Fig. 1. Comparison of surface temperatures and mass loss values of PP/G 30% at 21% O_2 concentration for varying heat fluxes.

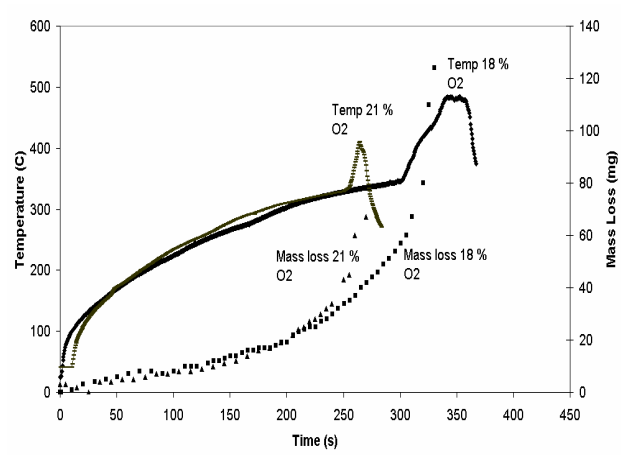

Fig. 2. Comparison of surface temperatures and mass loss values of PP/G 30% at 18 kW/m^2 for varying oxygen concentrations.

THE INTEGRATION OF A SMOKE DETECTOR MODEL WITH LARGE EDDY SIMULATION FIRE MODELING FOR PREDICTING SMOKE DETECTOR ACTIVATION IN MICROGRAVITY

Richard Roby, Wei Zhang, Glenn Gaines, Stephen Olenick, and Michael Klassen
Combustion Science & Engineering, Inc., 8940 Old Annapolis Road Suite L, Columbia, MD, 21045
Phone: 410-884-3266, Fax: 410-884-3267, Email: rroby@csefire.com

Jose L. Torero
Engineering and Electronics, The University of Edinburgh Edinburgh, EH9 3JL, United Kingdom

Fire safety on spacecraft, space stations, and in potential non-terrestrial environments (e.g. Mars) is an important consideration for any mission. Safety of the crews and spacecraft or space station, as well as continuation of the mission is dependent on adequate prevention, detection and suppression of fires in low- and micro-gravity environments. Early detection of fires relies on quickly identifying a fire signature by a detection device placed in an optimum location. Fire signatures and fire flows have been shown to be vastly different on spacecraft and in low-gravity environments; therefore, studies aimed at determining proper detector locations are necessary to provide adequate fire protection in low-gravity environments.

Since it is not practical to perform the large number of experiments necessary to determine optimal placement of detectors in the various low-gravity environments (e.g. the shuttle or varying racks and modules in ISS), a methodology must be developed which will allow for effective detector placement using a minimal number of experiments and a well-validated computational scheme. This study aims to integrate an algorithm that describes the response characteristics of the smoke detectors used in the ISS and the shuttle into a Large Eddy Simulation fire model (FDS [3]). The algorithm is restricted to two parameters, a dwell time and a mixing time, which was originally proposed by Cleary et al. [1]. A full scale room test with convective flows similar to the International Space Station is currently being conducted. Hence initially, experimental data from a multi-room compartment fire was used for validation. Overall, reasonable results were obtained when comparing the predictions to the experimental results. This result shows great potential of the smoke detector modeling combined with CFD (Computational Fluid Dynamics) fire modeling.

The two characteristic parameters that describe smoke model detector activation are: (1) the dwell time (or time lag δt) and the mixing time (τ). Both parameters are a function of the mass flow of smoke into the detector. The dwell time δt was defined as the mass of the smoke within the detector divided by the mass flow rate of smoke (Eq.2), and the mixing time τ was defined as the ratio between the mass of smoke in the sensing chamber divided by and the mass flow rate (Eq.3). Both can also be described by a power law dependence on velocity.

$$\delta t = \frac{L A \rho}{\dot{m}} = \frac{L}{u} \approx \alpha_1 u^{-\beta_1} \tag{1}$$

$$\tau = \frac{\rho V}{\dot{m}} = \frac{L'}{u} \approx \alpha_2 u^{-\beta_2} \tag{2}$$

where V is the sensing chamber volume (V=AL'), A is the effective area of the detector, $\dot{m}$ is the smoke flow rate into the detector and L is the characteristic distance represents smoke entry resistance and $\alpha_1, \alpha_2, \beta_1, \beta_2$ are proportionality constants that account for the detector geometry. The change of the mass of smoke in the sensing chamber volume should equal the difference of the mass fraction as it passes

though the distance L. If the initial mass fraction of smoke in the sensing chamber is zero, the mass fraction of smoke in the sensing chamber is given by:

$$Y_o(t) = \exp\left(-\int_0^t \frac{1}{\tau(t')} dt'\right)\left\{\int_0^t \left(\frac{1}{\tau(t')} \cdot \exp\left(\int_0^t \frac{1}{\tau(t')} dt'\right) \cdot Y_e(t'-\delta t)\right) dt'\right\} \tag{3}$$

where e represents the entrance of the model detector and o represents the sensing chamber. Y is the mass fraction of smoke.

In this validation case, the test geometry consisted of two compartments (2.4 m x 2.4 m x 2.4 m) connected by a corridor (4.9 m long with 2.4 m high ceiling) [2]. Ionization smoke detectors were used in this testing. In this study, the proportionality constants for ionization detectors [1] were used. A value of 7.6 m^2/g was used as the specific extinction coefficient, which is a typical value for a flaming fire.

Table 1 shows the comparison between experimental data and modeling results of the smoke model detector activation time. The experimental data was averaged from three independent test cases. Figure 1(a, b) provides the predictions of the external obscuration (%/ meter) and the predicted responses (internal obscurations) of the model detectors at five different detector locations. Work is currently ongoing to extend this technique to the detectors in use on the ISS and the Shuttle.

References:

[1] Cleary, T., Chernovsky, A. Grosshandler, W. and Anderson, M. (1999). "Particulate entry lag in spot-type-smoke detectors". Proceedings of the 6th international symposium 1999, pp 779-790.

[2] D'souza, V.T., Sutula, J.A., Olenick, S.M., Zhang, W. and Roby, R.J., (2002). "Predicting smoke detector activation using the fire dynamics simulator". Proceedings of 7th international symposium of fire safety science, 2002.

[3] Fire Dynamics Simulator (Version 4.0)–User's Guide, National Institute of Standards and Technology (NIST), NISTIR 6784. 2003 Ed.

Table 1.—Measured and predicted detector activation times(s) for experimental setup.

Detector	D# 1	D# 2	D# 3	D#4	D# 5
Experiment (sec)	14	31	43	64	60.1
Model Detector I1	18.8	14.1	50.6	50.1	60.1
Model Detector I2	19.0	14.1	52.2	50.6	59.9

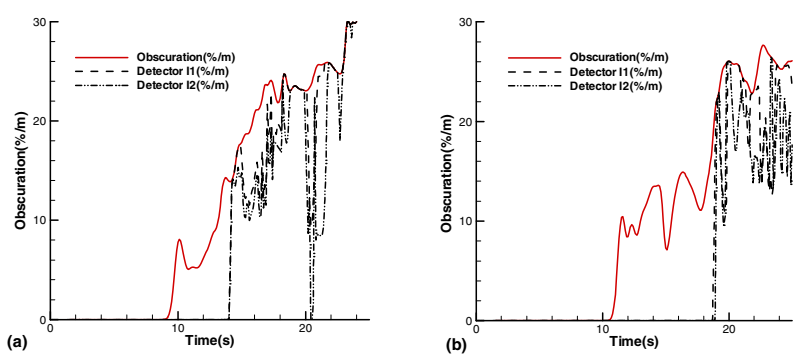

Figure 1.—Predicted obscuration (%/m) and detector (I1 & I2) responses in the fire room.

STUDY OF THE VON-KÁRMÁN VORTEX STREET CLOSE TO ONSET OF SHEDDING

Pedram Roushan and Xiao-Lun Wu
Department of Physics and Astronomy
University of Pittsburgh
Pittsburgh, Pennsylvania 15260

The Bénard-von Kármán vortex street is studied in a flowing soap film channel. The two-dimensional fluid flow in the film allows stable vortex streets to be generated and investigated over a broad range of Reynolds numbers, $10<Re<2000$. Unlike previous studies, which concentrated on the temporal velocity oscillations at a single point in the wake region, the current study focuses on the entire near-wake region using image analysis techniques. The envelope of the von-Kármán vortex street is analyzed for different rod diameters, which span more than two orders of magnitude in their diameters. The parameters that characterize the envelope of the vortex street, such as the growth rate and the saturation amplitude, are measured for different Reynolds numbers. It is found that all of the curves representing the envelope can be collapsed onto a single master curve, suggesting that the shape of the von-Kármán vortex street is universal, independent of Re. We construct a simple model that takes into account the energy transfer into vortices by periodic oscillations of transverse velocity fluctuations beneath the rod. This simple model not only explains the near wake shape of the von-Kármán vortex street, but also allows extraction of useful information about the wake, such as the kinetic energy injected into the fluid and the drag coefficient (C_D).

VISUALIZATION OF ELECTRIC FIELD EFFECTS ON NUCLEATE AND FILM BOILING

Subramanian Sankaran and Jeffrey S. Allen
National Center for Microgravity Research
NASA Glenn Research Center
Cleveland, Ohio

Film boiling is the phenomena whereby a layer of vapor completely covers a heated surface resulting in extreme surface temperatures; a potentially catastrophic condition. Film boiling can easily occur in microgravity and in microscale systems because the characteristic dimension of the vapor bubble is much larger than that of the heater. Electric fields may be employed to provide an effective means to bring liquid into contact with the heater surface thereby maintaining low surface temperatures at high heat fluxes.

Nucleate and film boiling of PF-5060 over a 127 micrometer diameter electrically heated wire are observed. High resolution, high speed imaging show the nature of nucleate and film boiling and the enhancement to heat transfer afforded by the use of electric fields. Preliminary experiments conducted at 12 C and 27 C subcooling levels showed increases in the q_max and q_min heat flux levels by up to 50% when using 2kv across the heater and the screen, compared to the heat fluxes without electric fields. Using electric fields 1) we can enhance the nucleate boiling heat transfer (increase q_max), 2) make the transition, from nucleate boiling to film boiling at the critical heat flux, a slower and controllable process, and 3) destabilize the vapor film earlier and achieve nucleate boiling (increased q_min is a desirable safety/recovery characteristic).

NICKEL-COATED ALUMINUM PARTICLES: A PROMISING FUEL FOR MARS MISSIONS

Evgeny Shafirovich and Arvind Varma
Purdue University, School of Chemical Engineering
480 Stadium Mall Drive, West Lafayette, IN 47907-2100

Combustion of metals in carbon dioxide is a promising source of energy for propulsion on Mars. This approach is based on the ability of some metals (e.g. Mg, Al) to burn in CO_2 atmosphere and suggests use of the Martian carbon dioxide as an oxidizer in jet or rocket engines [1, 2]. Analysis shows that CO_2/metal propulsion will reduce significantly the mass of propellant transported from Earth for long-range mobility on Mars and sample return missions. Recent calculations for the near-term missions indicate that a 200-kg ballistic hopper with CO_2/metal rocket engines and a CO_2 acquisition unit can perform 10-15 flights on Mars with the total range of 10-15 km, i.e. fulfill the exploration program typically assigned for a rover [3].

Magnesium is currently recognized as a candidate fuel for such engines owing to easy ignition and fast burning in CO_2 [1, 2, 4]. Aluminum may be more advantageous if a method for reducing its ignition temperature is found. Coating it by nickel is one such method. It is known that a thin nickel layer of nickel on the surface of aluminum particles can prevent their agglomeration and simultaneously facilitate their ignition, thus increasing the efficiency of aluminized propellants [5, 6].

Combustion of single Ni-coated Al particles in different gas environments (O_2, CO_2, air) was studied using electrodynamic levitation and laser ignition [7]. It was shown that the combustion mechanisms depend on the ambient atmosphere. Combustion in CO_2 (see Fig. 1) is characterized by the smaller size and lower brightness of flame than in O_2, and by phenomena such as micro-flashes and fragment ejection (see image 4). The size and brightness of flame gradually decrease as the particle burns.

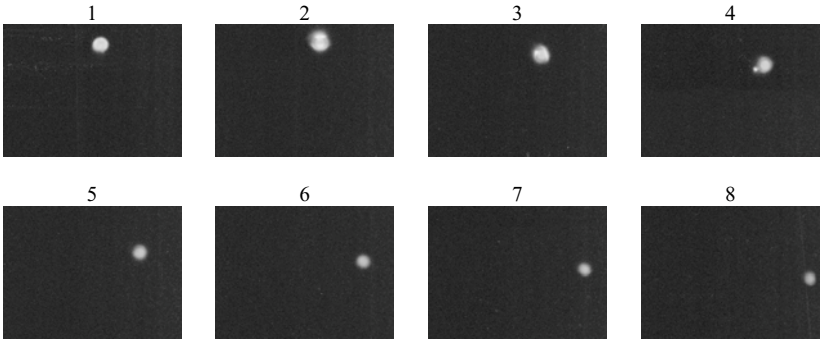

Figure 1: Combustion of Ni-clad Al particle in CO_2.
(0.5 μs between images, viewing area 1236 x 921 μm)

Remarkably, burning of Ni-clad Al particles in air (see Fig. 2) involves two stages, with inverse images of flame (bright core-dark flame and dark core-bright flame). Such images have never been observed in prior experiments with pure Al particles. Thus, we expect that this new phenomenon is caused by the presence of two elements (Al and Ni) in the particles.

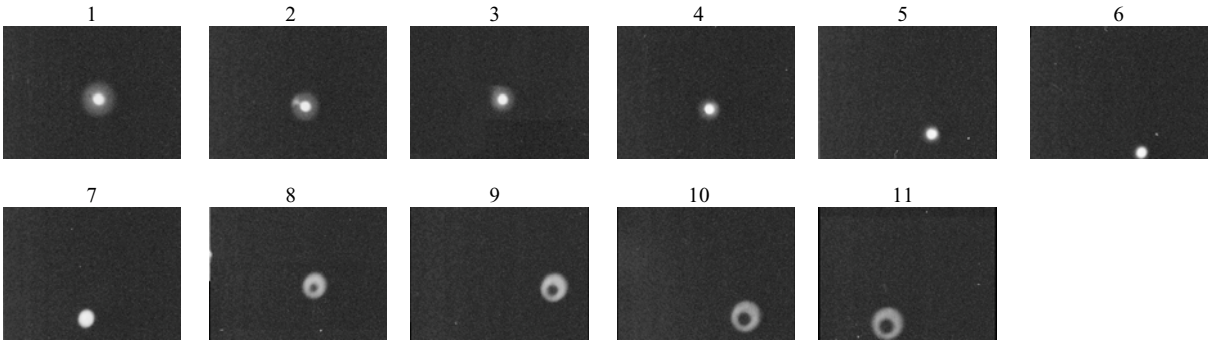

Figure 2: Combustion of Ni-clad Al particle in air.
(1.3 μs between images, viewing area 1236 x 921 μm)

Recent studies [8] show that the Ni coating dramatically decreases both the ignition delay time of laser-heated Al particles and the critical ignition temperature of gas-heated Al particles. Exothermic intermetallic reactions between liquid Al and solid Ni are considered as the main reason for the lowered ignition temperature of Ni-coated Al particles.

The detailed characterization of the process requires spatial and temporal resolutions that can be achieved only with relatively larger particles (1-5 mm). To avoid the natural convection and liquid flow effects, experiments on combustion of such particles will be conducted in microgravity environment using NASA research aircraft. The ignition and combustion will be studied by using high-speed and infra-red video cameras, and product composition analysis. Special attention will be devoted to elucidating the roles of inter-metal reaction and physical processes in surface layers (e.g. cracking of the shell, melt spreading).

This work is supported by NASA (Grant NNC04AA36A).

REFERENCES

1. Yuasa, S., and Isoda, H. (1989) *25th AIAA/ASME/SAE/ASEE Joint Propulsion Conference & Exhibit, July 1989*, AIAA Paper 89-2863.
2. Shafirovich, E.Ya., Shiryaev, A.A., and Goldshleger, U.I. (1993) *Journal of Propulsion and Power*, **9**(2), 197.
3. Shafirovich, E., Salomon, M., and Gökalp, I. (2003) *Proceedings of the Fifth IAA International Conference on Low-Cost Planetary Missions*, *ESTEC, Noordwijk, The Netherlands, 24-26 September 2003,* ESA SP-542, p. 97.
4. Shafirovich, E.Ya., and Goldshleger, U.I. (1997) *Journal of Propulsion and Power*, **13**(3), 395.
5. Breiter, A.L., Mal'tsev, V.M., and Popov E.I. (1988) *Combustion, Explosion, and Shock Waves* **26**, 86.
6. Yagodnikov, D.A., and Voronetskii, A.V. (1997) *Combustion, Explosion, and Shock Waves* **33**, 49.
7. Shafirovich, E., Mukasyan, A., Thiers, L., Varma, A., Legrand, B., Chauveau, C., and Gökalp, I. (2002) *Combustion Science and Technology*, **174**(3), 125.
8. Shafirovich, E., Escot Bocanegra, P., Chauveau, C., Gökalp, I., Goldshleger, U., Rosenband, V., and Gany, A. (2004) To be presented at the *30th International Symposium on Combustion, Chicago, July 25-30, 2004*.

COMPUTER MODELING OF CARDIOVASCULAR RESPONSES TO GRAVITY

M. Keith Sharp
Department of Mechanical Engineering
University of Louisville
Louisville, KY 40292

A recently initiated computer modeling project will investigate a possible contributing factor to postflight orthostatic intolerance (POI) that has to date received little attention. POI compromises crew safety and could have disastrous consequences in emergency situations during landing. A potentially revealing characteristic of POI is that even susceptible astronauts are able to stand postflight for several minutes without symptoms. Many astronauts become dizzy only after 5-10 minutes of standing. Therefore, compensatory reflexes are apparently sufficient to prevent symptoms initially. While many factors, including a well-documented decrease in postflight blood volume, may increase sensitivity, the final cause of POI must have a delayed action consistent with the range of times astronauts are able to tolerate standing. Onset of symptoms during orthostatic stress in nonastronauts is correlated with the gradual rate of loss of blood volume by capillary filtration, which provides a potential explanation for the delayed occurrence of POI. Furthermore, astronauts have increased lower body capillary permeability in space. If permeability remains elevated, then capillary transport may also be responsible for the reduced tolerance of astronauts to upright posture postflight. *Accordingly, it is hypothesized that capillary filtration explains the delayed onset, as well as the increased postflight incidence of dizziness.* The hypothesis will be tested with a computer model of the cardiovascular system that incorporates fundamental biomechanical responses and reflex control. Posture-dependent capillary filtration will be represented with local permeability values and models of local intra- and extra-vascular pressure. A model of cerebral circulation will be included to provide a prediction of dizziness by direct comparison with established thresholds for cerebral flow. Because data is currently unavailable in astronauts, the model will be validated with heart rate, stroke volume and arterial pressure measurements and capillary filtration estimates derived from experiments on nonastronauts. Finally, the plausibility of the hypothesis will be tested by comparing the permeability required in the model to cause dizziness during simulated stand tests to the preliminary inflight values. This modeling effort will elucidate the potential importance of capillary filtration in producing POI and may guide the design of experiments to investigate this mechanism in astronauts.

BI-COMPONENT DROPLET COMBUSTION IN REDUCED GRAVITY

Benjamin D. Shaw
Mechanical and Aeronautical Engineering Department
University of California, Davis

ABSTRACT

This research deals with reduced-gravity combustion of bi-component droplets initially in the mm size range or larger. The primary objectives of the research are to study the effects of droplet internal flows, thermal and solutal Marangoni stresses, and species volatility differences on liquid species transport and overall combustion phenomena (e.g., gas-phase unsteadiness, burning rates, sooting, radiation, and extinction). The research program utilizes a reduced-gravity environment so that buoyancy effects are rendered negligible. Use of large droplets also facilitates visualization of droplet internal flows, which is important for this research.

In the experiments, droplets composed of low- and high-volatility species are burned. The low-volatility components are initially present in small amounts. As combustion of a droplet proceeds, the liquid surface mass fraction of the low-volatility component will increase with time, resulting in a sudden and temporary decrease in droplet burning rates as the droplet rapidly heats to temperatures close to the boiling point of the low-volatility component. This decrease in burning rates causes a sudden and temporary contraction of the flame. The decrease in burning rates and the flame contraction can be observed experimentally. Measurements of burning rates as well as the onset time for flame contraction allow effective liquid-phase species diffusivities to be calculated, e.g., using asymptotic theory [1]. It is planned that droplet internal flows will be visualized in flight and ground-based experiments. In this way, effective liquid species diffusivities can be related to droplet internal flow characteristics.

This program is a continuation of extensive ground-based experimental and theoretical research on bi-component droplet combustion that has been ongoing for several years. The focal point of this program is a flight experiment (Bi-Component Droplet Combustion Experiment, BCDCE). This flight experiment is under development. However, supporting ground-based studies have been performed. Some of the most recent ground-based research is summarized below.

Reduced Gravity Experiments

Experiments on combustion of fiber-supported propanol droplets with initial droplet diameters of about 1 mm were conducted in air at standard temperature and with pressures ranging from 0.1 to 1.0 MPa [2]. The experiments were conducted using the 2.2 Second Drop Tower at the NASA John H. Glenn Research Center at Lewis Field in Cleveland, OH. The results indicate significant differences in combustion of propanol droplets at 0.1 MPa relative to higher pressures. The flame at 0.1 MPa is non-sooting with blue coloring during most of the combustion process. For higher pressures, flames exhibited somewhat non-spherical shapes as well as significant amounts of sooting during most of the combustion history. The non-spherical flame shapes were likely a

result of the increased importance of buoyant convection at elevated pressure as inferred from Grashof numbers that were calculated based on flame dimensions. Droplet burning rates were also observed to increase with increasing pressure. Theory indicates that these increases resulted mainly from decreases in liquid densities and enthalpies of vaporization, where these decreases are caused by increases in liquid saturation temperatures.

Analytical Modeling

Simplified analyses of spherically symmetrical combustion of an isolated fuel droplet were developed to account for fuel pyrolysis [3]. Fuel pyrolysis is modeled as a high activation-energy process that occurs within a thin zone between the droplet and the flame. Accounting for fuel pyrolysis changes classical expressions for the transfer number because the flame must supply energy for fuel pyrolysis, which requires the flame to be located closer to the droplet. Sample calculations for combustion of heptane droplets in air at one atm indicate that transfer numbers, burning rates and quasisteady flame standoff ratios can be appreciably reduced when fuel pyrolysis effects are included in the analyses.

Soot shell standoff ratios in reduced-gravity droplet combustion were also investigated analytically [4]. Analysis of energy conservation between the droplet and the flame shows that temperature gradients between the droplet and a flame are influenced by variations in specific heats as well as fuel pyrolysis, which influences thermophoretic soot transport. Analyses show that if endothermic fuel pyrolysis is neglected, soot shells are predicted to be close to the fuel oxidation zone where fuel mass fractions are small. Analyses that account for endothermic fuel pyrolysis indicate that the onset of fuel pyrolysis can be abrupt, leading to local increases in temperature gradients. These temperature gradient changes can be large enough to influence soot transport, causing soot-shell standoff ratios to be smaller than if fuel pyrolysis is neglected. Theoretical predictions of pyrolysis-controlled soot-shell standoff ratios compare favorably with experimental data on reduced-gravity combustion of n-heptane droplets in air at 1 atm

References

1. I. Aharon and B. D. Shaw, Estimates of Liquid Species Diffusivities from Experiments on Reduced-Gravity Combustion of Heptane-Hexadecane Droplets, Combustion and Flame 113, 507 (1998).

2. S. M. Dakka and B. D. Shaw, Combustion of Propanol Droplets in Reduced Gravity, paper 04S-46 presented at the 2004 Spring Meeting of the Western States Section of the Combustion Institute, University of California, Davis, March 29-30.

3. B. D. Shaw, Theory of Spherically Symmetrical Droplet Combustion with Gas-Phase Fuel Pyrolysis, Combustion Science and Technology (submitted).

4. Theory of Influence of Fuel Pyrolysis on Soot-Shell Standoff Ratios in Reduced-Gravity Droplet Combustion, paper 04S-50 presented at the 2004 Spring Meeting of the Western States Section of the Combustion Institute, University of California, Davis, March 29-30.

REDUCED GRAVITY STUDIES OF SORET TRANSPORT EFFECTS IN LIQUID FUEL COMBUSTION

Benjamin D. Shaw
Mechanical and Aeronautical Engineering Department
University of California, Davis

Soret transport, which is mass transport driven by thermal gradients, can be important in practical flames as well as laboratory flames by influencing transport of low molecular weight species (e.g., monatomic and diatomic hydrogen). In addition, gas-phase Soret transport of high molecular weight fuel species that are present in practical liquid fuels (e.g., octane or methanol) can be significant in practical flames (Rosner et al., 2000; Dakhlia et al., 2002) and in high-pressure droplet evaporation (Curtis and Farrell, 1992), and it has also been shown that Soret transport effects can be important in determining oxygen diffusion rates in certain classes of microgravity droplet combustion experiments (Aharon and Shaw, 1998). It is thus useful to obtain information on flames under conditions where Soret effects can be clearly observed.

This research is concerned with investigating effects of Soret transport on combustion of liquid fuels, in particular liquid fuel droplets. Reduced-gravity is employed to provide an ideal (spherically-symmetrical) experimental model with which to investigate effects of Soret transport on combustion. The research will involve performing reduced-gravity experiments on combustion of liquid fuel droplets in environments where Soret effects significantly influence transport of fuel and oxygen to flame zones. Experiments will also be performed where Soret effects are not expected to be important. Droplets initially in the 0.5 to 1 mm size range will be burned. Data will be obtained on influences of Soret transport on combustion characteristics (e.g., droplet burning rates, droplet lifetimes, gas-phase extinction, and transient flame behaviors) under simplified geometrical conditions that are most amenable to theoretical modeling (i.e., spherical symmetry). The experiments will be compared with existing theoretical models as well as new models that will be developed. Normal gravity experiments will also be performed.

Experimental research will involve performing reduced-gravity droplet combustion experiments in a NASA Glenn drop tower (the 2.2 s tower). Use will be made of an existing droplet combustion rig. Digital images of the drop rig are shown in Fig. 1. This rig will be used to provide results on Soret effects for droplets initially from about 0.5 mm to 1 mm in diameter. The pressure will range from subatmospheric to as high as about 1.2 MPa (and possibly higher).

The drop rig has a pressure vessel mounted on a NASA-supplied drop frame with associated control electronics and gas and liquid handling systems. Orthogonal views are used with the drop rig; one view is used to image droplets and the other view is used to image flames. The flame view is not backlit, and a Xybion intensified-array CCD camera can be used to image OH emissions in this view (CH emissions can also be imaged).

Theoretical modeling will employ further development of analytical models beyond that described by Aharon and Shaw (1998). Further development of analytical theory will involve accounting for transient effects as well as developing models of Soret effects and multicomponent diffusion effects between droplet and flames. A goal of this modeling will be to develop simplified analytical models that retain the essential physics of Soret transport. In this way, Soret effects can be illustrated in a transparent manner.

Use will also be made of a computer code being developed as part of a NASA-sponsored program to study combustion of bi-component droplets. The numerical modeling involves development of a three-dimensional model for combustion of a droplet on a fiber (as well as a free droplet). The code includes important effects such as gas-phase radiant losses, detailed chemical kinetics, and realistic fiber effects (e.g., a nonslip condition, and fiber radiation in the vicinity of the flame). Soret transport can be turned on or off in the model.

References

Aharon, I., and Shaw, B.D. (1998) Microgravity Science and Technology X/2: 75.
Curtis, E.W., and Farrell, P.V. (1992) Combustion and Flame 90: 85.
Dakhlia, R.B., Giovangigli, V., and Rosner, D.E. (2002) Combustion Theory and Modeling 6: 1.
Rosner, D.E., Israel, R.S., and La Mantia, B. (2000) Combustion and Flame 123: 547.

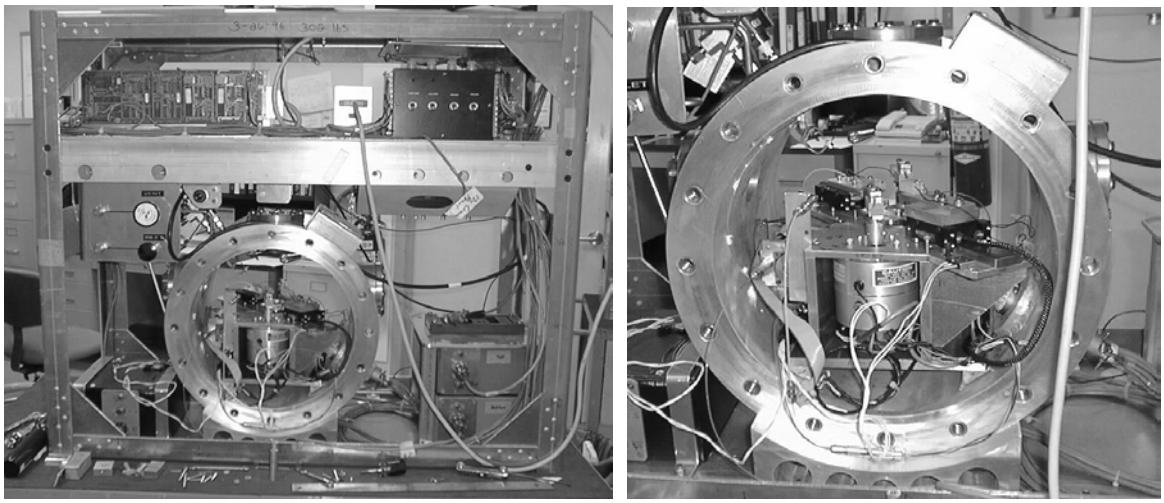

(a) (b)

Figure 1. Digital images of the drop rig: (a) overall rig; and (b) closeup of the pressure chamber interior. The endcaps for the pressure chamber are not shown.

COMPARISON OF CARBON DIOXIDE AND HELIUM AS FIRE EXTINGUISHING AGENTS FOR SPACECRAFT

Youngjin Son and Paul D. Ronney
University of Southern California, USA

Suleyman Gokoglu
NASA Glenn Research Center, USA

The effects of radiation heat transfer in microgravity compared to convection heat transfer in earth gravity for opposed-flow (downward) over thermally-thick fuel using low density foam fuel were investigated. Microgravity experiments on flame spread over thermally-thick fuels were conducted using foam fuels to obtain low density and thermal conductivity, and thus large flame spread rate compared to dense fuels such as PMMA. And thereby valid microgravity results were obtained even in 2.2 second drop-tower experiments not to mention for the longer duration tests in Zero Gravity Facility. Contrast to the conventional understanding, it was found that steady flame spread can occur over thick fuels in quiescent microgravity environments, especially when radiatively-active diluent gases such as CO_2 were employed. This is proposed to result from radiative heat transfer from the flame to the fuel surface, which could lead to steady spread even when the amount of the heat transfer via conduction from the flame to the fuel bed is negligible. Radiative effects are more significant at microgravity conditions because the flame is thicker and thus the volume of radiating combustion products is larger as well.

These results suggested that helium may be a better inert or extinguishment agent on both a mass and a mole bases at microgravity even though CO_2 is much better on a mole bases at earth gravity, and these are relevant to studies of fire safety in manned spacecraft, particularly the International Space Station that uses CO_2 fire extinguishers. CO_2 may not be as effective as an extinguishing agent at μg as it is at earth gravity in some conditions because of the differences in spread mechanisms between the two cases. In particular, the difference between conduction-dominated heat transport to the fuel bed at earth gravity and radiation-dominated heat transport at μg indicates that radiatively-inert diluent such as helium could be preferable in μg applications. Helium may be a superior fire suppression agent at μg on several bases. First, helium is more effective than CO_2 on a mole basis (thus pressure times storage volume basis) at μg, meaning that the size and weight of storage bottles would be smaller for the same fire-fighting capability. Second; helium is much more effective on a mass basis (by about 11 times) at μg. Third; helium has no physiological activity, unlike CO_2 that affects human respiration. Fourth, as compared to N_2 or CO_2, is not very soluble in water and thus has fewer tendencies to cause bloodstream bubble formation following rapid spacecraft cabin depressurization.

Paul D. Ronney
3650 McClintock Ave. OHE430
Los Angeles, CA, 90089
ronney@usc.edu
TEL: 213-740-0490
FAX: 213-740-8071

AGGREGATES AND SUPERAGGREGATES OF SOOT WITH FOUR DISTINCT FRACTAL MORPHOLOGIES

C.M. Sorensen, W. Kim, D. Fry, and A. Chakrabarti
Department of Physics
Kansas State University
Manhattan, KS 66506

Soot formed in laminar diffusion flames of heavily sooting fuels evolves through four distinct growth phases which give rise to four distinct aggregate fractal morphologies. These results were inferred from large and small angle static light scattering from the flames, microphotography of the flames, and analysis of soot sampled from the flames. The growth stages occur approximately over five successive orders of magnitude in aggregate size. Computer simulations can reproduce the kinetics observed in aggregation and aerogelation of soot clusters and indicate that these four growth stages involve either diffusion limit aggregation or percolation in either three or two dimensions.

DYNAMICS AND STABILITY OF CAPILLARY SURFACES: LIQUID SWITCHES AT SMALL SCALES

Paul H. Steen, Anand Bhandar, and Michael J. Vogel,
School of Chemical and Biomolecular Engineering
Cornell University
Ithaca, NY 14850

Amir H. Hirsa
Rensselaer Polytechnic Institute
Troy, NY 12180

The dynamics and stability of systems of interfaces is central to a range of technologies related to the Human Exploration and Development of Space (HEDS). Our premise is that dramatic shape changes can be manipulated to advantage with minimal input, if the system is near instability. The primary objective is to develop the science base to allow novel approaches to liquid management in low-gravity based on this premise. HEDS requires efficient, reliable and lightweight technologies. Our poster will highlight our progress toward this goal using the capillary switch as an example.

A 'capillary surface' is a liquid/liquid or liquid/gas interface whose shape is determined by surface tension. For typical liquids (e.g., water) against gas on earth, capillary surfaces occur on the millimeter-scale and smaller where shape deformation due to gravity is unimportant. In low gravity, they can occur on the centimeter scale. Capillary surfaces can be combined to make a switch – a system with multiple stable states. A capillary switch can generate motion or effect force. To be practical, the energy barriers of such a switch must be tunable, its switching time (kinetics) short and its triggering mechanism reliable. We illustrate these features with a capillary switch that consists of two droplets, coupled by common pressure. As long as contact lines remained pinned, motions are inviscid, even at sub-millimeter scales, with consequent promise of low-power consumption at the device level. Predictions of theory are compared to experiment on i) a soap-film prototype at centimeter scale and ii) a liquid droplet switch at millimeter-scale.

FIRE SUPPRESSION IN LOW GRAVITY USING A CUP BURNER

Fumiaki Takahashi
National Center for Microgravity Research on Fluids and Combustion
NASA Glenn Research Center
Cleveland, OH 44135
E-mail: Fumiaki.Takahashi@grc.nasa.gov, Fax: (216) 977-7065, Phone: (216) 433-3778

Gregory T. Linteris
Fire Research Division
National Institute of Standards and Technology
Gaithersburg, MD 20899

Viswanath R. Katta
Innovative Scientific Solutions Inc.
Dayton, OH 45440

Longer duration missions to the moon, to Mars, and on the International Space Station increase the likelihood of accidental fires. The goal of the present investigation is to: (1) understand the physical and chemical processes of fire suppression in various gravity and O_2 levels simulating spacecraft, Mars, and moon missions; (2) provide rigorous testing of numerical models, which include detailed combustion-suppression chemistry and radiation sub-models; and (3) provide basic research results useful for advances in space fire safety technology, including new fire-extinguishing agents and approaches.

The structure and extinguishment of enclosed, laminar, methane-air co-flow diffusion flames formed on a cup burner have been studied experimentally and numerically using various fire-extinguishing agents (CO_2, N_2, He, Ar, CF_3H, and $Fe(CO)_5$). The experiments involve both 1*g* laboratory testing and low-*g* testing (in drop towers and the KC-135 aircraft). The computation uses a direct numerical simulation with detailed chemistry and radiative heat-loss models. An agent was introduced into a low-speed coflowing oxidizing stream until extinguishment occurred under a fixed minimal fuel velocity, and thus, the extinguishing agent concentrations were determined. The extinguishment of cup-burner flames, which resemble real fires, occurred via a blowoff process (in which the flame base drifted downstream) rather than the global extinction phenomenon typical of counterflow diffusion flames. The computation revealed that the peak reactivity spot (the reaction kernel) formed in the flame base was responsible for attachment and blowoff of the trailing diffusion flame. Furthermore, the buoyancy-induced flame flickering in 1g and thermal and transport properties of the agents affected the flame extinguishment limits.

This research was supported by NASA's Office of Biological and Physical Research, Washington, D.C.

A BIOSENSOR FOR SINGLE-MOLECULE DNA SEQUENCING

Nerayo P. Teclemariam and Susan J. Muller*
Department of Chemical Engineering, University of California, Berkeley, CA 94720-1462
Phone: 510-642-4525, fax: 510-642-4778, e-mail:muller2@socrates.berkeley.edu

Victor A. Beck and Eric S.G. Shaqfeh
Department of Chemical Engineering, Stanford University, Stanford, CA 94305-5025

ABSTRACT

This project is a collaborative effort to develop a biosensor for obtaining sequence information from single DNA molecules. The sensor will allow rapid screening for specific genes which may be indicators of susceptibility to space radiation damage. The basic concept is to use hydrodynamics to fully extend genomic DNA in a microfluidic device. Fluorescent beads with surface-bound, complementary oligonucleotide probe sequences (corresponding to genes or sequences of interest) will be introduced and hybridized to the stretched DNA. Any unhybridized beads will be separated from the DNA-bead complexes. Imaging of the bead positions along the stretched, linear DNA backbone will then provide sequence information since the beads act as position and sequence sensitive markers. Realization of the device will require both detailed experiments and simulations aimed at designing flow geometries to stretch the DNA, optimizing the hybridization and transport of the DNA-bead complexes, and determining the resolution and limits of this sequencing method.

Introduction & Research Plan

In a series of seminal papers, Chu and co-workers used epifluorescence microscopy and fluorescently labeled DNA to directly visualize the effects of simple flows on DNA conformation (Perkins, Smith, and Chu, *Science* 276:2016 (1997), Smith and Chu, *Science* 281: 1335 (1998), Smith, Babcock, and Chu, *Science* 283:1724 (1999)). These studies provided unprecedented insights into the dynamics of single, macromolecular chains in steady shear and planar extensional flows; they also revealed the potential for direct comparisons between experiments and Brownian dynamics simulations of DNA chain trajectories in flow. Such simulations by Shaqfeh and Larson and co-workers have been successful in capturing the DNA dynamics observed in direct visualization experiments (Larson, Hu, Smith, and Chu, *J. Rheol.* 43:267 (1999), Hur, Shaqfeh, Babcock, Smith, and Chu,, *J. Rheol.* 45:421 (2001)). However, to date, very few *complex* flows of DNA have been simulated and compared to experiments. Moreover, it appears that no work has been done on designing flow geometries to produce specific DNA conformation fields.

The use of flow to control macromolecular conformation has wide-ranging potential applications. Here we propose using hydrodynamics to produce stretched, linear DNA for subsequent hybridization to fluorescently labeled beads; subsequent imaging of the beads will provide information about the location of certain genetic markers. Existing experimental and simulation capabilities will be extended to 1) identify the flow geometries that are most effective in stretching DNA in a microfluidic device, 2) determine the bead transport and binding kinetics for formation of the complementary DNA-bead complex, 3) quantify transport of the DNA-bead complex through the microdevice and its relaxation dynamics, 4) identify appropriate geometries

and flow parameters for separation of the unbound beads from the DNA-bead complexes, and 5) determine the resolution and limitations of this technique for sequencing.

Preliminary Results

Initial work has focused on identifying the flow geometries that will be most effective in stretching DNA. Several candidate geometries consisting of high aspect ratio post arrays of varying spatial arrangements, extents, and post densities have been fabricated in silicon at the Berkeley Microlab. Posts, flow channels, and deep trenches for capillary interconnects are defined through a series of lithography and etching steps. The final step is anodic bonding of the silicon device to a glass cover, which seals the flow channel and provides optical access. Optimization of the fabrication processing steps is currently underway. In particular, the deep reactive ion etch used to create the posts is extremely sensitive to operating parameters in the etch chamber; non-optimal conditions can result in undercutting of the posts or "grass" – i.e., large scale roughness on the bottom of the etched channels. To date, a number of fairly dense post arrays have been completed; a scanning electron micrograph of one such array, a 15 row hexagonal array of 2 micron diameter posts in a rectangular flow channel, is shown in figure 1.

Fluorescence microscopy will be used to visualize stretching of λ-DNA immediately upstream and immediately downstream of the arrays. Preliminary results for a 7 row post array are shown in figure 2. Under the flow conditions examined, this 7 row array results in a significant amount of stretching of DNA molecules as evidenced by the shift in the histogram to higher extensions after the post array. The array results in an increase in the mean extension of a DNA molecule of approximately 124%.

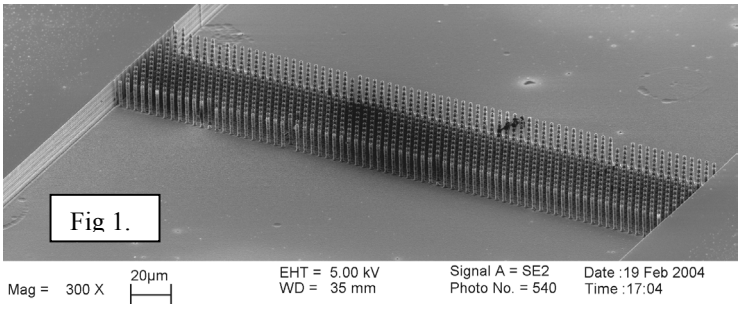

Preliminary Brownian dynamics simulations of DNA interactions with single posts and with extended post arrays are also underway. These simulations indicate that, through appropriate post column and row spacing, up to 42% of the DNA molecules can be extended past 80% of full extension after twenty rows of posts. Thus, fully stretched DNA molecules should be achievable through the use of appropriately designed post arrays, or through a combination of post arrays and contraction flows. A quantitative comparison of experiments to simulations, using the measured initial DNA extension and center of mass position upstream of the post array as inputs for the Brownian dynamics simulations, will be completed in the near future. Successful comparison will validate the simulations in these complex flows and allow us to use simulations to rapidly screen potential stretching geometries. Results will then guide the design and fabrication of the next generation of microfluidic devices.

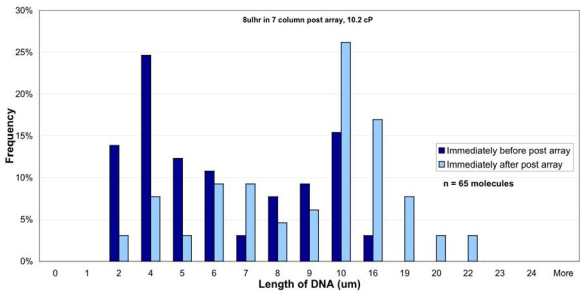

Figure 2. Histogram of λ-DNA extension in a 7 row post array.

SUPPORTED CAPILLARY PIPES

David B. Thiessen and Philip L. Marston
Department of Physics
Washington State University
Pullman, WA 99164-2814

Preliminary experiments have been conducted in a Plateau tank on supported capillary structures, which might have application to chemical separations and other processes in zero gravity including those associated with life support. Countercurrent flow of gas and liquid or of two liquids is ubiquitous in chemical processing. Examples include distillation, absorption, stripping, and extraction. A large amount of surface area is necessary for efficient operation of such processes. On earth, gravity drives the countercurrent flow because of a density difference between the two phases. Various support structures are used to create large amounts of surface area between the two phases such as structured or dumped packings or bubble-cap trays. In zero gravity, free-surface liquid flow can be inertial or driven by capillary forces or applied forces. It is proposed that supported capillary pipes can sustain sufficient pressure gradients to drive flow over significant distances for liquid-gas or liquid-liquid contacting. Liquid tubes of arbitrary length can be supported by parallel wires with the proper wetting characteristics arranged in regular polygonal arrays or by a helical coil of wire. The static stability of these structures has recently been investigated theoretically.

OSCILLATORY FLOWS AS A MEANS OF SEPARATION OF CONTAMINANTS FROM AIR

Aaron Thomas
University of Idaho

Oscillatory flows in tubes can be used as a mechanical means to separate species and enhance mass transport. This work applies the theory of oscillating flows toward the removal of trace organic contaminants and submicron particles from air that can be the result of off gassing, chemical spills, or even a fire that may occur in areas occupied by humans. For long-manned space missions, oscillating flows will reduce the load placed on traditional separation methods such as membranes, molecular sieves, and the like. These separation devices require replacement and/or regeneration of materials, so decreasing the load on these materials will increase their effective life and reduce the amount of material and man-hours needed (at some cost to extra power requirements). The current focus of our work is in a) optimization of the separation process using the tuning of geometric length scales with transport length scales in irregular geometries b) the enhancement of separation by operating the flows under increased concentration gradients and c) extension of this work to heat transfer as well as liquid phase systems.

This research is of use in space-enabling technologies but also has terrestrial applications to a) enhanced heat transport, b) separation of species in the liquid phase for biomedical devices and c) pre concentrators for detection of small concentration species in Homeland Security. Past results on experiments in regular geometries as well as preliminary results on velocity profiles and mass transfer in irregular geometries (wavy-walled tubes) will be presented during this poster session.

Reducing Fuel Slosh in Spacecraft Propulsion Systems

Erik Tolmachoff and Michael T. Kezirian

Department of Chemical Engineering
University of Southern California

Understanding the sloshing motion of liquid propellants in a partially-filled fuel tank is essential for determining and controlling spacecraft attitude (pointing). This investigation evaluates the importance of incorporating dynamic surface properties into the complete fluid transport model used to determine hydrodynamic flow stability.

Pointing stability requirements necessitate an understanding of the fuel motion and its interaction with the complete spacecraft flexible dynamic model. This investigation relates the fluid fuel motion, which at launch can account for approximately one half of the total spacecraft mass, to the overall attitude control. The numerical model developed for this investigation simulates the motion of a liquid fuel and quantifies the surface waves which appear at the interface and the internal waves in the bulk fluid.

COMPARISON OF THE STABILITY OF AN ELLIPTICAL LIQUID BRIDGE WITH A COMPANION CIRCULAR LIQUID BRIDGE

A. Kerem Uguz and R. Narayanan
Chemical Engineering Department
University of Florida
Gainesville, FL, 32611, USA
auguz@che.ufl.edu/ Fax: +1-352-392-9513

Liquid bridges have applications in microgravity contexts in connection to human health as well as materials processing. The small airways of the lungs are covered with a thin viscous film. The surface tension between the film and the air may induce the formation of a liquid bridge blocking the airflow and which might even damage the airway walls because of the pressure build-up. This disease is mostly seen in newborn premature babies who lack enough surfactant. Another application of the liquid bridges is seen in the float-zone crystal growth, which is a crucible-free technique to grow especially silicone. In this technique, in zero gravity, even if the strong thermocapillary flows are neglected, the melt zone, which can be represented by liquid bridge configuration, collapses at what is known as the Plateau limit. In most of the liquid bridge studies, the end disks are considered to be circular. In this presentation, the effect of distortion of the circular end plates to the nearby elliptical ones is studied wherein the volume of the companion cylindrical bridge is conserved. Also, the end plates are deviated from the companion circular plates by keeping either the area or the perimeter of the circular disks constant. We conclude that elliptical liquid bridge is more stable than its nearby circular bridge. A movie of the break-up of an elliptical liquid bridge is also provided.

ELECTRIC CURRENT ACTIVATED COMBUSTION SYNTHESIS AND CHEMICAL OVENS UNDER TERRESTRIAL AND REDUCED GRAVITY CONDITIONS

Unuvar, C.[1]; Fredrick, D.[1]; Anselmi-Tamburini U. [1]; M.; Manerbino, A.[3]; Guigne, J. Y.[3]; Munir, Z. A.[1]; Shaw, B. D.[2]

[1]Department of Chemical Engineering and Materials Science,
[2]Department of Mechanical and Aeronautical Engineering,
University of California, Davis
[3]Guigne Int. Ltd., 685 St. Thomas Line, Paradise, Newfoundland A1L 1C1, Canada

Combustion synthesis (CS) generally involves mixing reactants together (e.g., metal powders) and igniting the mixture. Typically, a reaction wave will pass through the sample. In field activated combustion synthesis (FACS), the addition of an electric field has a marked effect on the dynamics of wave propagation and on the nature, composition, and homogeneity of the product as well as capillary flow, mass-transport in porous media, and Marangoni flows, which are influenced by gravity. The objective is to understand the role of an electric field in CS reactions under conditions where gravity-related effects are suppressed or altered. The systems being studied are Ti+Al and Ti+3Al. Two different ignition orientations have been used to observe effects of gravity when one of the reactants becomes molten. This consequentially influences the position and concentration of the electric current, which in turn influences the entire process. Experiments have also been performed in microgravity conditions. This process has been named Microgravity Field Activated Combustion Synthesis (MFACS). Effects of gravity have been demonstrated, where the reaction wave temperature and velocity demonstrate considerable differences besides the changes of combustion mechanisms with the different high currents applied. Also the threshold for the formation of a stable reaction wave is increased under zero gravity conditions. Electric current was also utilized with a chemical oven technique, where inserts of aluminum with minute amounts of tungsten and tantalum were used to allow observation of effects of settling of the higher density solid particles in liquid aluminum at the present temperature profile and wave velocity of the reaction.

Conference-Workshop on Strategic Research to Enable NASA's Exploration Missions
June 22 - 23, 2004; Cleveland, Ohio USA

Droplet-Surface Impingement Dynamics for Intelligent Spray Design

Randy L. Vander Wal, John P. Kizito, Gretar Tryggvason,*
Gordon M. Berger, and Steven D. Mozes

The NCMR c/o NASA-Glenn
Cleveland, OH 44135

* Worcester Polytechnic Institute
Worcester, MA 01609

Spray cooling has high potential in thermal management and life support systems by overcoming the deleterious effect of microgravity upon two-phase heat transfer. In particular spray cooling offers several advantages in heat flux removal that include the following:

1. By maintaining a wetted surface, spray droplets impinge upon a thin fluid film rather than a dry solid surface
2. Most heat transfer surfaces will not be smooth but rough. Roughness can enhance conductive cooling, aid liquid removal by flow channeling.
3. Spray momentum can be used to a) substitute for gravity delivering fluid to the surface, b) prevent local dryout and potential thermal runaway and c) facilitate liquid and vapor removal. Yet high momentum results in high We and Re numbers characterizing the individual spray droplets. Beyond an impingement threshold, droplets splash rather than spread. Heat flux declines and spray cooling efficiency can markedly decrease.

Accordingly we are investigating droplet impingement upon a) dry solid surfaces, b) fluid films, c) rough surfaces and determining splashing thresholds and relationships for both dry surfaces and those covered by fluid films. We are presently developing engineering correlations delineating the boundary between splashing and non-splashing regions.

Determining the splash/non-splash boundary is important for many practical applications. Coating and cooling processes would each benefit from near-term empirical relations and subsequent models. Such demarcations can guide theoretical development by providing definitive testing of its predictive capabilities. Thus, empirical relations describing the boundary between splash and non-splash are given for drops impinging upon a dry solid surface and upon a thin fluid film covering a similar surface. Analytical simplification of the power laws describing the boundary between the splash and non-splash regions yields insight into the engineering parameters governing the splash and non-splash outcomes of the fluid droplets.

Figure 1 shows the power law correlation separating the splashing versus non-splashing regions as developed for droplets impinging upon a dry solid surface. Splashing upon a dry surface is reasonably described by $Ca > 0.85$, reflecting the competing roles of surface tension and viscosity. Figure 2 shows the power law correlation separating the splashing versus non-splashing regions as developed for droplets impinging upon a thin fluid film covering the solid surface. Splashing upon a thin fluid film, as described by $v\,(pd/s) > 63$, is governed by fluid density and surface tension, but is rather independent of viscosity. Finally, the data presented here suggests that a more direct dependence upon the surface tension and viscosity, given a better understanding of their interplay, would allow accurate description of the droplet-surface impacts for more complicated situations involving non-Newtonian fluids, specifically those exhibiting viscoelastic behavior.

Acknowledgment
This work was supported by a NASA NRA 01-HEDs-03 Fluid Physics award administered through NASA cooperative agreement NCC3-975 with The National Center for Microgravity Research on Fluids and Combustion (NCMR) at the NASA Glenn Research Center.

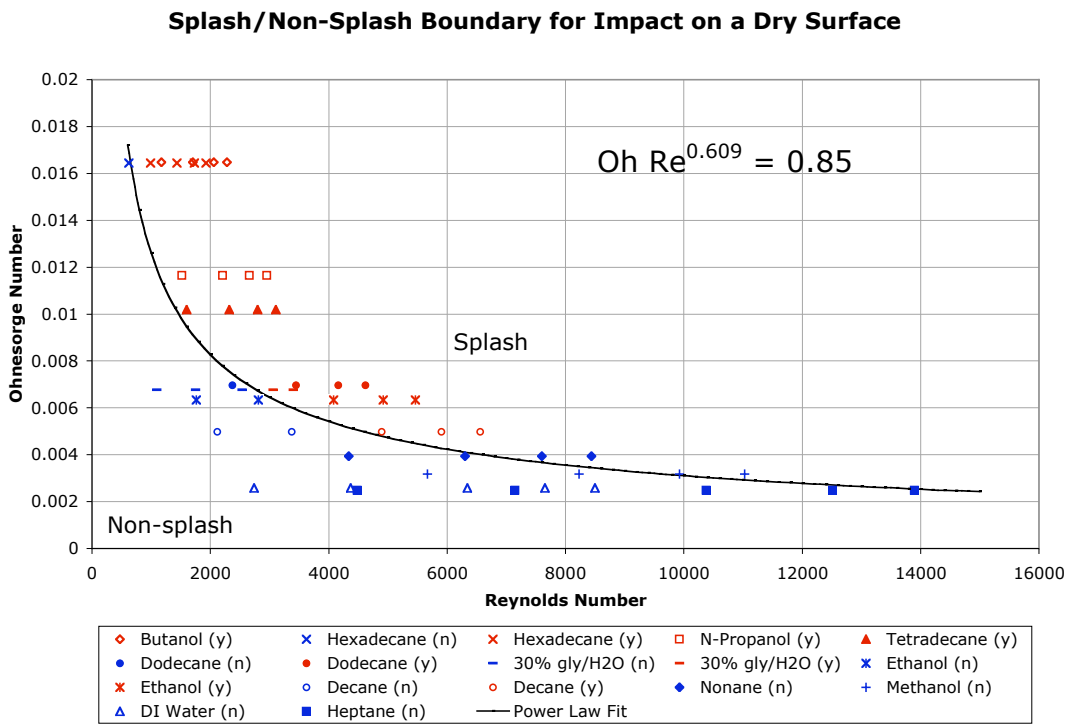

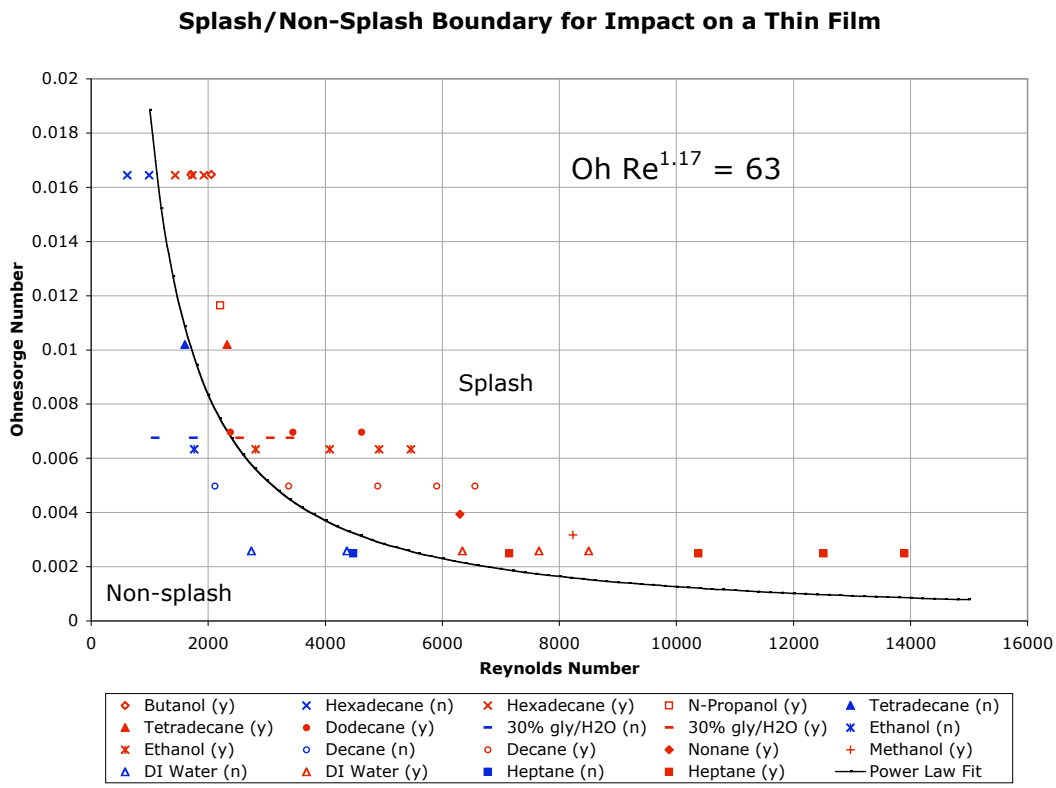

Figures 1&2. Splash behavior on a dry solid surface and on covered by a thin film, respectively, each plotted with respect to Ohnesorge and Reynolds number values. Red plot marks correspond to splashing behavior and blue to non-splash. The equation for the boundary fit line is included on the graph.

CONVECTIVE INSTABILITIES IN LIQUID FOAMS

Igor Veretennikov,
Department of Chemistry and Biochemistry, University of Notre Dame, Notre Dame, IN 46556,
email: ivereten@nd.edu, phone: (574)-631-7601, fax: (574)-631-6652

James A. Glazier,
Department of Physics, Indiana University, Bloomington, IN 47405

ABSTRACT

The main goal of this work is to better understand foam behavior both on the Earth and in microgravity conditions and to determine the relation between a foam's structure and wetness and its rheological properties. Our experiments focused on the effects of the bubble size distribution (BSD) on the foam behavior under gradual or stepwise in the liquid flow rate and on the onset of the convective instability. We were able to show experimentally, that the BSD affects foam rheology very strongly so any theory must take foam texture into account.

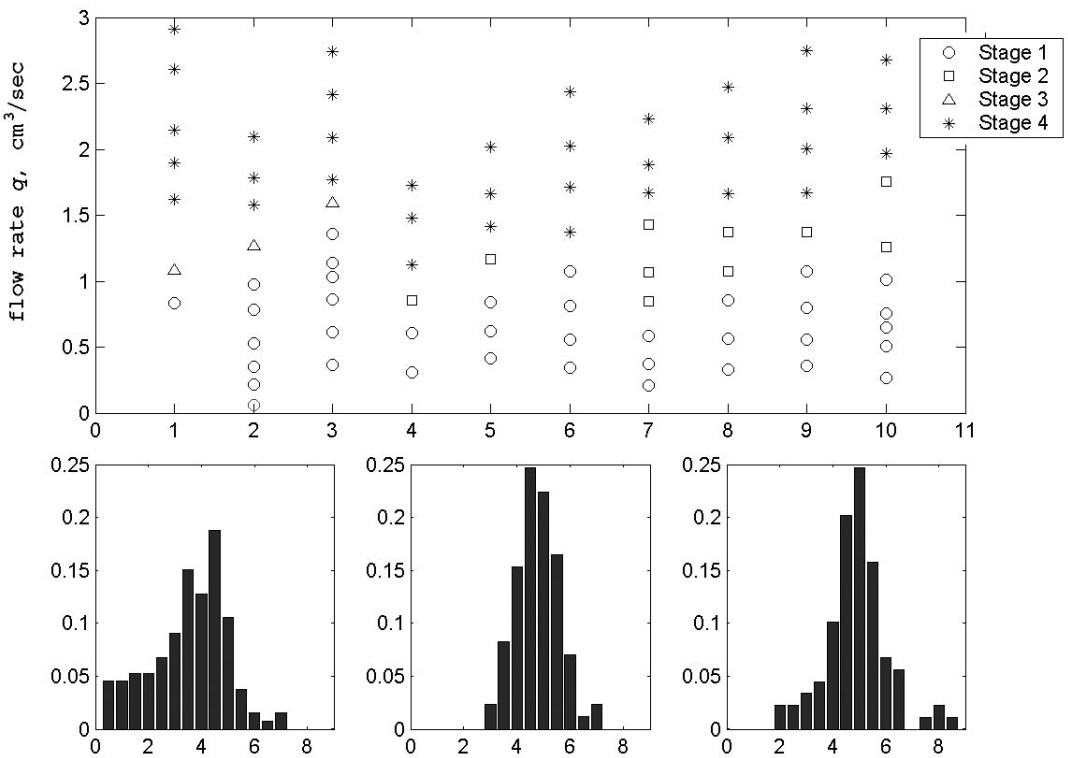

Figure 1: Behavior of stabilized foams as a function of liquid flow rate *q*. The BSD histograms corresponding to data sets 1-3, 4-6 and 7-10 are shown in a lower row.

When we change liquid flow rate by small increments, we detected four different stages of foam evolution. At low flow rates, increase in liquid supply produces only thickening of membranes and borders but does not induces bubbles motion (Stage1). For larger flow rate, but before the onset of global convection, we observed two possible types of foam behavior. One of them includes localized bubbles rearrangements in response to variations in liquid supply, which

stop after few minutes (Stage 2). For almost monodispersed foams (data sets 4-6) this stage presents for the narrow range of liquid flow rates or may be even absent. If the BSD is wide, with appreciable fraction of large bubbles (data sets 7-10), these rearrangements are typical for larger liquid flow rates range. Such "placing right bubbles to the right place" reduces stress in foam lattice and delays the onset of global convection for polydispersed foams. This stage was not observed for foams containing relatively large fraction of small bubbles. Instead, we have seen "scattered motion" (Stage 3): bubble cluster start to move, stops after few seconds or minutes, then similar motion begins at other place at the foam column, and so on. Such flow pattern persists as long as liquid flow rate does not change. Both Stages 2 and 3 for the same foam were never observed. "Scattered" motion always starts from the displacement of the smallest bubbles while the larger ones become involved later. Small bubbles, which may travel along the borders between large ones, may acts as increase effective viscosity of basic fluid, such that the passage of small bubbles between larger ones locally destabilizes the foam. The large-bubble motion stops after structure adjustment, but may start again if another cluster of small bubbles will be provided by incoming liquid flow.

We also examine the development of convective pattern under rapid increase in liquid flow rate from subcritical (Stage 1) to supercritical value (Stage 4). Typically, the melting wave propagates down along one side of the cell while the much slower upward foam flow develops on the other side. During few seconds after the flow rate change, there is no bubble motion while liquid flow through the foam slightly increases. After that, the entire foam downstream of the convective front moves down. Bubbles slightly compresses, but still do not moves relative to each other. When the melting wave passes few centimeters, the upward counterflow begins to develop. If the difference in flow rate is large, bubbles at the front of the wave may be significantly compressed. Behind the front, the borders thicknesses increase and bubbles may rotate while moving down. When the melting front reaches the bottom of the column, steady convective pattern develops. We captured the foam motion by digital video camera and measured the averaged image density. Borders are darker than lamellae, such that the average density provides information about liquid distribution in the foam. During the initial prewetting, the wetness of motionless foam increases uniformly over entire column. For the compression stage, we see the growth of wetness fluctuations and beginning of development of wetness maximum in front of approaching melting wave. The position of moving melting front is clearly seen on the vertical density profile. The wetness difference behind the front and downstream and the front slope are related to the wave speed and, in turn, to jump in liquid flow rates. When the convective roll is fully developed, vertical profiles of relative density again become uniform, while on horizontal profiles typically appear two maxima corresponding to downward and upward foam flows. The amplitude of these intensity maxima is roughly proportional to the foam velocity. The surprising is the overall decrease of the relative density during the compression stage. The physical mechanism behind it is not clear and requires additional study.

SEPARATION OF CARBON MONOXIDE AND CARBON DIOXIDE FOR MARS ISRU

Krista S. Walton and M. Douglas LeVan
Department of Chemical Engineering, Vanderbilt University
VU Station B #351604, 2301 Vanderbilt Place, Nashville, TN 37235
krista.s.walton@vanderbilt.edu
m.douglas.levan@vanderbilt.edu
Ph: (615) 322-2441 Fax: (615) 343-7951

The atmosphere of Mars has many resources that can be processed to produce things such as oxygen, fuel, buffer gas, and water for support of human exploration missions. Successful manipulation of these resources is crucial for safe, cost-effective, and self-sufficient long-term human exploration of Mars. In our research, we are developing enabling technologies that require fundamental knowledge of adsorptive gas storage and separation processes. In particular, we are designing and constructing an innovative, low mass, low power separation device to recover carbon dioxide and carbon monoxide for Mars ISRU (in-situ resource utilization). The technology has broad implications for gas storage and separations for gas-solid systems that are ideally suited for reduced gravitational environments. This paper describes our separation process design and experimental procedures and reports results for the separation of CO_2 and CO by a four-step adsorption cycle.

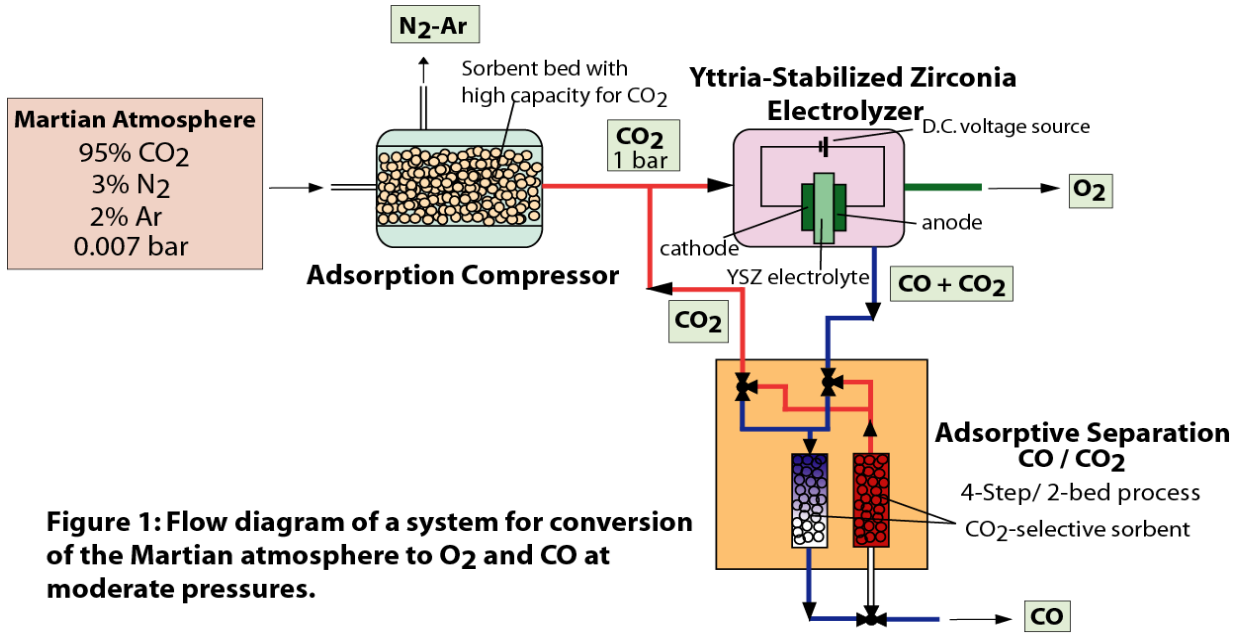

Figure 1: Flow diagram of a system for conversion of the Martian atmosphere to O_2 and CO at moderate pressures.

As illustrated in Figure 1, this work comprises one-third of an overall process for producing O_2 and CO at moderate pressures from the Martian atmosphere. An adsorption compressor, developed by Dr. John E. Finn at NASA Ames Research Center, adsorbs CO_2 from the atmosphere and compresses it to a pressure of 1 bar. The CO_2 is then passed to a solid oxide electrolysis cell developed by K. R. Sridhar at the University of Arizona. This electrolysis cell makes use of yttria-stabilized zirconia to produce oxygen from the compressed planetary CO_2 and will then reject CO and unreacted CO_2 in a separate stream. The efficiency of the oxygen-production process is greatly improved if the unreacted CO_2 is separated and recycled back into the feed stream. The separation will also have a positive impact on the mass of the adsorption compressor because less CO_2 will needed from the atmosphere. Additionally, the CO by-product is a valuable fuel for space exploration and habitation, with applications from fuel cells to production of hydrocarbons and plastics.

Our separation device contains a CO_2-selective sorbent such that when the mixture is fed from the electrolyzer, CO_2 adsorbs and CO passes through the bed with minimal adsorption. The cycle is illustrated by Figure 2. The mixture is fed at a temperature of 273K. When the bed reaches capacity, it is isolated and heated with no flow at 398K to desorb the CO_2. CO_2 at high pressure is then allowed to pass to a storage tank at sufficient pressure to feed the electrolyzer. The bed is then cooled back to 273K prior to returning to the feed step. We envision a two-bed system in which one bed is onstream for the feed step while the other is undergoing regeneration and blowdown of CO_2.

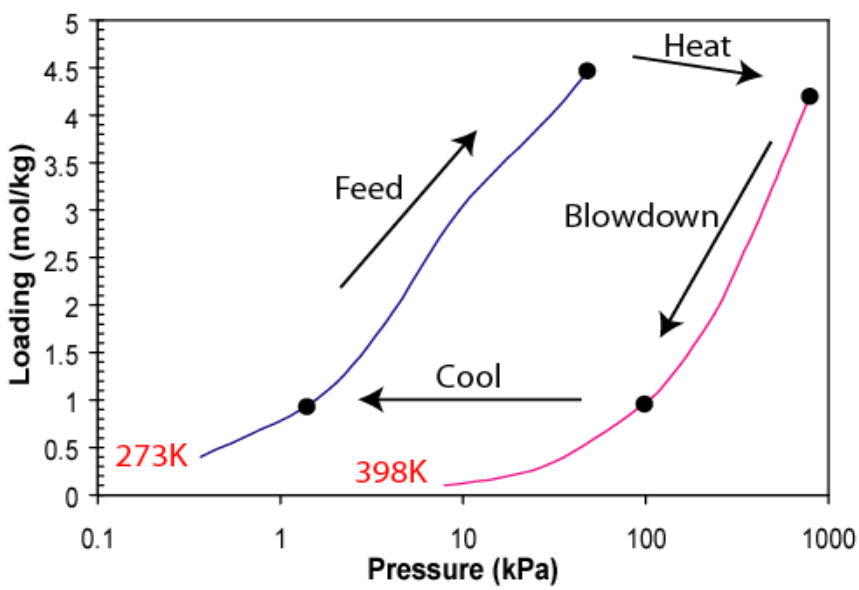

Figure 2: Depiction of four-step adsorption cycle between CO_2 adsorption isotherms on NaY zeolite.

We have a working prototype and have performed the proposed cycle. We have developed process models and are continuing to optimize the separation. All of these results will be discussed.

ENHANCED DAMPING FOR CAPILLARY BRIDGE OSCILLATION USING VELOCITY FEEDBACK

Wei Wei, David B. Thiessen, and Philip L. Marston
Department of Physics
Washington State University
Pullman, Washington 99164-2814

The stability of cylindrical liquid bridges in reduced gravity is affected by ambient vibrations of the spacecraft. Such vibrations are expected to excite capillary modes of the bridge. The lowest-order unstable mode is particularly susceptible to vibration as the length of the bridge approaches the stability limit. This low-order mode is known as the (2,0) mode and is an axisymmetric varicose mode of one wavelength in the axial direction. In this work, an optical system is used to detect the (2,0)-mode amplitude. The derivative of the error signal produced by this detector is used to produce the appropriate voltages on a pair of ring electrodes which are concentric with the bridge. A mode-coupled Maxwell stress profile is thus generated in proportional to the modal velocity. Depending on the sign of the gain, the damping of the capillary oscillation can be either increased or decreased. This effect has been demonstrated in Plateau-tank experiments. Increasing the damping of the capillary modes on free liquid surfaces in space could be beneficial for containerless processing and other novel technologies. [work supported by NASA]

THE STUDY OF TOPOLOGICAL STRUCTURE DISTRIBUTIONS IN STRATIFIED SOAP FILM CONVECTIONS

Jie Zhang, Yonggun Jun, and X.L. Wu
Department of Physics
University of Pittsburgh
Pittsburgh, PA 15260

The statistical properties of local topological structures (centers and saddles) are studied using a vertically suspended soap film. The turbulent convection of the film is created by a vertical temperature gradient (ΔT). The quantitative description of local topology is given by $\Lambda(x,y) \equiv \frac{1}{4}(\omega^2 - \sigma^2)$, where ω is the local vorticity and σ is the local strain rate. The PDFs of Λ were measured within a broad range of ΔTs. After normalizing Λ by its Λ_{rms}, one found that the PDFs of Λ were collapsed to two different curves at low and high ΔT regimes. Interestingly, the non-dimensional compressibility $C \equiv \frac{<(\nabla \bullet \vec{v})^2>^{\frac{1}{2}}}{<(\nabla \vec{v})^2>^{\frac{1}{2}}}$ was found to have two different constant values at these low and high ΔT regimes within experimental uncertainties. At low ΔT, C was found 0.32, and at high ΔT was 0.24. We believe the two different behaviors of Λ PDFs and C at low and high ΔTs are closely related and are result of the vertical stratifications of the soap film

REPORT DOCUMENTATION PAGE

Form Approved
OMB No. 0704-0188

Public reporting burden for this collection of information is estimated to average 1 hour per response, including the time for reviewing instructions, searching existing data sources, gathering and maintaining the data needed, and completing and reviewing the collection of information. Send comments regarding this burden estimate or any other aspect of this collection of information, including suggestions for reducing this burden, to Washington Headquarters Services, Directorate for Information Operations and Reports, 1215 Jefferson Davis Highway, Suite 1204, Arlington, VA 22202-4302, and to the Office of Management and Budget, Paperwork Reduction Project (0704-0188), Washington, DC 20503.

1. AGENCY USE ONLY (*Leave blank*)

2. REPORT DATE
June 2004

3. REPORT TYPE AND DATES COVERED
Technical Memorandum

4. TITLE AND SUBTITLE
Strategic Research to Enable NASA's Exploration Missions Conference
Abstracts

5. FUNDING NUMBERS
WBS–22–101–58–09

6. AUTHOR(S)
Henry Nahra, compiler

7. PERFORMING ORGANIZATION NAME(S) AND ADDRESS(ES)
National Aeronautics and Space Administration
John H. Glenn Research Center at Lewis Field
Cleveland, Ohio 44135–3191

8. PERFORMING ORGANIZATION REPORT NUMBER
E–14590

9. SPONSORING/MONITORING AGENCY NAME(S) AND ADDRESS(ES)
National Aeronautics and Space Administration
Washington, DC 20546–0001

10. SPONSORING/MONITORING AGENCY REPORT NUMBER
NASA TM—2004-213114

11. SUPPLEMENTARY NOTES
Abstracts from a conference sponsored by the NASA Office of Biological and Physical Research and hosted by NASA Glenn Research Center and the National Center for Microgravity Research on Fluids and Combustion, Cleveland, Ohio, June 22–23, 2004. Responsible person, Bhim Singh, organization code 6712, 216–433–5396.

12a. DISTRIBUTION/AVAILABILITY STATEMENT
Unclassified - Unlimited
Subject Category: 34 Distribution: Nonstandard
Available electronically at http://gltrs.grc.nasa.gov
This publication is available from the NASA Center for AeroSpace Information, 301–621–0390.

12b. DISTRIBUTION CODE

13. ABSTRACT ***(Maximum 200 words)***

The primary focus of the Conference on Strategic Research to Enable NASA's Exploration Missions is to inform the research community of the changing direction of the NASA Office of Biological and Physical Research programs to support the future exploration missions. The conference includes invited plenary talks, technical paper presentations, poster presentations, and exhibits in the areas of Human Life Support Technology and Human Health. This Technical Memorandum is a compilation of abstracts of the papers and the posters presented at the conference. Web-based proceedings, including the charts used by the presenters, will be posted on the Web shortly after the conference.

14. SUBJECT TERMS
Fluid dynamics; Fluid physics; Fluid mechanics; Microgravity; Reduced-gravity; Heat transfer; Multiphase flow; Complex fluids

15. NUMBER OF PAGES
199

16. PRICE CODE

17. SECURITY CLASSIFICATION OF REPORT
Unclassified

18. SECURITY CLASSIFICATION OF THIS PAGE
Unclassified

19. SECURITY CLASSIFICATION OF ABSTRACT
Unclassified

20. LIMITATION OF ABSTRACT